

**LOWER LIMB EXOSKELETON OF  
ROBOT ASSISTED GAIT TRAINER**

**ELANG PARIKESIT**

**A DISSERTATION SUBMITTED IN PARTIAL FULFILLMENT OF THE  
REQUIREMENTS FOR THE DEGREE OF DOCTOR OF ENGINEERING  
MECHATRONICS ENGINEERING PROGRAM  
(INTERNATIONAL PROGRAM)**

**FACULTY OF TECHNICAL EDUCATION**

**RAJAMANGALA UNIVERSITY OF TECHNOLOGY THANYABURI**

**ACADEMIC YEAR 2023**

**COPYRIGHT OF RAJAMANGALA UNIVERSITY  
OF TECHNOLOGY THANYABURI**

This dissertation consists of research materials conducted at Faculty of Technical Education, Rajamangala University of Technology Thanyaburi and hence the copyright owner. I hereby certify that the thesis doesn't contain any forms of plagiarism.

(Elang Parikesit)



COPYRIGHT © 2023

FACULTY OF TECHNICAL EDUCATION

RAJAMANGALA UNIVERSITY OF TECHNOLOGY THANYABURI

**Dissertation Title** Lower Limb Exoskeleton of Robot Assisted Gait Trainer  
**Name-Surname** Mr. Elang Parikesit  
**Program** Mechatronics Engineering  
**Dissertation Advisor** Associate Professor Dechrit Maneetham, D.Eng., Ph.D.  
**Academic Year** 2023

---

**DISSERTATION COMMITTEE**



..... Chairman  
(Professor Worawat Sa-ngiamvibool, Ph.D.)



..... Committee  
(Assistant Professor Evi Triandini, Ph.D.)



..... Committee  
(Assistant Professor Petrus Sutiyasadi, D.Eng.)



..... Committee  
(Associate Professor Ren Jean Liou, Ph.D.)



..... Committee  
(Associate Professor Dechrit Maneetham, D.Eng., Ph.D.)

Approved by the Faculty of Technical Education, Rajamangala University of Technology Thanyaburi in Partial Fulfillment of the Requirements for the Degree of Doctor of Engineering



..... Dean of Faculty of Technical Education

(Assistant Professor Arnon Niyomphol, M.S.Tech.Ed.)

8 July 2023

<b>Dissertation Title</b>	Lower Limb Exoskeleton of Robot Assisted Trainer
<b>Name-Surname</b>	Mr. Elang Parikesit
<b>Program</b>	Mechatronics Engineering
<b>Dissertation Advisor</b>	Associate Professor Dechrit Maneetham, D.Eng., PhD.
<b>Academic Year</b>	2023

## ABSTRACT

In this research, a low-cost lower limb exoskeleton has been developed for those who struggle with their lower legs, the exoskeleton works as a gait trainer. It is crucial for patients' lower extremity rehabilitation since it provides aid in their physical recovery. Although, there are robotic assisted gait trainers available in the market, the cost is high. Hence the objective of the study is to create a low-cost lower-limb exoskeleton for gait training with good performance. This research proposes a controller for a robot-assisted gait trainer's lower limb exoskeleton. The study focuses on 1) development of mechanism of two joints (hip and knee) of a lower-limb exoskeleton for gait training, 2) development of an electric motor driver for two joints (hip and knee) of a lower-limb exoskeleton for gait training, 3) development of control algorithm for two joints (hip and knee) of a lower-limb exoskeleton for gait training, and 4) an evaluation of the control algorithm's performance on the lower-limb exoskeleton of the robot-assisted gait training.

The human gait movement is not linear. Proportional-Integral Derivative (PID) appeared as a popular controller does not work on nonlinear system either. As a consequence, the PID could not be used in this system. Two experiments on controlling the gait trainer by using two different controllers were carried out: the one using hybrid PID-ILC and the other using Computed Torque Controller (CTC). The former, PID-ILC was an unmodelled control algorithm while the latter, CTC was a modelled controlled algorithm. The computed torque

controller was a vital nonlinear controller when the system's dynamic parameters were merely partially understood. A mathematical model was the foundation of this kind of controller. This proposed control was evaluated employing a scaled-down model. The methodological instruments used to achieve these goals were 1) an investigation and data collection using updated references, 2) a design and development of hardware and software of the system, and 3) a testing and a performance evaluation of the system.

An inexpensive robot-assisted gait trainer has been produced successfully. In the first experiment the robot-assisted gait trainer could follow gait trajectories with the support of the proposed hybrid PID-ILC controller even when there were unmodelled dynamics, uncertainty, and distractions. Real studies utilizing a specific controller load and gain showed that the PID-controlled system had possessed stability, but with an error of up to 10 degrees at steady state. Stability was demonstrated by the recommended hybrid PID-ILC controller. Initially the PID-ILC had steady state errors, notwithstanding after more than ten iterations, less than 1 degree of steady state error was attained. Up to 50% of the steady state error was greatly reduced. The performance of CTC was also evaluated and it was contrasted with that of the PID controller. CTC had better responses than PID for both joint 1 and joint 2. Nonetheless, for the downward direction, the response of joint 2 using CTC was not as good as PID.

**Keywords: computed torque controller, exoskeleton, gait trainer, Iterative learning control, lower limb, PID, robotics**

## **Acknowledgments**

First, I would want to convey my thanks and admiration to my advisor, Assoc. Professor Dr. Dechrit Maneetham, and my co-advisor, Asst. Professor Petrus Sutyasadi. The success of this thesis has been largely attributed to his willingness to put in a significant amount of time, consistent encouragement, wise counsel, and continuous direction and support throughout the research process. The examination committee members also deserve our sincere gratitude. We appreciate the objective analysis and helpful criticism provided by the outside reviewers, as they helped to elevate the quality of this work.

I want to express my gratitude to all the professors and students of the Mechatronics Department at the Rajamangala University of Technology Thanyaburi (RMUTT), also all my colleagues at Vocational Faculty, Sanata Dharma University, who have already made various contributions. Thanks also to the Sanata Dharma Foundation, Sanata Dharma University, and Rajamangala University of Technology Thanyaburi for supporting my scholarship and my studies.

I want to close by expressing my sincere gratitude to my loving family for their continuous love, support, and enthusiasm throughout my life. I want to express my gratitude to my parents for their work and their earnest prayers that their son attains the best level of education imaginable. I dedicate this work to my supportive family.

Elang Parikesit

## Table of Contents

	Page
ABSTRACT .....	(4)
Acknowledgments .....	(6)
Table of Contents .....	(7)
List of Figures .....	(11)
List of Tables.....	(15)
CHAPTER 1 INTRODUCTION .....	17
1.1 Background .....	17
1.2 Problems Statement.....	18
1.3 Purpose of the Study .....	19
1.4 Scope of the Study .....	19
1.5 Methodology .....	20
1.6 Dissertation Structure.....	22
CHAPTER 2 LITERATURE REVIEW .....	24
2.1 Spinal Cord Injuries .....	24
2.1.1 Strokes.....	26
2.1.2 Rehabilitation.....	27
2.1.3 Functional Ambulation Classification (FAC).....	29
2.1.4 Assistive device.....	30
2.1.5 Orthosis .....	32
2.2 Gait and Human Anatomy .....	36

2.2.1 Anatomical Terminology .....	36
2.2.4 Gait Analysis.....	37
2.2.2 Muscles and Bones.....	38
2.2.3 Walking cycle.....	40
2.3 Walking rehabilitation.....	43
2.3.1 End Effector Type Walk Trainer.....	43
2.3.2 Exoskeleton Type Walk Trainer .....	43
2.3.3 Walking Rehabilitation and Body Weight Support .....	45
2.4 Medical Robot and Exoskeleton .....	46
2.4.1 Medical Robot.....	48
2.4.2 Exoskeleton .....	53
2.4.3 Robot assisted walk trainers.....	75
<b>CHAPTER 3 RESEARCH METHODOLOGY.....</b>	<b>89</b>
3.1 System Design.....	89
3.2 The lower limb exoskeleton's kinematics .....	90
3.3 Lower limb exoskeleton dynamics.....	93
3.4 Mechanical Design.....	94
3.5 Actuator Selection.....	98
3.6 Control Theory .....	102
3.6.1 PID Control .....	103
3.6.2 Hybrid Feedback Control.....	105
3.6.3 Feedback Linearization and Computed torque control .....	106
3.7 Microcontroller and motor driving system .....	107



3.7.1 Arduino .....	107
3.7.2 Motor Driver .....	114
3.7.3 DC Motor .....	119
3.7.4 Gearbox .....	121
CHAPTER 4 RESULTS AND DISCUSSION .....	122
4.1 Control of Robot Assisted Gait Trainer Using Hybrid Proportional Integral Derivative Learning Control .....	122
4.1.1 Advantage of Iterative Learning Control (ILC) .....	122
4.1.2 Dataset of normal gait .....	123
4.1.3 Result and discussion .....	124
4.2 Two-link Lower Limb Exoskeleton Enhancement Using Computed Torque .....	127
4.2.1 Computed torque control .....	127
4.2.2 Microcontroller and motor driving circuit .....	130
4.2.3 Results and discussion .....	136
CHAPTER 5 CONCLUSIONS AND FUTURE WORKS .....	143
5.1 Conclusions .....	143
5.1.1 Hybrid PID ILC .....	143
5.1.2 Computed Torque Control .....	144
5.2 Future Works .....	144
List of Bibliography .....	146
APPENDICES .....	169
APPENDIX A MICROCONTROLLER SOURCE CODE .....	170
APPENDIX B INTERNATIONAL PUBLICATIONS .....	180



## List of Figures

	Page
Figure 2. 1 Levels of SCI and the area of the body effect .....	25
Figure 2. 2 Ischemic strokes and Hemorrhagic strokes and the effect .....	27
Figure 2. 3 (A) Crook-top or C-handle cane (B) aluminum cane that is adjustable (C) Cane with a good grip (D) Adjustable quad cane with a wide base.(E) Hemiwalker. (F) Wooden axillary crutch that can be adjusted. (G) Lofstrand crutch made of adjustable aluminum. (H)Support with the forearms or a platform. (I) either a walker or walkerette.....	32
Figure 2. 4 Clutch Spring Knee Exoskeleton for Running .....	34
Figure 2. 5 PAFO device .....	35
Figure 2. 6 Three reference planes represent the anatomical position.....	36
Figure 2. 7 Knee and hip movements .....	37
Figure 2. 8 An overview of the bones of the lower limb .....	39
Figure 2. 9 The lower limbs' bones and muscles .....	40
Figure 2. 10 Phases of gait cycle .....	41
Figure 2. 11 Normal adult walking joint trajectories.....	42
Figure 2. 12 Graphs of angular kinematics across the gait cycle .....	42
Figure 2. 13 BWS systems are classified as (a) static and (b) passive counterweight dependent, (c) passive spring based, and (d) active systems .....	45
Figure 2. 14 Medical robotics systems based on classification .....	50
Figure 2. 15 Robotic assistive technologies.....	51
Figure 2. 16 An outline of rehabilitation robots in recent literature .....	52
Figure 2. 17 Classification of exoskeletons according to their usage.....	55
Figure 2. 18 Enactment Exoskeletons : (a) Walsh soft exosuit (Awad et al., 2020) .....	57
Figure 2. 19 BLEEX Exoskeleton .....	59
Figure 2. 20 ReWalk Exoskeleton .....	60
Figure 2. 21 Indego Exoskeleton .....	61
Figure 2. 22 HAL-3 exoskeleton .....	62

## List of Figures (Continued)

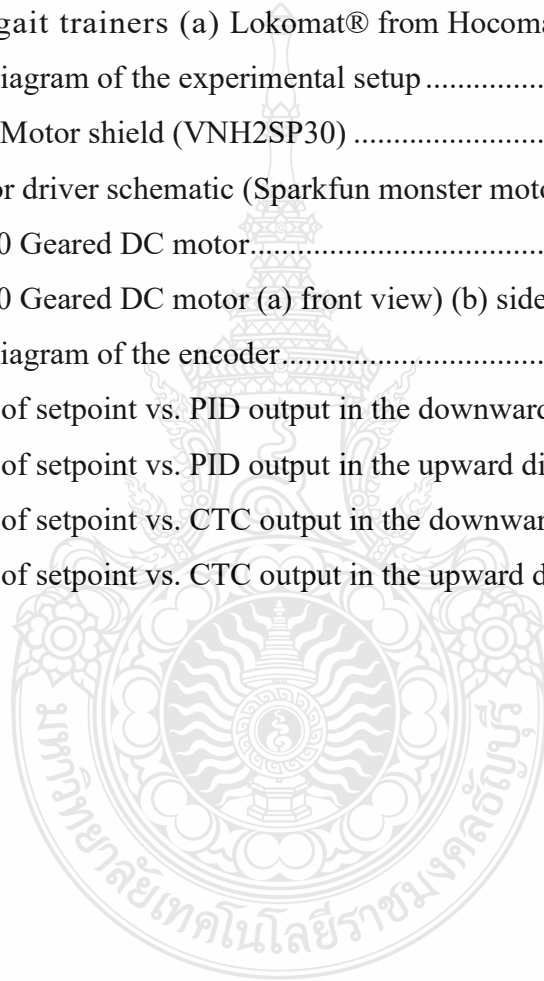
	wPage
Figure 2. 23 Characteristics of Robots for Lower Limb Rehabilitation .....	63
Figure 2. 24 Classification of exoskeletons .....	64
Figure 2. 25 Main Upper Limb Exoskeleton Robots Companies. a Hocoma, b Bionik, c BKINTechnologies, d Motorika, Medical, e Wereable Robotics, f AURA Robotics .....	65
Figure 2. 26 Characteristics of Robots for Upper Limb Rehabilitation.....	67
Figure 2. 27 MIT-MANUS.....	68
Figure 2. 28 UL-EXO7 .....	69
Figure 2. 29 Exoskeleton concept solutions for actuation and power. ....	71
Figure 2. 30 Exoskeleton actuation principles. (A) Transmission of gears. (B) A joint with a force sensor. Tendon transmission (C). Variable impedance (D). Elastic in the (E) sequence. Hydraulic-pneumatic (F).....	72
Figure 2. 31 List of existing rehabilitation robot with their actuator type.....	72
Figure 2. 32 Different approaches to robotic gait trainers .....	76
Figure 2. 33 Most recent lower-limb therapy robots and their category .....	78
Figure 2. 34 Passive mode and active mode .....	83
Figure 2. 35 Classification of control modes.....	83
Figure 2. 36 Summary of robot-assisted rehabilitation control strategies and their outcomes .....	85
Figure 2. 37 Mechanical compensation using control algorithm.....	88
Figure 3. 1 Framework for hierarchical control in the robotic gait trainer .....	89
Figure 3. 2 The gait rehabilitation control system's architecture.....	90
Figure 3. 3 General closed-loop control of Robotic Gait Trainer.....	90
Figure 3. 4 Kinematics of lower limb exoskeleton.....	91
Figure 3. 5 Knee joints from human(a) and exoskeleton(b) are compared. ....	94
Figure 3. 6 Exoskeleton of the lower limb in mechanical illustration .....	96
Figure 3. 7 Exoskeleton support (top and side mechanical illustration).....	96

## List of Figures (Continued)

	Page
Figure 3. 8 a) PG56 brushless DC motor with encoder b) Gearbox Shaft Ratio 1:50.....	97
Figure 3. 9 The physical appearance of the gait trainer .....	97
Figure 3. 10 A dc motor (a) electrical schematic (b) sketch of the parts.....	98
Figure 3. 11 DC motor field-controlled type .....	100
Figure 3. 12 DC motor (armature-controlled type).....	101
Figure 3. 13 PID controller structure. ....	104
Figure 3. 14 IPD controller structure. ....	104
Figure 3. 15 Hybrid control system illustration.....	105
Figure 3. 16 A generalized hybrid closed loop system block diagram.....	105
Figure 3. 17 Computed torque control.....	106
Figure 3. 18 Arduino UNO .....	111
Figure 3. 19 Arduino Mega 2560.....	112
Figure 3. 20 Diagram of the system for driving a motor and a microcontroller.....	114
Figure 3. 21 BTS7960 H-Bridge DC Motor Driver.....	115
Figure 3. 22 Schematic of BTS7960 H-Bridge DC Motor Drive.....	115
Figure 3. 23 BTS 7960B MOSFET .....	117
Figure 3. 24 Inside BTS 7960 IC .....	118
Figure 3. 25 Pinout BTS 7960P MOSFET .....	118
Figure 3. 26 Block Diagram of TLE4278G.....	119
Figure 3. 27 Sideview of PG 56 motor .....	120
Figure 3. 28 Yuema Gearbox.....	121
Figure 4. 1 Schematic representation of a hybrid PID-ILC system.....	123
Figure 4. 2 Hip flexion and extension based on the dataset .....	123
Figure 4. 3 Knee flexion and extension depending on the dataset .....	124
Figure 4. 4 PID-only hip flexion and extension in an exoskeleton.....	125
Figure 4. 5 PID-ILC control of exoskeleton hip flexion and extension .....	125

## List of Figures (Continued)

	Page
Figure 4. 6 PID-only control of knee flexion and extension in an exoskeleton .....	126
Figure 4. 7 PID-ILC control of knee flexion and extension in an exoskeleton .....	126
Figure 4. 8 Computed-torque control scheme .....	129
Figure 4. 9 Robotic gait trainers (a) Lokomat® from Hocoma; .....	130
Figure 4. 10 Wiring diagram of the experimental setup .....	131
Figure 4. 11 Monster Motor shield (VNH2SP30) .....	132
Figure 4. 12 DC motor driver schematic (Sparkfun monster motoshield) .....	133
Figure 4. 13 JG25-370 Geared DC motor.....	134
Figure 4. 14 JG25-370 Geared DC motor (a) front view) (b) side view .....	135
Figure 4. 15 Wiring diagram of the encoder.....	135
Figure 4. 16 The plot of setpoint vs. PID output in the downward direction .....	136
Figure 4. 17 The plot of setpoint vs. PID output in the upward direction .....	137
Figure 4. 18 The plot of setpoint vs. CTC output in the downward direction.....	138
Figure 4. 19 The plot of setpoint vs. CTC output in the upward direction.....	139

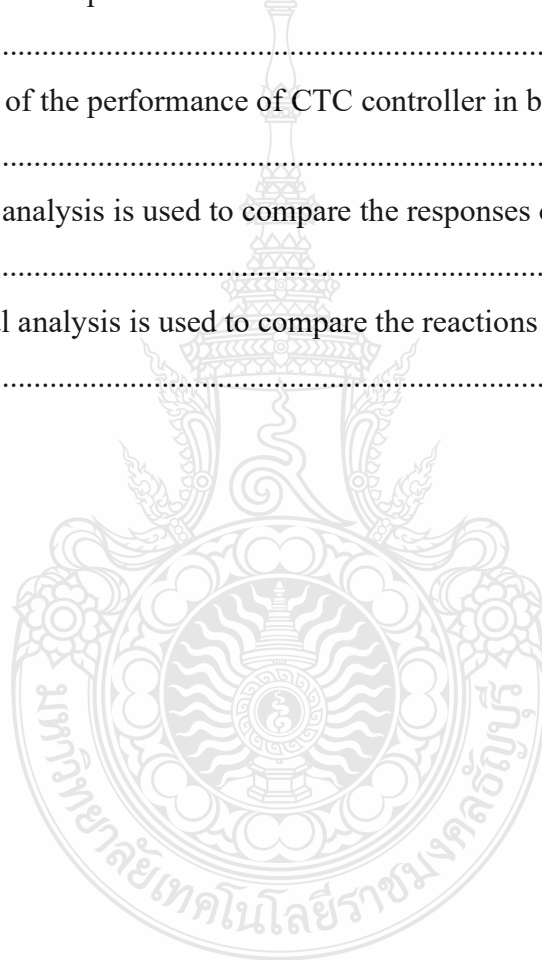


## List of Tables

	Page
Table 1. 1 Phases and stages of the methodology.....	20
Table 2. 1 Functional ambulation scale .....	30
Table 2. 2 Categories of orthoses.....	33
Table 2. 3 Historical evolution of robots in medical industry .....	48
Table 2. 4 Classifications of upper-limb exoskeletons according to actuation and kinematic .....	69
Table 2. 5 Comparison of actuator types implemented on robot assisted gait trainer .....	73
Table 2. 6 Powering source and methods of various exoskeletons .....	74
Table 2. 7 Commercial robot assisted walk trainers .....	75
Table 2. 8 Actuated DOF and characteristics of the most recent lower limb therapy robots .....	79
Table 2. 9 Some of the most common training modes for robots that help with lower limb rehabilitation. ....	83
Table 2. 10 A summary of robot-assisted gait trainer control algorithm.....	85
Table 2. 11 Comparison of Hybrid Controller for robot assisted gait trainer.....	87
Table 3. 1 Kinematics of the Hip and Knee.....	95
Table 3. 2 Timeline of Arduino products .....	109
Table 3. 3 Hardware specification of Arduino UNO (Arduino).....	111
Table 3. 4 Hardware specification of Arduino MEGA2560 (Arduino).....	112
Table 3. 5 Brief data of BTS7960.....	116
Table 3. 6 Pin function and description.....	116
Table 3. 7 Key elements of BTS 7960B.....	117
Table 3. 8 Gearbox data.....	120
Table 3. 9 Motor data.....	120
Table 4. 1 PID controller tuning parameters.....	124
Table 4. 2 A numerical comparison of the PID-ILC and PID responses.....	127
Table 4. 3 Parameters with two links.....	130

### List of Tables (Continued)

	Page
Table 4. 4 Operating ratings of Monster Moto Shield.....	132
Table 4. 5 Characteristics of VNH2SP30-E .....	134
Table 4. 6 Datasheet of the encoder.....	135
Table 4. 7 Evaluation of the performance of PID controller in both the downward and upward directions.....	139
Table 4. 8 Evaluation of the performance of CTC controller in both the downward and upward directions.....	140
Table 4. 9 Numerical analysis is used to compare the responses of CTC and PID (upward direction).....	141
Table 4. 10 Numerical analysis is used to compare the reactions of CTC and PID (downward direction).....	141





# CHAPTER 1

## INTRODUCTION

### 1.1 Background

The term "cardiovascular disease" refers to a group of conditions that include heart disease, vascular disease of the brain, and diseases of other blood artery conditions. Stroke is classified as a kind of cardiovascular disease (CVD). Around the world, strokes are responsible for the most prevalent cause of motor impairment. Every year, 15 million people suffer from stroke. More than 85 percent are healthy, but only 10 percent fully recovered (Benjamin et al., 2017).

Globally, CVD mortality increased by 46% between 1990 and 2013. The increase in CVD mortality is mainly due to the increase in CVD mortality and stroke. In 2013, CHD was responsible for 15% of all deaths worldwide. The second cause of death was stroke (12%) (evenly distributed between ischemic and hemorrhagic stroke). An estimated 14.5 million people died of heart disease and stroke, accounting for nearly a quarter of all deaths worldwide in 2013 (Zipes et al., 2019). Stroke is a particularly serious problem in Asia. Asia has a higher stroke mortality rate than Western Europe, America, or Australia, with the exception of Japan (Venketasubramanian et al., 2017). Physical conditions that impair a person's ability to walk are frequently caused by neurological injuries (van Nunen, 2013). When one loses their ability to walk, they frequently become dependent on wheelchairs or other mobility devices like orthotics or ankles.

Daily tasks require the ability to walk. One of the key healing objectives for many people with neurological illnesses is regaining the ability to walk. Therefore, walking is an important part of these people's rehabilitation program. In addition, the ability to walk greatly contributes to the whole fitness of the patient and affects the patient's health status. In many rehabilitations and research, optimizing therapeutic methods/techniques to walking improvement has received considerable attention. Various therapies have been utilized to help people regain their performance and motor skills (Gassert & Dietz, 2018). However, in

many cases, treatment results remain unsatisfactory, so many scientists are investigating how best to improve the mobility of neurological patients.

Given the need for proper medical care, delicate and precise procedures, and the lack of doctors and specialists, various alternatives have been proposed to address the problem of medical rehabilitation. Many new devices are being developed every year, and robotic rehabilitation field is growing fast (Xue et al., 2022).

## **1.2 Problems Statement**

Cerebrovascular accident (CVA) is the medical term for a stroke. It results from hypoxia due to a blockage or rupture of blood vessels that cause bleeding (Hankey et al., 2019). Without oxygen or glucose, the brain can work for about 10 minutes before this happens (Mohr et al., 2011). In this case, the person with that condition usually has one or more extremities on one side of the body paralyzed because the affected area on the other side of the brain can no longer function. In case of damage to the lower extremities, recovery is necessary to restore independent gait and gait. Various approaches to rehabilitation have been proposed to improve walking ability.

In most cases, recovery occurs within the first 6 months after a stroke. Healing may happen later, but it will be slower (Ponsford et al., 2004). At this stage, an intervention program is conducted to retrain their abilities in day-to-day activities. Neuroplastic changes (brain remodeling) are much more likely if the movement trying to repeat is part of the real problem (Levine, 2018). There are robot-powered walking trainers like Lokomat and Gait Trainer, but the price is still very high (€ 330,000 for Lokomat and € 30,000 for Gait Trainer GT1)(Esquenazi, 2018).

The ability to "do more with less" — that is, to provide much more commercial and societal gain while using fewer finite resources (electricity, money, and time), is referred to as frugal innovation (Radjou & Prabhu, 2015). Healthcare professionals frequently develop unique strategies in circumstances with limited resources to provide patients with adequate

care. These inexpensive yet useful discoveries have the ability to alter people's lives by making wellness available to everyone, despite its flaws (Tran & Ravaud, 2016).

Mechatronics uses interdisciplinary expertise from mechanical engineering, electronics, and information science to solve technical problems. Component and device modeling are important in the mechatronics development process because they allow flexibility and sophistication to be exchanged between disciplines to iteratively arrive at the best system architecture (Onwubolu, 2005).

### **1.3 Purpose of the Study**

The goals of this research are:

- 1.3.1 To optimize control algorithm for Robot Assisted Walking Trainer that can assist the user in performing movements in real environment and improving walking ability.
- 1.3.2 To design cost effective mechanical design exoskeleton of Robot Assisted Gait Trainer

### **1.4 Scope of the Study**

The study will focus on

- 1.4.1 Development of mechanism of two joints (hip and knee) of lower limb exoskeleton gait trainer
- 1.4.2 Development of electric motor driver for two joints (hip and knee) of lower limb exoskeleton gait trainer
- 1.4.3. Development of control algorithm for two joints (hip and knee) of lower limb exoskeleton gait trainer
- 1.4.4 Evaluation of the control algorithm's performance on the lower limb exoskeleton of the robot-assisted gait trainer.

## 1.5 Methodology

The process, which contains nine steps and three phases, involves developing the device from the point at which a problem first arises all the way through to the point at which, after numerous iterations, the technological transition can be made one step after the answer has been solidified. Table 1.1 shows the methodology used in this research

**Table 1. 1** Phases and stages of the methodology

No	Stages	Phases	Activities	Output
1	Investigation and data collection	Investigate current patient rehabilitation methods	In this step, the kind of human disorders that relate to the human walking are investigated. Information about instruments being used in this field is collected. From many potential methods and variety of injuries are grouped and selected to find the most subject and appropriate way to solve in the research	Information about the kind of walking disorders and its rehabilitation devices.
2		Data collection of methods being used in recent research and then compare those research's	The chosen topic will be studied to find its state of the art. Recent methods that have been used are studied deeper to get the	State of the art of the topic chosen.

		methods against the patient improvements	benefits and the drawbacks respectively.	
3	Design and development	Design new control method of the rehabilitation hardware and software	Design of new rehabilitation hardware software will be conducted according to the previous study about the current systems and the patient improvement.	Hardware and software design of Exoskeleton of Robot Assisted Gait Trainer
4		Design optimization using model optimization algorithm test or Computer Aided Engineering.	To test the hardware model using some optimization algorithms or Computer Aided Engineering software to get the full system characteristic and performance.	Simulation and optimization test result.
5		Finalizing the hardware and software design.	Re-design and improve the design of the Exoskeleton of Robot Assisted Gait Trainer hardware and software according to the data from the previous test.	Improved design

6		Development of the overall system	Start to develop the hardware and software of Exoskeleton of Robot Assisted Walk Trainer	Prototype of Exoskeleton of Robot Assisted Gait Trainer
7	Testing and implementation	System test and improvement	Test the system to investigate the reliability, repeatability, robustness, etc. Compared to the previous model experiment.	Performance test result of the system.
8		User implementation and feedback	Test the system to the human or real patient and get the feedback data about the performance of the system.	Performance test result of the system.
9		Finalization and improvement	Update the system using the data feedback from the previous implementation test.	The final Exoskeleton of Robot Assisted Gait Trainer

### 1.6 Dissertation Structure

The following is the structure of the dissertation:

Chapter 1 : background, problems statement, and scope of the study are presented here.

Chapter 2: several literature studies of robot-assisted gait trainer designs and control algorithms that were carried out by earlier researchers are discussed.

Chapter 3: the kinematics and hardware design of the recently built robot aided gait trainer are broken down and explained.

Chapter 4: an algorithm that utilizes hybrid PID-ILC is shown. Both the results of the experiment and a discussion of them are offered here. A control algorithm that makes use of computed torque control is also presented. . The discussion and the results of the experiment are presented here.

Chapter 5: all the research is brought to a close, which also provides some suggestions for further research in the area.



## **CHAPTER 2**

### **LITERATURE REVIEW**

Today, a variety of illnesses are treated using rehabilitation robotics systems. Strokes and spinal cord injuries (SCI) are two common illnesses. While SCI and strokes are two distinct medical disorders, both are extremely stressful to the body and can harm one or all the limbs' motor functions, based on how severe the injury is and how quickly can receive medical help. People with both injuries are currently being treated with robotic devices and similar rehabilitation techniques.

#### **2.1 Spinal Cord Injuries**

Injuries to the spinal cord affect between 250,000 and 500,000 persons annually. Most of these cases are the result of avoidable events like violence and auto accidents (Bennett et al., 2022). SCI causes the loss of sensor and motor function. The amount of functionality loss depends on the injury level. Generally, as the injury location goes up a person's spinal cord, more functionality is lost, as shown in Figure 2.1. According to American Spinal Injury Association (ASIA) recommendations, the damage levels classified by the American Spinal damage Association (ASIA) scale are as follows: A-B; cervical (C7-C8) or thoracic (T1-T12) (Glasper et al., 2010). Grade A describes a total impairment in which there is no residual sensory or motor function. Grade B is a partial impairment with no motor functions below the damage level but some sensory functions. As a result, it is decided that the target requirement for investigations using lower limb exoskeletons is injury levels between C7 and T12 (Esquenazi et al., 2012). The injury level results in one of many classifications that define their functional ability. Paraplegia results in impairment of the trunk, legs, and pelvis. Tetraplegia affects the arms, trunk, and other parts of the upper and lower body. An incomplete SCI is when some remaining sensory or motor function is below the injury level. There is no motor or sensory functionality below the injury level in a complete SCI injury. The cost of lifetime treatment is between \$500k -\$2M depending on the injury level (McDonald & Sadowsky, 2002). This cost includes the initial cost



immediately after the injury and the treatment of secondary health side effects throughout life. A secondary health side effect is a physical or psychological health condition caused by the injury (Jensen et al., 2012). These side effects include the decrease in the bone density of the femur, decrease in blood pressure, and reduced muscle mass (Haisma et al., 2007)(Hitzig et al., 2010) and result in a significantly reduced Quality of Life (QoL) of the person (Craven et al., 2012). Prevention of these side effects through rehabilitation will help increase the QoL and overall health of the person.

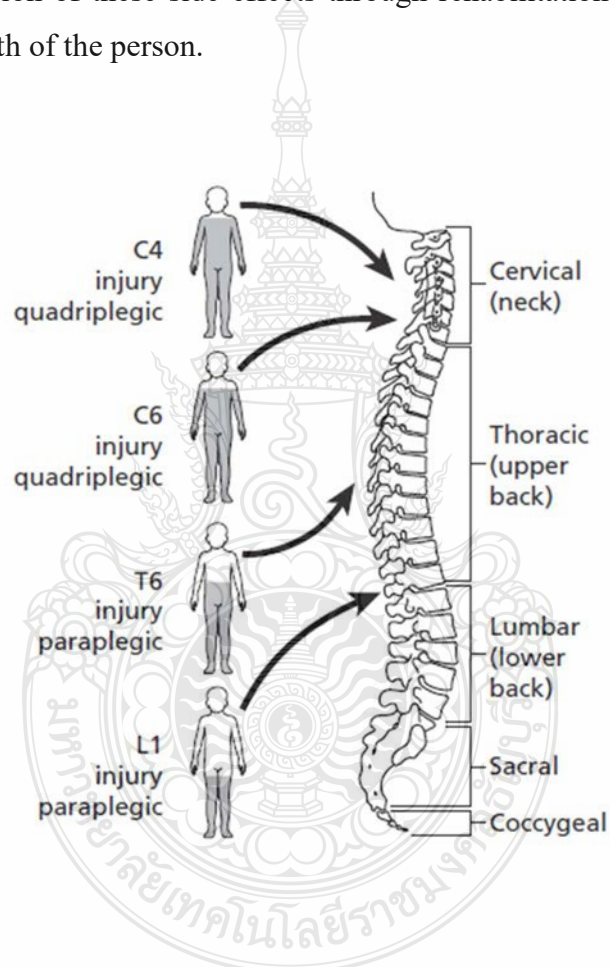


**Figure 2. 1** Levels of SCI and the area of the body effect  
(SOURCE: Developing Practical Skills for Nursing Children and Young People, Hoder Arnold, 2010.)

### 2.1.1 Strokes

Stroke ranks third in global disability and second in global mortality according to disability-adjusted life-years lost (DALYs). Stroke is predicted to cost the world economy about \$721 billion annually, or 0.66 percent of GDP. The burden (measured regarding the overall quantity of cases) rose substantially between 1990 and 2019 (stroke mortality increased by 43.0%, stroke incidence increased by 102.0%, and the number of disability-adjusted life years (DALYs) increased by 143.0%), with low- and middle-income nations bearing the brunt of the cost (LMIC) (89.0% of DALYs and 86.0% of fatalities) (Peng et al., 2022).

Strokes have been on the decline globally, however younger adults (18–54 years old) are now experiencing a higher rate of strokes. Increased lipid diseases, obesity, diabetes, hypertension, and tobacco use are the likely causes. A stroke is a medical disorder in which the blood arteries leading to the brain get blocked or rupture; as a result, the brain is deprived of the required blood supply, and the tissue starts to deteriorate. Ischemic strokes and hemorrhagic strokes, which are depicted in Figure 2.2, are the two main forms of strokes (Peng et al., 2022). Blood artery obstructions are what lead to an ischemic stroke. Approximately 85% of strokes are this type. When the brain's blood vessels rupture, a hemorrhagic stroke results.

Following a stroke, it's imperative to get medical attention right away. About 1.9 million neurons are lost per minute due to increasing tissue and brain damage (Saver, 2006), which can lead to both upper and lower limb paralysis as well as other cognitive issues (Pennycott et al., 2012). It has been demonstrated that immediate blood flow restoration therapy improves outcomes, which are crucial for returning the patient to normal life with reduced functional loss (Sakuta et al., 2016).

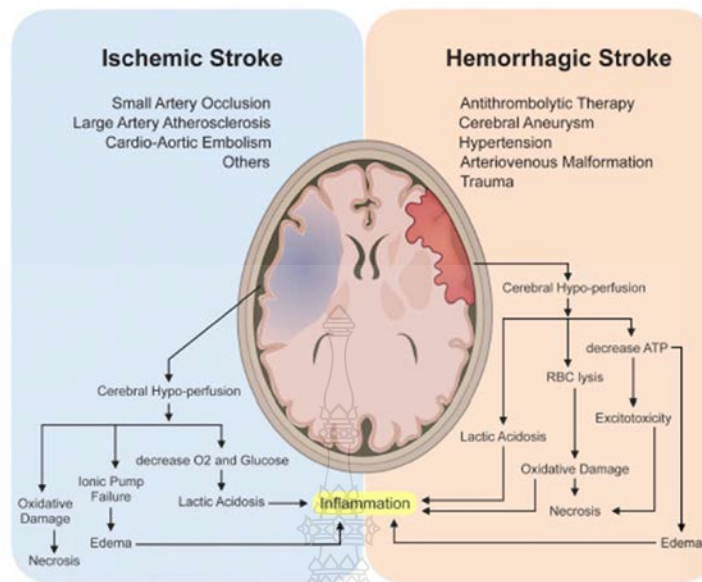


**Figure 2. 2** Ischemic strokes and Hemorrhagic strokes and the effect  
 (SOURCE: Stroke and molecular imaging: a focus on FDG-PET. American Journal of Nuclear Medicine and Molecular Imaging, 2023)

### 2.1.2 Rehabilitation

Rehabilitation is essential for regaining lost functionality and gaining independence to lead a long, fulfilling life; this does not imply that motor and sensory functionality will be fully or partially recovered but rather to lessen other medical side effects, be able to navigate the world and carry out daily activities (ADL), and improve quality of life (QoL). Improved mental and emotional health is a component of quality of life, along with the physical side effects of the injury being lessened. The person's quality of life is enhanced by improving their physical capacity with physical therapy and exercises (Noreau & Shephard, 1995). A person should learn how to physically traverse the world and be motivated to engage with their society as part of a successful recovery (Whalley Hammell, 1995).

As soon as a traumatic injury occurs, the rehabilitation process should begin. It has been demonstrated that early therapy has better long-term outcomes than delayed therapy (Scivoletto et al., 2005)(Piepmeier & Jenkins, 1988), with most of the healing progress occurring within the first year following the injury. Numerous long-term health issues result

from the limitations of the wheelchair. Leg muscles atrophy (Castro et al., 2000), leg bones weaken (Goemaere et al., 1994) without a gravitational force, and pressure sores (Wall & Colley, 2003) are all consequences of spending the entire day on a chair. The abnormalities cause the person to feel a great deal of discomfort and can result in cardiac issues and bone fractures (Giangregorio & McCartney, 2006).

A mechanical orthosis aids the patient in walking and standing up straight while minimizing and reversing some of these negative effects (Palermo et al., 2017). Knee-Ankle-Foot-Orthosis (KAFO) or hip-KAFO (HKAFO) were some of the earliest mechanical systems that helped in ambulatory treatment. These gadgets were ineffective and used a lot of metabolic energy (del-Ama et al., 2012). As technology advanced, these gadgets were made active using robotics, which reduced the demand from the patient. Section 2.2 goes into more detail about these gadgets. A hybrid exoskeleton is a combination of an active exoskeleton and FES (Ha et al., 2012)(Alouane et al., 2019).

Therapy with robotic exoskeletons does not always result in more functional improvements than therapy using standard methods. Robotic therapy has other advantages, though, one of which is that it lightens the therapist's workload. Both the patient and the therapist benefit from the gait and balance training that robotic exoskeletons can provide (Martínez et al., 2018), which is more than a single therapist might be able to do. The therapist's physical workload is reduced because of the patient receiving gait training that follows a precise and repeatable motion, allowing them to devote more time to patients and provide more individualized care.

The advantages of robotic therapy for rehabilitation have been extensively studied and published. It has been utilized for post-stroke and post-SCI rehabilitation. Lower limb exoskeletons have received a lot of attention recently for SCI, with various research being undertaken (Esquenazi et al., 2012)(Zeilig et al., 2012)(S. A. Murray et al., 2015). Similar research was done for stroke recovery, although it's important to note that upper arm exoskeletons have also been studied (Chang & Kim, 2013)(Ho et al., 2011).

The two measurements and tests with robotic lower limb exoskeletons that are most frequently utilized include the 10-meter walk test (10MWT) and the 6-minute walk test (6MWT)(Amatachaya et al., 2014). All measured parameters have seen improvements, according to research. generally increased walking speed, endurance, and distance. The degree of improvement varied from subject to subject and depended on several variables, including the severity of the injury.

### **2.1.3 Functional Ambulation Classification (FAC)**

As shown in Table 2.2, a traditional system for categorizing mobility is the Functional Ambulation Classification (FAC). Establishing a mobility outcome measure that is clinically significant was the main goal of the FAC's development. The creation of a cheap measure that needed little therapist training and administration time but was accurate and dependable was one of the secondary goals. The FAC comprises six categories, between 0 (non-functional ambulation) and 5 (independent)(Jeffrey et al., 2018).

According on how much personal support a participant needs, the FAC classifies them into one of six functional groups, regardless of whether they utilize a mobility aid while walking. According to Holden and colleagues, classifying subjects by functional category or motor ability is more crucial than grouping them according to other gait markers. Their system defines six functional categories. Ineffective ambulation is indicated by a score of 0. People who are significantly and continuously dependent on another person for support and balance are given a score of 1. With a score of 2, it's necessary to use light contact or provide brief physical support; a score of 3 indicates that verbal cues or brief safety aid are necessary. A score of 4 indicates that the person is independent in ambulation on flat terrain, while a score of 5 indicates that the person is independent in ambulation on flat and uneven surfaces, including stairs and inclines. Despite being a generic ambulation test, the FAC's results showed a positive linear correlation along the lines of the 6-minute walk test, step size, and speed of gait. The FAC has been most frequently used to evaluate functional locomotion and track the success of stroke patients' rehabilitation (Chui et al., 2020).

**Table 2. 1** Functional ambulation scale

<b>Score</b>	<b>Category</b>	<b>Interpretation</b>
0	Ambulation do not function	
1	In need of substantial help walking or standing (I level)	need continual manual assistance to support body weight and to help with coordination or balance.
2	Needs regular or constant physical help (II)	needs regular or infrequent gentle touch to aid in balance or coordination.
3	Dependent on supervision	can navigate a level area by themselves, but who still requires one person to be nearby to offer verbal clues or physical safety.
4	Independent level surface only	can move about on a flat area by themselves, but still needs a backup person to offer instructions or provide physical protection.
5	Independent	can move on any surface, even stairs.

#### **2.1.4 Assistive device**

Various products that improve or make it easier to operate or engage in activities are included in the category of assistive devices. While assistive devices are an extension of the body and enable control over the environment, orthotic devices are placed to the body to stabilize and facilitate movement. These technologies could make up for a disability or make an activity easier. They increase independent control of users to manipulate their

surroundings at will. Assistive devices are used in rehabilitation to promote the process of compensation and restoration of function (Hsu et al., 2008).

Many devices are standard and have not changed over several decades because they are ideal in simplicity and effectiveness. Newer devices, such as robotics and computers, are allowing more complex controls over the world around us. Keeping up with new technology as it improves in efficiency and user friendliness is necessary to provide clients with access to devices that best suit their needs. Assistive technology performs one or more tasks (Webster & Murphy, 2009):

- Increase propulsion
- Enhance balance
- Lessen compressive strain on one or both lower limbs
- Send sensory signals to the hand(s).
- Allow the user to move around in small spaces not suitable for a wheelchair and to maintain an upright posture
- Let other people know that the user needs special consideration, such as extra time when crossing the street or a seat on the bus.

Canes, crutches, and walkers are examples of assistive devices, as depicted in Figure 2.3.

Canes, crutches, and walkers help with balance, facilitate walking, lighten the strain on the lower limbs, relay sensory cues, and allow maneuvering in spaces in which a wheelchair is impractical.



**Figure 2.3** (A) Crook-top or C-handle cane (B) aluminum cane that is adjustable (C) Cane with a good grip (D) Adjustable quad cane with a wide base.(E) Hemiwalker. (F) Wooden axillary crutch that can be adjusted. (G) Lofstrand crutch made of adjustable aluminum. (H) Support with the forearms or a platform. (I) either a walker or walkerette. (SOURCE : Atlas of Orthoses and Assistive Devices (5th ed.), Elsevier, 2009)

### 2.1.5 Orthosis

" A piece of equipment that is applied externally and is used to alter the anatomical and functional properties of the musculoskeletal and neuromuscular systems, that is how an orthosis is described. " The art and science of treating patients with orthoses" is how orthotics is defined. " A person who is qualified to design, measure, and fit orthoses after completing a recognized educational or training program and being approved by the relevant national authorities" is the definition of an orthotist."(Hsu et al., 2008).

An orthosis is a wearable device that can be passive or active, has built-in sensors, and can give structure or power to a joint. Robotic orthoses are smart orthoses that have actuators. Numerous books on various orthotic mechanisms have been written because of



research. Every joint in a person has various needs, and each one requires a particular kind of technology to sustain and supply additional power. Knee orthoses and ankle-foot orthoses are two of the topics undergoing the greatest research. categories of orthoses is shown in Table 2.2.

**Table 2. 2** Categories of orthoses

Foot Orthosis (FO)	Finger Orthosis (FO)	Sacroiliac Orthosis (SIO)
Ankle Foot Orthosis (AFO)	Hand Orthosis (HdO)	Lumbosacral Orthosis (LSO)
Knee Orthosis (KO)	Wrist Hand Orthosis (WHO)	Thoracolumbosacral Orthosis (TLSO)
Knee Ankle Foot Orthosis (KAFO)	Wrist Hand Finger Orthosis (WHFO)	Cervical Orthosis (CO)
Hip Orthosis (HpO)	Elbow Orthosis (EO)	Cervicothoracic Orthosis (CTO)
Hip Knee Orthosis (HKO)	Elbow Wrist Hand Orthosis (EWHO)	Cervicothoracolumbosacral orthosis (CTLSO)
Hip Knee Ankle Foot Orthosis (HKAFO)	Shoulder Orthosis (SO)	
	Shoulder Elbow Orthosis (SEO)	
	Shoulder Elbow Wrist Hand orthosis (SEWHO)	

For exoskeletons, the power to the knee and prevention of buckling are provided by a variety of knee orthoses designs. Typically, knee orthoses are built as a clutch or brake system. As shown in Figure 2.4 a running exoskeleton with a clutch spring knee joint was presented by Elliott et al (Elliott et al., 2014). This system activates, based on the gait phase,

and disengages the leaf spring. The system has a mass of 0.710kg and can retain about 190Nm.



**Figure 2. 4** Clutch Spring Knee Exoskeleton for Running  
(SOURCE: Design of a clutch-spring knee exoskeleton for running. Journal of Medical Devices, Transactions of the ASME, 8(3), 2014)

For rehabilitation, Farris et al. developed a brand-new form of brake called Wafer Disc Brakes (Farris et al., 2009). The brake operates in a typically closed condition that is still in place in the event of a power outage, ensuring the user's safety. The stator and rotor discs are positioned alternately over a narrow space in a succession of high-strength wafer stacks that make up the brake. The central shaft is connected to a motor. When it is turned on, a ball screw applied to the discs creates a compressive force. The brake can maintain a static torque of 73Nm with this configuration. The Wrap Spring Clutch/Brake mechanism-based version control method used in the Austin exoskeleton project was naturally performed to manufacture many knee joints.

Ankle-Foot Orthoses (AFO) are devices that either completely restrict the motion of the foot itself or fully actuate the ankle. Most of these models fall into one of two categories: Dynamic, Advanced Ankle Foot Orthoses (DAFO) or Solid Ankle Foot Orthoses (SAFO)(Bai et al., 2012). SAFOs are completely static devices made to keep the user's foot firmly in place (Chern et al., 2013). These usually consist of a single plastic piece. To prevent limiting the foot's full range of motion, DAFO devices, in contrast, are made up of numerous parts that are joined around a single adjustable hinge joint (Bai et al., 2012). DAFO designs can be passive, non-powered objects, electrical parts that are powered actively, or passively powered non-electrical objects (Russell Esposito et al., 2018). The angular position of the ankle throughout the gait cycle can be controlled using both actively and passively driven devices (Bai et al., 2012)(Yoshizawa, 2012)(Chin et al., 2009). Examples of several Powered AFO device types are shown in Figure 2.5. An actively powered device adds heft and cost to the system while providing torque to help with walking.

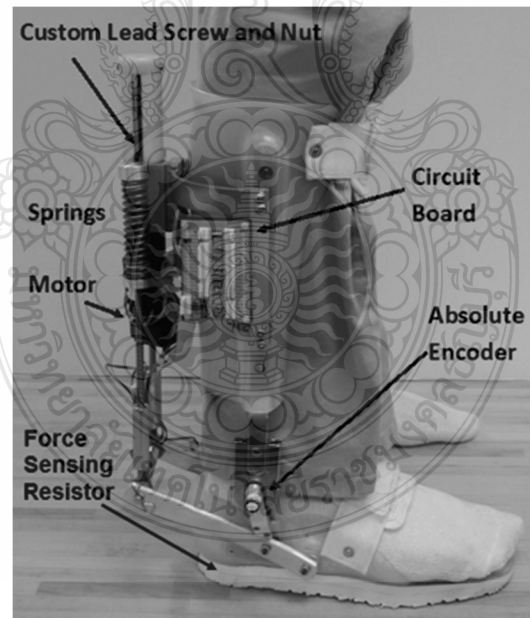


**Figure 2.5** PAFO device  
(SOURCE: Stroke survivors' gait adaptations to a powered ankle-foot orthosis. *Advanced Robotics*, 25(15), 2011)

## 2.2 Gait and Human Anatomy

### 2.2.1 Anatomical Terminology

Anatomical placement serves as the foundation for all subsequent anatomical descriptions. Figure 2.6 illustrates the explanation. The eyes are pointed ahead, the arms are at the side of the body, palms pointing forward, feet and legs are in proximity parallel in the anatomical posture. Three anatomical planes may be defined in this position: the sagittal the transverse plane and plane the coronal plane (Whittle, 2007).

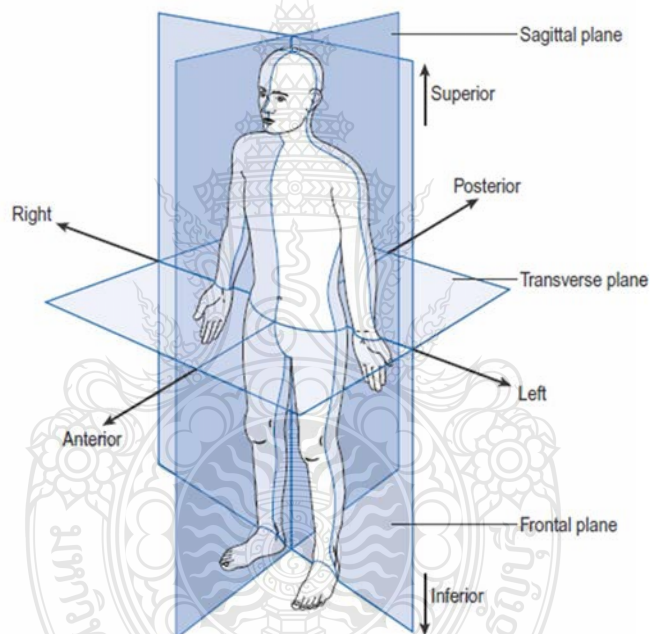


**Figure 2. 6** Three reference planes represent the anatomical position  
(SOURCE: An Introduction to Gait Analysis (4th ed.). Elsevier, 2007)

The body is split in half by the coronal plane: front(anterior) and back(posterior) respectively. The superior (upper) and inferior (lower) sections of the body are divided by the transverse plane. The body's left and right sides are separated by the sagittal plane. The bulk of motions in gait take place in sagittal plane 3. Only one or two of these planes are

available to most joints (Figure 2.7). Abduction and adduction are movements in the coronal plane. Spreading and shutting the legs, for example. Internal and exterior rotations are internal and external rotations in the transverse plane. For instance, turning human head from left to right. Flexion and extension are two types of sagittal plane movements. Plantarflexion refers to the movement of pointing the toes, whereas dorsiflexion refers to the movement of bringing the toes closer to the torso.

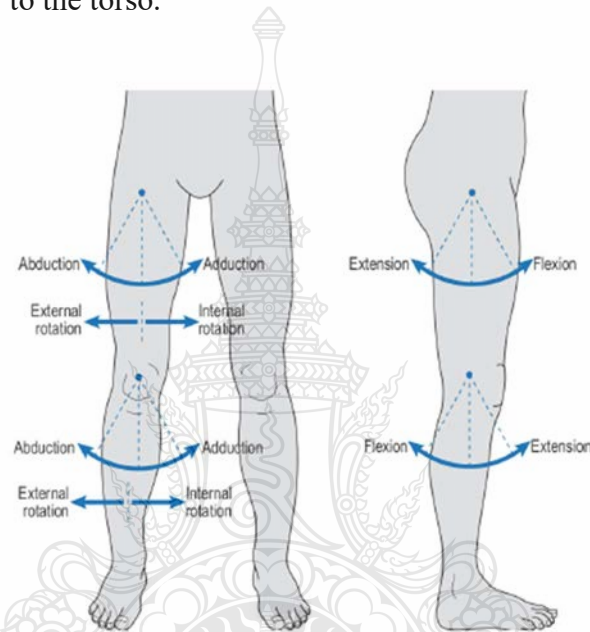


**Figure 2. 7** Knee and hip movements  
(SOURCE: An Introduction to Gait Analysis (4th ed.). Elsevier, 2007)

#### 2.2.4 Gait Analysis

The systematic study of human walking, also known as gait analysis, is performed with the help of experienced observers' eyes and brains, as well as with the assistance of apparatus for recording muscle activity, joint position, and other bodily motions. Gait analysis is a tool that can be used to make precise diagnoses and to devise the most effective treatment strategies for patients who are afflicted with illnesses that impair their ability to walk (Whittle, 2007).

In the past few years, gait analysis has "come of age," and it is now utilized frequently in various facilities to provide the best possible care for certain groups of patients, most notably patients who have cerebral palsy. This is because gait analysis has "come of age" and "matured" during the previous few years. It is intended that this strategy will continue to gain popularity considering the well-documented advantages it offers, and thus more people will be able to profit from the improved therapeutic choices that can be reached through the utilization of gait analysis.

### **2.2.2 Muscles and Bones**

Walking is a full-body exercise that requires the use of all the muscles in the body. When it comes to gait research, the bones and muscles of the pelvis and legs usually get the most attention (Pandy & Andriacchi, 2010)(Butler et al., 2007)(Kumar et al., 2013). The pelvis is a multi-layered bone structure that connects the base of the spine to the femur. On its proximal end, the femur articulates with the pelvis, and on its distal end, it articulates with the tibia and fibula. The 26 bones that make up the foot are joined by the complex ankle joint between the tibia and fibula (Figure 2.8). The movement of the joints is triggered by muscles. The musculoskeletal system is a redundant mechanical system. The same joint can be controlled by several muscles. The three degrees of freedom in the hip, for example, are controlled by 15 muscles (Pandy & Andriacchi, 2010). As a result, multiple combinations of muscle activations may produce the same movement. The iliopsoas and rectus femoris are the primary hip flexion movers. Knee extension is also caused by the rectus femoris and the vastus muscles. The hips are extended by the gluteal muscles and hamstrings. The hamstrings also extend past the knee. The tibialis anterior provides dorsiflexion at the ankle, whereas the gastrocnemius and soleus both cause plantarflexion (Figure 2.9).

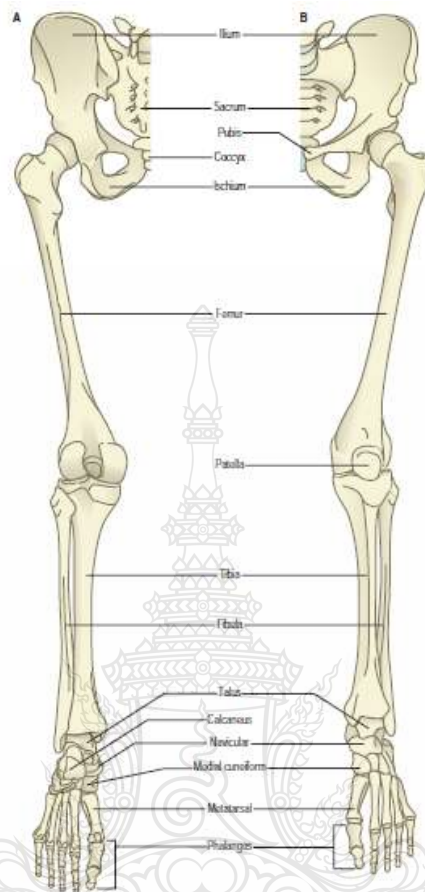


**Figure 2. 8** An overview of the bones of the lower limb  
 (SOURCE: GRAY'S Anatomy : The Anatomical Basis of Clinical Practice (41st ed.).  
 Elsevier, 2016)

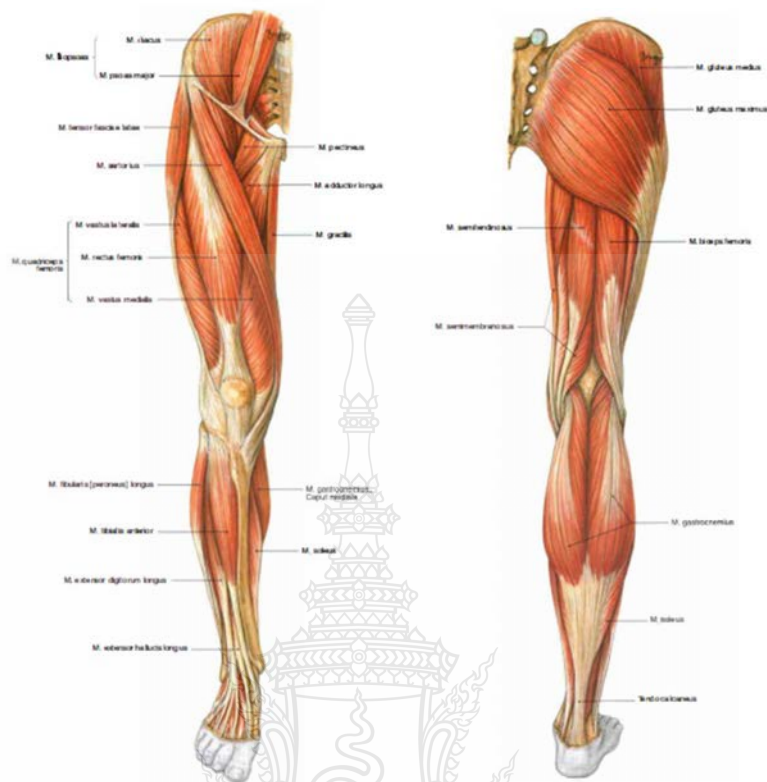


**Figure 2.9** The lower limbs' bones and muscles  
 (SOURCE: Sobotta:Atlas of Human Anatomy, (22th ed., Vol. 2). Elsevier, 2006).

### 2.2.3 Walking cycle

To create a controller capable of recovering walking motion, it is crucial to comprehend how to walk healthfully. Two stages make up a normal walking cycle, swing phase, also known as the short phase, and stance phase, also known as the long phase. The first one deals with the actual stepping, while the second one discusses the time when the foot is on the ground and swinging while supporting the opposing leg. Figure 2.10 illustrates the division of attitude into four sub-phases: loading reaction, mid-stance, terminal stance, and pre-swing (Cifu & Johns, 2021). Each sub-phase's starting positions are as follows: left initial contact, right toe off, right heel off, and left initial contact. Three sections make up the swing phase: the initial swing, the mid-swing, and the final swing. As these stages start, the



right toe is off, both feet are lined up, and the right tibia is upright but not in touch with the ground (Okamoto & Okamoto, 2007).

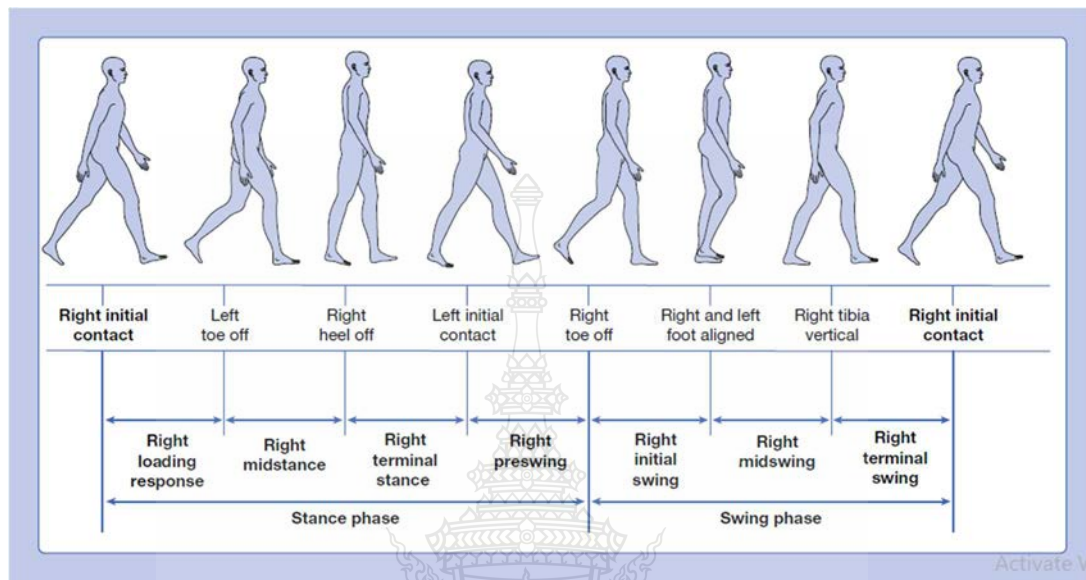


**Figure 2. 10** Phases of gait cycle

(SOURCE: Braddom ' s Physical Medicine and Rehabilitation (6th ed.). Elsevier, 2021)

Six main motions may be seen throughout the walking cycle: dorsiflexion and plantar flexion of the ankle, flexion and extension of knee joint, and flexion and extension of hip. Figure 2.11 depicts the toe and heel locations throughout the walking cycle, as well as knee, hip joints and ankle alignments. When moving at a 5 kph walking pace and 76 cm stride length. Each step taken by one leg during a walking cycle, or 1.1 seconds in total, is average. The swing phase lasts for roughly 40% of the cycle (Bartlett, 2007).

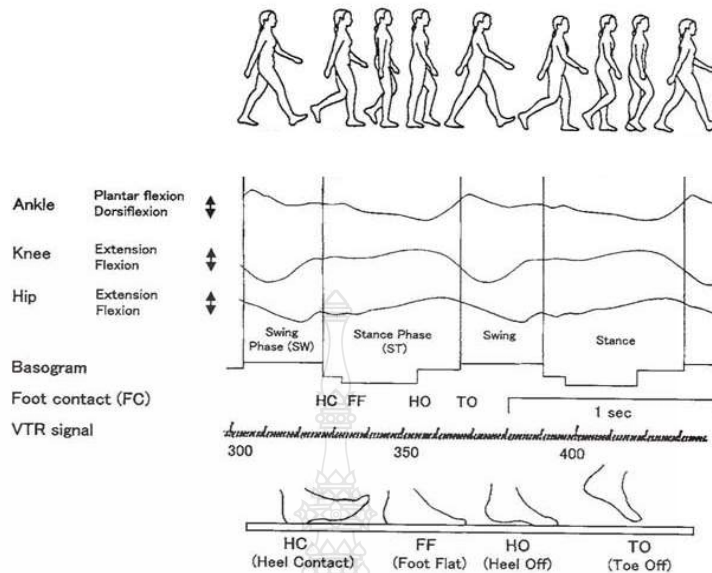


**Figure 2. 11** Normal adult walking joint trajectories  
 (SOURCE: Introduction to sports biomechanics: Analysing human movement patterns (2nd). Routledge., 2007)

The graphs in Figure 2.12 illustrate the angular kinematics throughout the gait cycle. The support phase and the swing phase are shown on the graphs (Hamill et al., 2015).

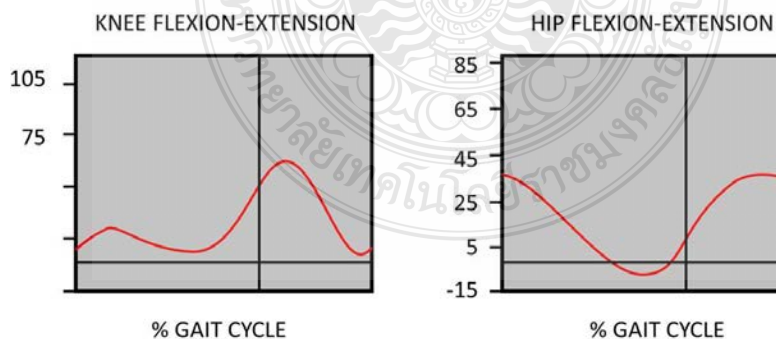


**Figure 2. 12** Graphs of angular kinematics across the gait cycle  
 (SOURCE: Biomechanical Basis of Human Movement (4th ed.). Lippincott Williams & Wilkins, 2015)

## **2.3 Walking rehabilitation**

Stroke illnesses can result in significant knee discomfort, abnormal walking patterns, immobility, and defective lower limbs. Stroke patients must go through gait rehabilitation in order to regain their gait mobility. Patients are forced to move their limb regularly to mimic normal gait patterns as part of the rehabilitation procedure (Singh et al., 2023). A wheeled device called a gait trainer aids in walking for both children and adults. Patients with neurological problems have employed a variety of devices to improve their gait. Some of them are goods that may be purchased, while others have only been developed and used in laboratories (Smania et al., 2018).

### **2.3.1 End Effector Type Walk Trainer**

The patient is attached to the end effector walk trainer at one point, and only that point exerts movement/force on the patient. Any of the instruments that are available include: the LokoHelp (*LokoHelp - Electromechanical Gait Trainer | Woodway, n.d.*), GT II gait trainer (*GT II - Reha-Stim, n.d.*), Haptic Walker (Schmidt et al., 2005), MIT-Skywalker (Artemiadis & Krebs, 2010) and NEUROBike (Monaco et al., 2012). The movement of this device is not compatible with human joints, and certain joint treatments cannot be performed without external restrictions. In addition, the device allows the patient to compensate for movement, which may force him to adapt to an improper gait. Therefore, we will not discuss this type of device.

### **2.3.2 Exoskeleton Type Walk Trainer**

Exoskeleton-style walk trainers are put in parallel and in sync with individual joints, allowing for targeted joint therapy. Individual joints can be given trajectories, pressures, and regulated moments, making these machines a true upgrade over trained human therapists. Advanced features such as immersive training and patient success assessment are also possible. Exoskeleton-like systems have been demonstrated for both treadmill and overground exercise. In terms of gait recovery, these devices currently have limited

capabilities. It also provides advanced features such as interactive training and patient measurement. Introducing exoskeleton equipment for treadmill training and floor training. Wearable exoskeletons (Esquenazi et al., 2012) are lightweight and can move with people. These devices have limited functionality in gait restoration, so they will not be discussed further. Lokomat is the most successful Robot Assisted Gait Trainer (RAGT) equipment (Munawar, 2017). This is a treadmill-based system that can regulate the sagittal plane movement of the knees and hips to keep the legs moving at a regular speed. The optional FreeD module enables active regulation of lateral pelvic movement while leaving other pelvic movements uncontrolled.

The shadow leg system, used in LOPES II (Meuleman, 2015), a treadmill-based exoskeleton, allows for eight complicated degrees of freedom, including hip extension/flexion, hip adduction/abduction, anterior/posterior pelvis, and lateral pelvis. The pelvis may have other degrees of freedom when it is passive, but it cannot control it. Both units concentrate on sagittal plane hip and knee rotation. Because of the irregular gait induced by unnatural pelvic motions, these systems pay careful attention to balance, and compensatory action is ineffective. The Pelvic Assist Manipulator (PAM) can help move the pelvis during treadmill training. During BWSTT treatment, this device uses six pneumatic cylinders to enable 5 degrees of pelvic freedom of movement (sagittal pelvic tilt is passive)(Ichinose et al., 2003). Since PAM does not include hip rotation, synchronizing the natural movement of the pelvis and lower extremities is difficult, necessitating additional control (Aoyagi et al., 2005). To help with pelvic movement, the system of Robotic Gait Rehabilitation (RGR) employs two unique DoF linear actuators on either side of the hip (Pietrusinski et al., 2014).

Since the device only activates vertical movement, it can actively maintain vertical pelvic movement and coronary pelvic tilt, but it can't monitor other pelvic rotations or lateral movement. The Motorized Reoambulator is a commercial rehabilitation system that helps patients to do recovery exercises on the treadmill regularly (Díaz et al., 2011). Abduction, pelvic movement, and pelvic rotation are all restricted by the system. The pelvis cannot shift forward or backward or rotate differently than standing in ALEX (Banala et al., 2008).

### 2.3.3 Walking Rehabilitation and Body Weight Support

Patients often cannot carry their own weight during gait rehabilitation. They often rely on a weight-bearing system (BWS). Clinical trials have demonstrated that transferring a portion of one's body weight to the thoracic spine system improves gait recovery (Barbeau & Visintin, 2003)(Mehrholtz et al., 2017)(Mao et al., 2015). BWS will also help people stay healthy when exercising, keep the balance, and avoid falling. BWS will enhance the patient's lateral balance to restore gait (Frey et al., 2006).

They can be classified into two categories in terms of weight reduction:

- i) static systems,
- ii) systems based on passive counterweights,
- iii) systems based on passive elastic springs, and
- iv) system of active.

Figure 2.13 depicts a diagram of these classes. The first three passive devices are not ideal for gait recovery because they cannot support steady weight while the pelvis moves vertically. The discharge force can be dynamically produced by the functional source system. These systems constantly calculate the intensity of the contact between the patient and the BSW driver, and the control system instructs the control unit to move through the audience based on these measures, even though the patient feels strong. Vertically, nothing changes. These systems have enough bandwidth to have a pleasant weight loss effect while encouraging a natural walk (Hidler et al., 2011).

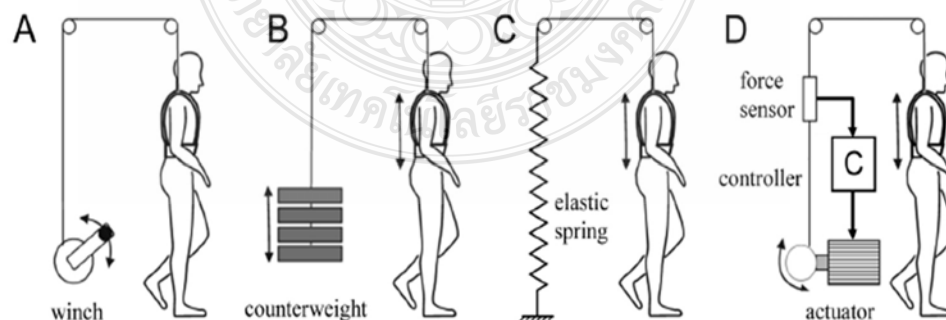


**Figure 2. 13** BWS systems are classified as (a) static and (b) passive counterweight dependent, (c) passive spring based, and (d) active systems  
(SOURCE: IEEE Transactions on Neural Systems and Rehabilitation Engineering,

A BWS system is used in the robot-assisted gait recovery equipment. HapticWalker (Hussein et al., 2009) is an end-effector that releases the patient as he walks using a passive suspension module. The BWS system keeps the CoM in full position in the human body, minimizing foot effect. Another end-effect device is the MIT Skywalker (Susko, 2015), which has a free chest brace to prevent patients from dropping, and the BVS passive spring system, which uses bicycle saddles to relieve patient tension. To obtain the desired weight support, pre-adjust the seat position and move the movable linear controller up and down with a remote control. To control the tension of the dangling cable in walking recovery schemes, the commercial Robomedica Active BWS unit is attached to the patient with a high safety belt (including POGO and PAM)(Aoyagi et al., 2007)(Burgess et al., 2010). The WalkTrainer (Stauffer et al., 2009) is a fast-recovery device with an active BWS system. It comprises a pre-tensioned control spring whose length can be modified based on the current sensor's calculated value. A tag is used to link the device to the patient. For an active customized seat belt fixed to the patient's pelvis, the KineAssist (Patton et al., 2007) gait training and balancing system supports the weight. The NaTure Gait(Luu et al., 2014) is a hybrid system that controls the movement of the feet and the sensation of walking on the ground using end effects technology (stirrups) and a movable foundation. In the pelvic module, there is an active BWS. ZeroG (Hidler et al., 2011) is an elevated BWS system that can fly over elevated tracks and employ force control techniques based on SEA (Series Elastic Actuator). With the aid of SEA, the device effectively monitors and manages the cable tension that is linked to the patient's sling.

#### **2.4 Medical Robot and Exoskeleton**

In the definition of a robot in the Dictionary of Robotics and Artificial Intelligence (Rosenberg, 1986), it is stated that a robot is:

- (1) a machine that has sensors for detecting input signals or ambient circumstances, but also has guidance or reaction mechanisms that can do calculations, sensing, and other tasks, as well as stored programs for subsequent actions; for instance, a machine that runs itself.
- (2) are machines that may be directed to carry out specific motions or manipulations.

Although they continue to capture the public's imagination, general-purpose, anthropomorphic (human-appearing) robots have not yet found many applications in medicine. The rehabilitation robots that have been created are specialized machines that are different in size, shape, and complexity from humans and have little to no similarity to them. They are similar in that their sophistication is rising along with their capabilities and programmability.

Wearable robotics that provides assistive torques and more robust structural support is known as a powered exoskeleton. The Human-Machine-Interface (HMI) used in this instance is an example. With the widespread adoption of robotic technology, there has been a rise in interest in exoskeleton research (Aliman et al., 2017)(B. Chen et al., 2016)(Mertz, 2012)(Gardner et al., 2017). Smart systems can now monitor movement, give feedback, and construct smooth trajectories by using more precise models thanks to robotics technology (Pons, 2010). Exoskeletons can be made lighter and more powerful thanks to the advancements in accurate sensors and compact actuators. This does, however, also make developing and constructing an exoskeleton more complex technologically. Exoskeletons have evolved over time from basic mechanical devices to wearable robots with independent intention detection and action. Treadmill-based systems and overground-based systems are two of the most frequently employed exoskeleton kinds nowadays (Díaz et al., 2011).

Unfortunately, accessible public areas are not always created with a wheelchair user in mind. In daily life, we climb stairs, reach for objects on high shelves, squeeze through small doors, and converse with individuals at eye level (Welage & Liu, 2011). All these ADLs provide difficulties for a wheelchair-bound individual. People can walk upright and lead more "normal" lives with the use of exoskeletons. Exoskeletons can be utilized to assist people with ADLs in the real world or to assist persons with health conditions in a rehabilitation setting.

### 2.4.1 Medical Robot

The term "medical robot" refers to any robot designed for use in the medical field that is either implanted in or otherwise physically connected to a human patient (Baratini et al., 2019). Medical robots are under regulatory control in many nations and regions as medical devices.

#### 2.4.1.1 History

Robots have several uses in the manufacturing sector. These days, robots are increasingly used in the medical field. Table 2.3 details the development of medical robots over time (Kasina et al., 2017).

**Table 2. 3** Historical evolution of robots in medical industry

YEAR	ROBOT	APPLICATION
1983		Laparoscopic surgery
1985	PUMA-560	Brain biopsy
1988	PROBOT	Prostate surgery
1989	AESOP endoscopic positioner	Endoscopic surgery
1991	MINERVA	Brain biopsy
1992	ROBODOC	Hip replacement surgery
1993		Prosthetic knee
1997	CASPAR	Knee and Hip surgery
1998	ZBUS surgical system	Endoscopic surgery



1999	ZBUS	Fallopian tubes operation
2000	DaVinci Surgical system	Laparoscopic surgery
2001	SOCRATES	Telepresence
2009	Freehand robot	Endoscopic holding
2011	Telelap AI.F-X	Laparoscopy
2011	ReWalk Rehabilitation	
2013	IGAR	Breast cancer detection
2014	INDIGO powered leg	Lower Body Exoskeleton
2014		Leg rehabilitation
2014	Luke Skywalker	Muscle contraction detection in prosthetics
2014	Three-armed robot	Surgery in womb
2014	LITTLE MOE	Disinfection
2014	SCALLOP	
2015	Magnetic rod	Spine surgery
2015	Nanometer drones	Drug delivery
2015	Robotic arm	Handling soft organ
2015	Rani robotic pill	Inject medication
2015	Origami robot	Remove cancer cell and unclog arteries
2015	Nanodrone	Deliver drugs to heal

### 2.4.1.2 Classification of Medical Robots

There are three main classes of medical robots (Boubaker, 2020).

- (1) robotic instruments for surgery, diagnosis, and drug delivery (medical devices)
- (2) robots for rehabilitation and robots that are wearable (assistive robots), and
- (3) prosthetics

Medical robots have a few benefits over traditional medical equipment. They are more cost-effective, and they are helping physicians to improve their precision and expertise while reducing human exhaustion. Classification of medical robots is shown in Figure 2.14, furthermore robotic assistive technologies are shown in Figure 2.15.

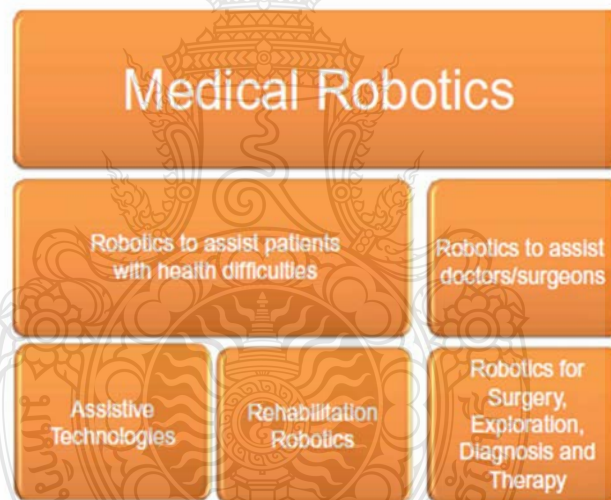
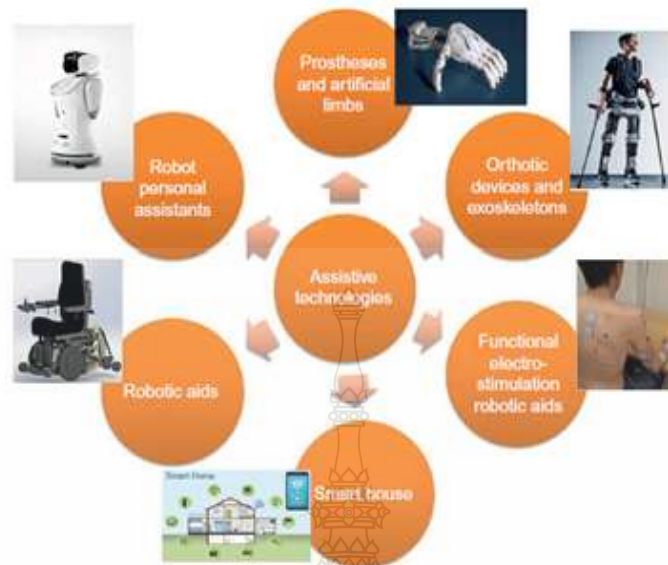


Figure 2. 14 Medical robotics systems based on classification



<https://www.limm.fr/UEE07/presentations/lecturers/Dombre.pdf>

**Figure 2. 15** Robotic assistive technologies

Assistive technologies can be categorized into:

- (1) Prostheses and artificial limbs
- (2) Orthotic devices and exoskeletons
- (3) Functional electro-stimulation robotic aids
- (4) Smart houses
- (5) Robotic aids
- (6) Robot personal assistants

Orthotic devices and exoskeletons can be utilized as a gait trainer. The different types of gait training robots are discussed in this chapter, as well as the related devices that have been mentioned in the literature.

### 2.4.1.3 Rehabilitation robot

Robotics for assistance and aid (also known as assistive robotics), on the one hand, and robotics for therapy and recovery (also known as therapeutic robotics), on the other, are the two primary subfields that make up the area of rehabilitation robotics. Patients who are unable to move their bodies due to age, accident, or stroke can move their bodies and do their daily duties more easily and quickly with the assistance of systems and equipment known collectively as assistive robotics. However, these robots do not necessarily engage the patient's neural system to regain control of the damaged or paretic limb, nor do they provide any feedback regarding the patient's progress in healing.

On the other hand, therapeutic systems contribute, even if only in a little way, to the process of supporting patients' recoveries. These systems are often utilised for a predefined period during which the patient's performance on a certain function is the primary area of focus. The patient receives treatment more quickly, and the therapist or carers experience less fatigue and strain as a result. Therapeutic robots can work in tandem with other medical professionals or with the patient themselves. An outline of rehabilitation robots is shown in Figure 2.16.

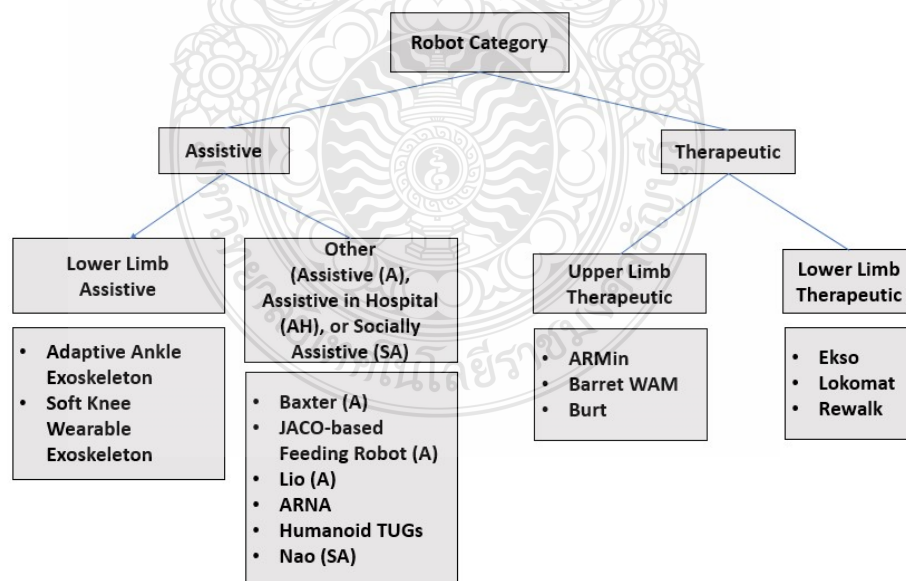


**Figure 2. 16** An outline of rehabilitation robots in recent literature (SOURCE: Medical and Healthcare Robotic, Academic Press., 2022)

## **2.4.2 Exoskeleton**

The term "exoskeleton" comes from the Greek word "exo," which means "outside." It refers to a skeleton that is found on the exterior of the body. When it comes to biological systems, the provision of protection or support typically takes the shape of a rigid exterior structure, such as the case or exoskeleton of an insect. An exoskeleton is a structure that a human wears and controls; it gives additional strength, or, in teleoperation, it allows for monitoring the movements and the forces that a human creates to utilize those to operate a robot. In robotics, an exoskeleton is a structure that a human wears and controls (Matarić, 2008).

### **2.4.2.1 History of Exoskeleton**

#### **EARLY EXOSKELETONS**

Robert Seymour's satirical article "Locomotion—Walking by Steam, Riding by Steam, Flying by Steam" published in London around the end of the 1820s contains what is believed to be the earliest illustration of what is essentially an exoskeleton. But it wasn't until 1890, some decades later, that Nicholas Yagn of St. Petersburg, Russia, received a patent for his invention known as a "Apparatus for Facilitating Walking" (Rosen & Ferguson, 2020). The apparatus, which was worn on the legs, was made to help with sprinting, jumping, and walking. Two models were either propelled by a massive bow spring or a compressed gas bag. The distinction between passive and active (powered) exoskeletons has never been made before, thanks to this patent. Although these early exoskeleton concepts were never put into production, their basic structure and design served as a model for powered armour and easily operated suits that amplified a user's force output that appeared in science fiction.

#### **1961-1973 PERIOD**

Over the course of the Man-Amplifier Project, powered exoskeletons started to materialise in the actual world, a 1961–1962 Cornell Aeronautical Labs programme that investigated technology that boosted human potential. The first medical powered exoskeleton was developed by researchers working at the Mihailo Pupin Institute on the campus of the

University of Belgrade in what is now the country of Serbia in the former Yugoslavia. The Institute conducted in-depth analysis of exoskeletons for the upper and lower bodies for patients with paralysis, and in 1972, several units were available for usage and testing in rehabilitation centers.

### **2001-2008 PERIOD**

Several research centers and startup businesses took the lead in rekindling interest in exoskeleton development at the turn of the century. The Hybrid Assistive Limb (HAL)(Siciliano et al., 2010) series was introduced in Japan by Cyberdyne under the direction of Yoshiyuki Sankai. Under the name Hexar Systems, Chang-Soo Han (Bock & Linner, 2016) developed a portfolio in Korea that included more than twenty exoskeletons. Ekso Bionics was cofounded by Homayoon Kazerooni (Popovic, 2019). Former University of Utah professor Stephen Jacobsen converted Sarcos Robotics (Meadows, 2011) into a company that developed exoskeletons for "disabled people" rather than just "disabled technology." Hocoma started selling the Lokomat robotic treadmill in Europe in the meantime. Considering all these businesses, 1000 devices have been sold overall in each one.

### **2015-2018 AND BEYOND**

Exoskeleton manufacturing companies have grown significantly in recent years. In East Asia, an aging population and labor force are the main drivers of the increase in interest. Exoskeletons created to avoid workplace accidents or in rehabilitation sessions. Fewer physical therapists are required are seen in North America as viable solutions to the country's fast rising healthcare expenses. However, the European Union is home to more kinematics and biomechatronics facilities that have only recently begun producing commercial devices. The Harvard soft exoskeleton (Tong, 2018) and the Keeogo (from B-Temia Inc., Quebec, Canada)(Scataglini et al., 2022), which have both military and medicinal purposes, are two examples of devices that might sometimes fit into more than one category.

### 2.4.2.2 Classifications of exoskeleton

Exoskeletons are mechanical structures that resemble the skeletal structure of a limb or body part (Tiboni et al., 2022)(Rupal et al., 2017). Figure 2.17 depicts the results of a comprehensive assessment of exoskeletons conducted to date(Rupal et al., 2017) which divided them into twocategories based on uses and needs: medical and non-medical systems.

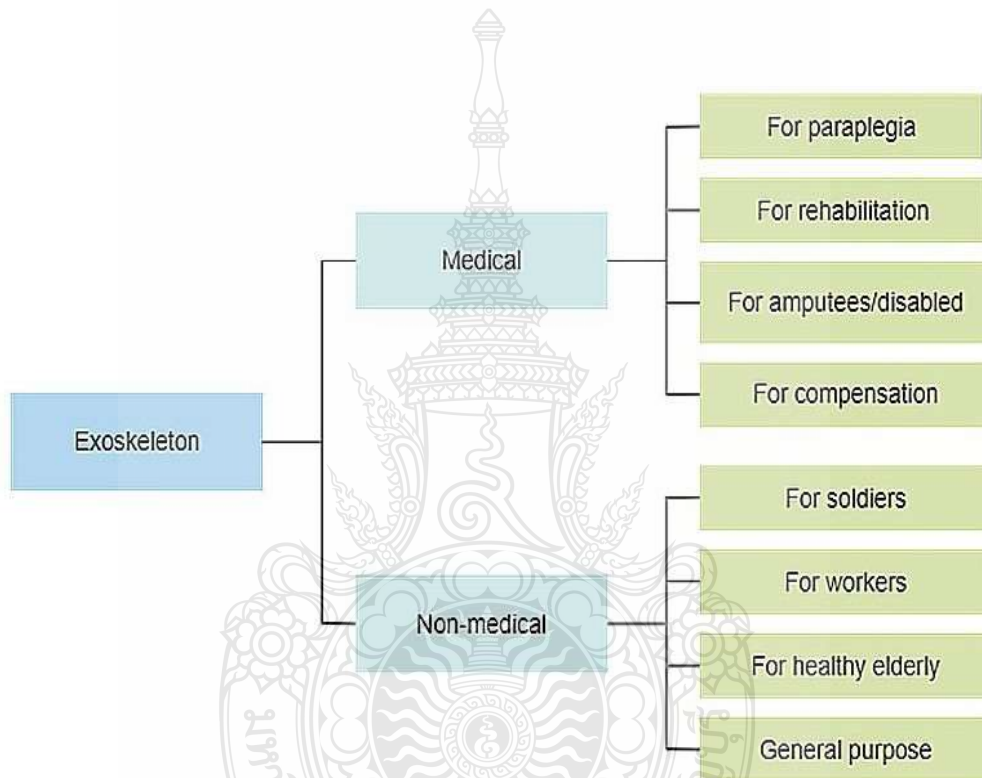


**Figure 2. 17** Classification of exoskeletons according to their usage

#### **Non-Medical Exoskeletons**

The development of exoskeletons designed to increase strength and reduce metabolic costs should be acknowledged, even if rehabilitation exoskeletons are the focus of this research. The use of these exoskeletons extends from military to industrial and construction

tasks that can improve the user's upper and lower bodies. Exoskeletons have also been investigated for various uses, both soft and rigid.

According to Walsh et al. in (Walsh et al., 2006), a lower-limb exoskeleton that was only half engaged could transfer 90% of the weights to the ground. Additionally, (Wehner et al., 2013) and (Alan T. Asbeck, 2013) investigated and developed a soft lower limb exoskeleton that was effective in reducing the metabolic cost of a gait cycle. Figure 2.18a depicts a soft exoskeleton of the lower limb. Actuated Bowden wires that are attached to the joints in these suits pull the joints through the gait cycle. Soft suits are advantageous since they are lightweight, but they do not provide structural support.

As was already mentioned, the BLEEX was developed for military use to enhance the amount of weight a person could carry and lower metabolic expenses. DARPA11 provided most of the funding for the study. Unlike the suite that Walsh provided, this suit has strong powered actuators and is a stiff system. The BLEEX military lower limb exoskeleton is depicted in Figure 2.18b.

Both upper and lower body systems are present in the HAL-5 exoskeleton. The HAL-5 exoskeleton is depicted in Figure 2.18c. Originally intended to be used with the upper body as a lower-body assistive device, this system enables users to boost their capacity for carrying loads. To determine the user's intent and offer support, this system employs electromyogram (EMG) signals(Casolo et al., 2008).



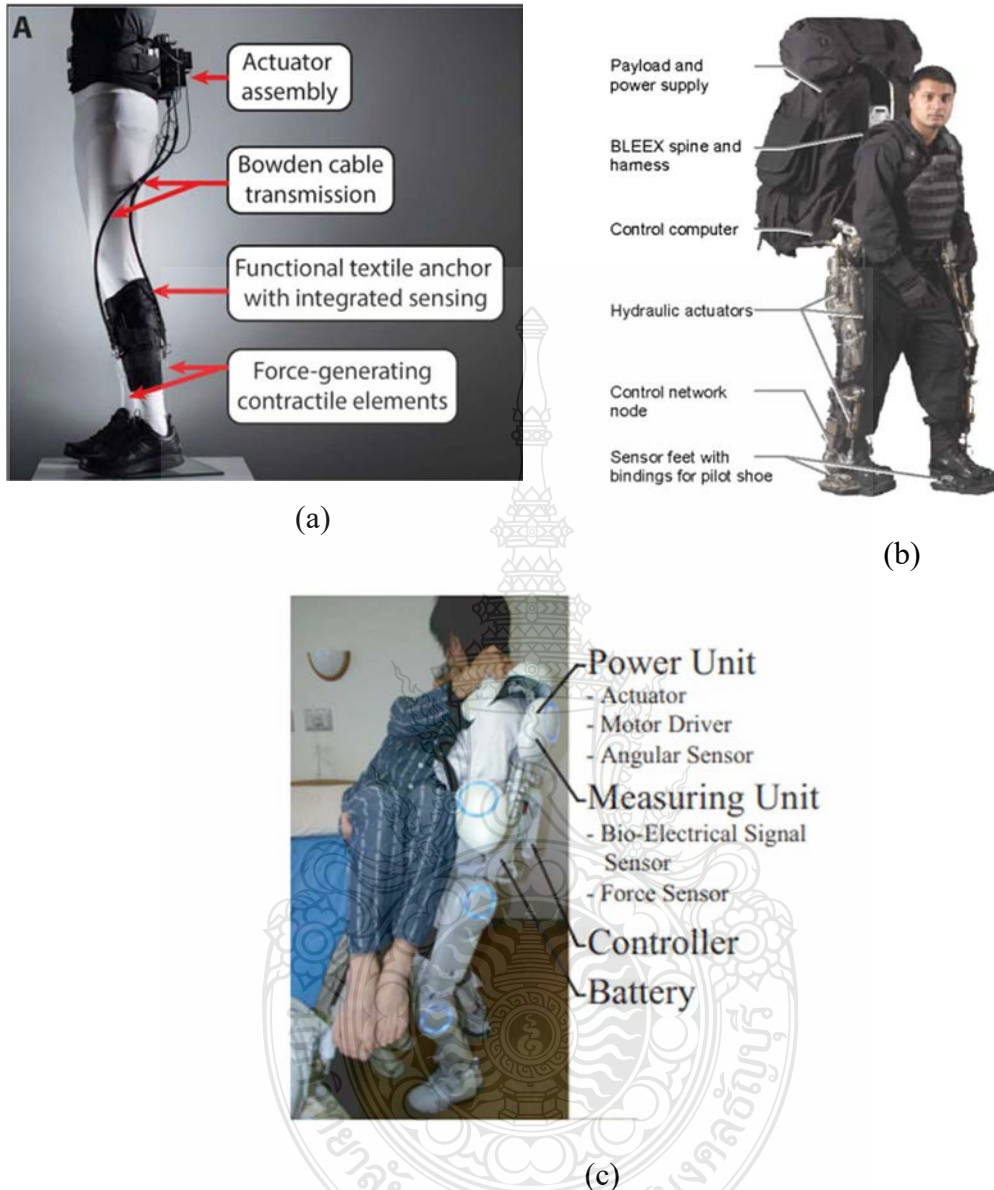


**Figure 2. 18** Enactment Exoskeletons : (a) Walsh soft exosuit (Awad et al., 2020)  
 (b) BLEEX (Flores, 2020), (c) HAL-5

(SOURCE: (a) Walking faster and farther with a soft robotic exosuit: Implications for post-stroke gait assistance and rehabilitation. IEEE Open Journal of Engineering in Medicine and Biology, December 2019, (b and c) Bathing care assistance with robot suit HAL. 2009 IEEE International Conference on Robotics and Biomimetics, ROBIO 2009)

### **2.4.2.3 Overground Exoskeletons**

Over the past few years, several overground walking exoskeletons have been researched and built and have become very popular. Since the person is not attached to a constricting gantry and all the power and control is on-board, they allow the therapist more freedom to design protocols and represent a more accurate representation of real-world ambulation (Martínez et al., 2018). As a result, the person is free to move around the environment. The system must be capable of supporting both the person and itself. This independence enables travel on stairs and difficult terrain. These systems have the drawbacks of being constrained by on-board power and having to consider the mass of the system. Maxon motors<sup>2</sup> and Harmonic gearboxes<sup>3</sup> are common design elements in most overground exoskeletons (Bortole et al., 2015)(Aliman et al., 2017). To support their upper bodies when walking, patients frequently use crutches. These systems typically cost around \$100,000 (Rupal et al., 2017).

#### **2.4.2.3.1 BLEEX**

One of the earliest exoskeletons available is the BLEEX. The BLEEX exoskeleton's most recent iteration is depicted in Figure 2.19. This exoskeleton differs significantly from the previous exoskeletons addressed in this study in that it is made of BLEEX. In order to enable soldiers to carry a significant amount of mass, design was required for military applications since it enhances the load that people can carry. Although it almost resembles human joints, it is not completely anthropomorphic. It has ball joints for the hip and ankle and pure rotation joints for the knee (Garcia et al., 2011). The joint design of the BLEEX exoskeleton was based on clinical gait studies. They were able to determine the joint ranges and torques for the exoskeleton by researching the motion of the human gait (A. Zoss et al., 2005)(A. B. Zoss et al., 2006). was developed to help soldiers to carry heavy loads (A. Zoss et al., 2005). About \$100,000 was spent on this system (B. Chen et al., 2016).



**Figure 2. 19** BLEEX Exoskeleton  
(SOURCE: <https://bleex.me.berkeley.edu/wp-content/uploads/2021/04/Berkeley-Exo-HR-scaled.jpg>)

#### 2.4.2.3.2 ReWalk

The Rewalk is a well-known rehabilitation exoskeleton available today. Figure 2.20 shows an image of the Rewalk. A closed-loop control system that uses the sensor suite to drive the motors, powered hip and knee joints, passive ankle joints covered by shoe ankle supports, and back support for the body's trunk are all features of the exoskeleton. The exoskeleton has various modes that include sitting, standing, walking, going up or down stairs, and standing and sitting simultaneously. Using tilt sensors in the trunk, the user is free to operate the exoskeleton. The controller is instructed to begin walking by stooping forward (Zeilig et al., 2012) Both inpatient therapy and at-home use are currently made of it. The benefits of the ReWalk for rehabilitation are supported by several well-researched studies (Esquenazi et al., 2012). The exoskeleton costs roughly \$70,000 (Bhatnagar et al., 2017).



**Figure 2. 20** ReWalk Exoskeleton

(SOURCE: Mobility Skills With Exoskeletal-Assisted Walking in Persons With SCI: Results From a Three Center Randomized Clinical Trial. *Frontiers in Robotics and AI*, 7(August), 2020)

#### **2.4.2.3.3 Indego**

Another well-liked exoskeleton for rehabilitation is the Vanderbilt model (Gasser et al., 2017). The Indego exoskeleton 7 is the system's commercial variant; it is depicted in Figure 2.21 This exoskeleton was initially created for stroke recovery, where one side of the patient has greater strength and function than the other. The added torque from the exoskeleton helps the wearer walk and restore strength.

The Indego exoskeleton has recently been utilized to treat SCI patients. A hybrid concept by Goldfarb et al combines FES and the motorized exoskeleton; this incorporates the user's muscles into the system and increases the torque with the motors (Ha et al., 2012).



**Figure 2. 21** Indego Exoskeleton

**(SOURCE:** An assistive robotic device that can synchronize to the pelvic motion during human gait training. Proceedings of the 2005 IEEE 9th International Conference on Rehabilitation Robotics, 2005)

#### **2.4.2.3.4 Hybrid Assistive Leg (HAL-3)**

As shown in Figure 2.22, the HAL-3 exoskeleton was developed at the University of Tsukuba in Japan, which also manufactured it (Sankai, 2010). This exoskeleton's primary purpose is to provide assistance in the process of rehabilitating people who have disabilities. HAL has a 160-minute continuous operating time (Venketasubramanian et al., 2017). The HAL-3 fits into the category of high-power exoskeletons because of the HAL-3's extensive usage of sensors, which has a high-power need. With a 100 V AC supply, HAL increases

joint torques at the ankle, hip, and knee. Power assist apparel A nurse may care for a crippled person using this exoskeleton.



**Figure 2. 22** HAL-3 exoskeleton

(SOURCE: <https://zhuanlan.zhihu.com/p/115288318>)

The exoskeletons mentioned above all have similar design elements. They have motorized knees and hips that can produce additional and helper torque, and the stiff frames offer support. Exoskeletons can be disassembled into several sections that can be altered to fit the wearer. These exoskeletons are tough to obtain and difficult to afford because to their exorbitant cost. Additionally, they are not transparent enough for controller research. Like

how it is challenging to test a controller without an exoskeleton, it is challenging to justify the purchase of an exoskeleton without a tested controller. An exoskeleton can be expensive and time-consuming to design and construct.

Maxon motors can cost more than \$350 each, while harmonic gearboxes can cost more than \$1000 each. These components also have lengthy lead times for internal evaluations. Including manufacturing time, the material cost for a building might range from hundreds to thousands of dollars. Additionally, the electrical components that drive the motors and enable real-time control must be specially built; this, too, necessitates expertise in every branch of engineering, from mechanical to computer science. It would also require a lot of effort to develop, produce, construct, and test the exoskeleton, which would divert attention from designing new controls. Figure 2.23 shows characteristics of Robots for Lower Limb Rehabilitation. Meanwhile Singla et. al. classifies exoskeletons as shown in Figure 2.24.

<b>Product :</b> Lokomat	<b>Product :</b> ReWalk	<b>Product :</b> HAL	<b>Product :</b> Ekso GT	<b>Product :</b> Rex	<b>Product :</b> Indego
<b>Company :</b> Hocoma	<b>Company :</b> ReWalk Robotics	<b>Company :</b> Cyberdine	<b>Company :</b> Ekso bionics	<b>Company :</b> Rex bionic	<b>Company :</b> Indego
<b>DoF :</b> 2 activos	<b>DoF :</b> 2 active	<b>DoF :</b> 2 activos	<b>DoF :</b> 2 active, 1 passive	<b>DoF :</b> 5 active	<b>DoF :</b> 2 active
<b>Approval :</b> CE, FDA	<b>Approval :</b> CE, FDA	<b>Approval :</b> CE	<b>Approval :</b> CE, FDA	<b>Approval :</b> CE	<b>Approval :</b> CE, FDA
<b>TRL :</b> 9	<b>TRL :</b> 9	<b>TRL :</b> 9	<b>TRL :</b> 9	<b>TRL :</b> 9	<b>TRL :</b> 9
<b>Pathologies :</b> <ul style="list-style-type: none"> <li>• Stroke</li> <li>• Traumatic brain injuries</li> <li>• Paraplegia</li> <li>• Cerebral Palsy</li> <li>• Multiple Sclerosis</li> <li>• Parkinson's</li> <li>• Endoprosthesis</li> <li>• Degenerative Diseases</li> <li>• Muscular Atrophy in the Column</li> </ul>	<b>Pathologies :</b> <ul style="list-style-type: none"> <li>• Stroke</li> <li>• Paralysis</li> <li>• Brain injuries</li> <li>• Spinal cord injuries</li> </ul>	<b>Pathologies :</b> <ul style="list-style-type: none"> <li>• Stroke</li> <li>• Cerebral palsy</li> <li>• Nervous or muscular disorders</li> <li>• Spinal cord injury</li> </ul>	<b>Pathologies :</b> <ul style="list-style-type: none"> <li>• Stroke</li> <li>• Spinal cord injury</li> <li>• Paralysis</li> <li>• Gait disorders</li> </ul>	<b>Pathologies :</b> <ul style="list-style-type: none"> <li>• Stroke</li> <li>• Spinal Cord Injuries</li> <li>• Muscular Dystrophy</li> <li>• Multiple Sclerosis</li> <li>• Postpolio Syndrome</li> </ul>	<b>Pathologies :</b> <ul style="list-style-type: none"> <li>• Spinal cord injuries</li> <li>• Gait rehabilitation</li> </ul>

**Figure 2. 23** Characteristics of Robots for Lower Limb Rehabilitation

(SOURCE: Robotics for Rehabilitation: A State of the Art, In Exoskeleton Robots for Rehabilitation and Healthcare Devices. Springer, 2020)

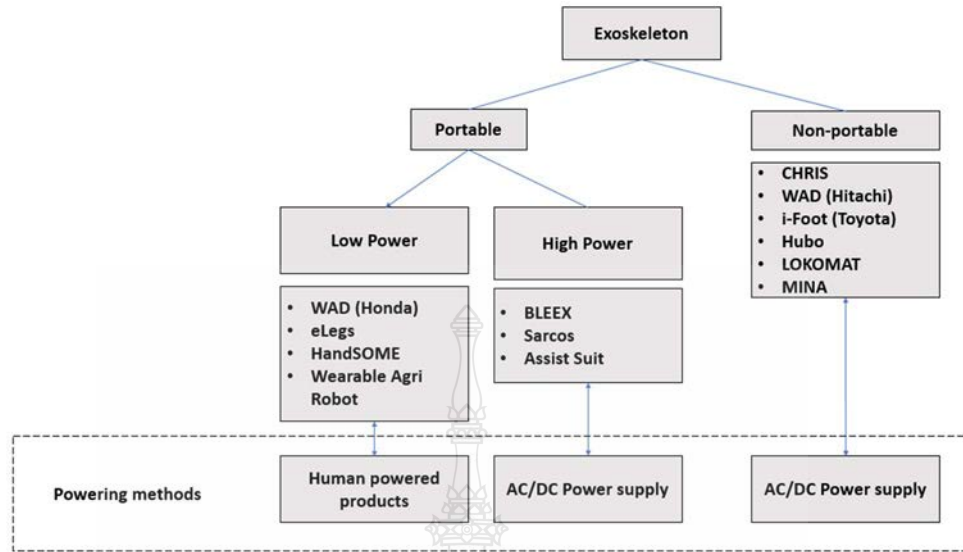


**Figure 2. 24** Classification of exoskeletons

#### 2.4.2.4 Upper Limb Exoskeletons

It is crucial to emphasize that several robotic systems have been created for upper limb rehabilitation, even though it isn't the paper's primary focus. Since lower limb exoskeletons also require the provision of assistive force to maintain a gait motion, these systems are primarily designed for repeated motion with assistive forces (Rehmat et al., 2018).

Products with a TRL 9 rating that are currently on the market include ArmeoPower, the InMotion ARM, the KINARM Lab, and the ReoGo. Although the ALEx and ORTE exoskeletons have not yet received authorization to be put on the market, their level of development, or TRL (7/8), already makes it possible to distinguish them from prototypes that are still being investigated.

Three devices are utilized in the "Armeo Therapy Concept" by the Swiss business Hocoma at various stages of the patient's rehabilitation. As the only device with actuators, the ArmeoPower can be used to treat a range of disorders where the functionality of the arm



is impaired, such as stroke, orthopedic or neurological illnesses, accidents, etc. (Nef & Riener, 2005).

ArmeoPower is depicted in Fig. 2.25 (a), and it has six active degrees of freedom (DoF) that cover 85% of a healthy arm's 3D workspace. It allows for the shoulder's adduction and abduction, flexion and extension, external and internal rotation, as well as extension and flexion of the elbow, wrist, and forearm. In individuals with multiple sclerosis, as well as stroke studies on the usage of this device have been conducted (Calabrò et al., 2017)(Klamroth-Marganska et al., 2014), reporting their success.

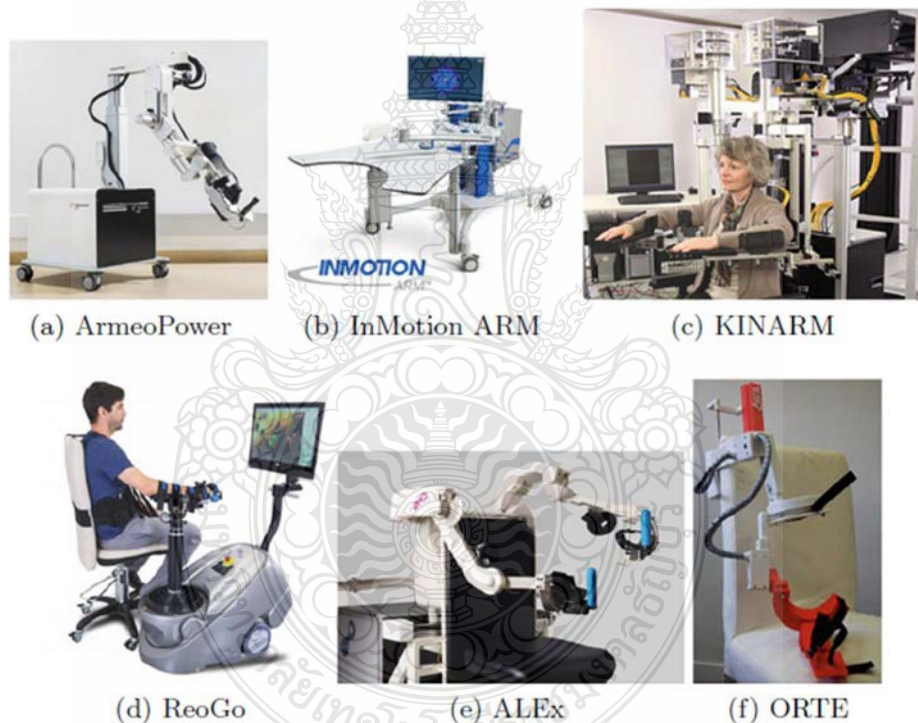


**Figure 2. 25** Main Upper Limb Exoskeleton Robots Companies. **a** Hocoma, **b** Bionik, **c** BKINTechnologies, **d** Motorika, Medical, **e** Werable Robotics, **f** AURA Robotics

(SOURCE: Robotics for Rehabilitation: A State of the Art, In Exoskeleton Robots for Rehabilitation and Healthcare Devices. Springer, 2020)

The MIT-Manus, sometimes known as the InMotion ARM, was created at the Massachusetts Institute of Technology (MIT), and today sold by Bionik (Lo & Xie, 2012), was one of the very first exoskeletons designed specifically for the purpose of aiding in the rehabilitation of the upper limbs. The flexion/extension of the elbow and the internal/external rotation of the shoulder are the active movements covered by the 2D rehabilitation that may be carried out with this device, as shown in Fig. 2.25 (b). It has a passive movement for rehabilitation called shoulder protraction/retraction. The InMotion ARM can be used to treat a several illnesses, such as multiple sclerosis, cerebral palsy, Parkinson's disease, and stroke. Children and adults alike can use the 2D rehabilitation tool known as the Kinarm Lab (Fig. 2.25 (c)). For the purposes of study, the developer gives the option of either renting it or purchasing it. One of its key characteristics is the ability to gather precise information regarding the effects of a brain disorder or damage on the patient's motor, sensory, and cognitive capabilities(Scott, 1999)(Ball et al., 2007).

The ReoGo gadget, shown in Fig. 2.25 (d), was created to treat a variety of neurological disorders as well as dysfunctions following surgery or caused by orthopedic difficulties. It has two active degrees of freedom and one passive degree that enable 3D rehabilitative and horizontal shoulder abduction/adduction movements as well as elbow and shoulder flexion/extension. Studies on stroke victims have been conducted, and the device's functionality has also been examined (Takahashi et al., 2016)(Bovolenta et al., 2009)(Bovolenta et al., 2011).

The Wearable Robotics firm (Italian company) created the Arm Lightweight Exoskeleton (ALEX). They develop robotic aids for physical therapy to help patients regain their strength and mobility. The company's themedical business, Kinetek, oversees developing ALEX.

A total of 4 active and 2 passive degrees of freedom (DoF) are present in ALEX. Flexo-extension, adduction/abduction, external/internal rotation, and extension-flexion of the elbow are among the motions that are engaged and detected. The wrist's flexo-extension and the forearm's pronosupination make up the passive DoF (Pirondini et al., 2016)(Auvray & Duriez, 2014).

One of ALEX's unique features is the shoulder's rotation mechanism, which the business patents and enables the alignment of the human arm with the joint axis. It has absolute angular position sensors, on the motor shafts are four incremental optical encoders, and on the device's, back are four regulated brushless motors. The motors and joints are connected by a system of cables for the transmission of torque. The device comes in two forms, one for unilateral therapy and the other for bilateral therapy. Figure 2.26 shows characteristics of Robots for Upper Limb Rehabilitation.

<b>Product :</b> ArmeoPower	<b>Product :</b> InMotion ARM	<b>Product :</b> KINARM lab	<b>Product :</b> ReoGo	<b>Product :</b> ALEX	<b>Product :</b> ORTE
<b>Company :</b> Hocoma	<b>Company :</b> Bionik	<b>Company :</b> BKINT Technologies	<b>Company :</b> Motorika Medical	<b>Company :</b> Motorika Medical	<b>Company :</b> Aura innovative robotics
<b>DoF :</b> 6 active	<b>DoF :</b> 2 active, 1 passive	<b>DoF :</b> 2 passive	<b>DoF :</b> 2 active, 1 passive	<b>DoF :</b> 2 active, 1 passive	<b>DoF :</b> 6 active
<b>Approval :</b> CE, FDA	<b>Approval :</b> CE, FDA	<b>Approval :</b> Pending	<b>Approval :</b> CE, FDA	<b>Approval :</b> Pending	<b>Approval :</b> Pending
<b>TRL :</b> 9	<b>TRL :</b> 9	<b>TRL :</b> 9	<b>TRL :</b> 9	<b>TRL :</b> 8/9	<b>TRL :</b> 7
<b>Pathologies :</b>	<b>Pathologies :</b>	<b>Pathologies :</b>	<b>Pathologies :</b>	<b>Pathologies :</b>	<b>Pathologies :</b>
<ul style="list-style-type: none"> <li>• Stroke,</li> <li>• Multiple sclerosis,</li> <li>• Cerebral palsy</li> <li>• Parkinson</li> <li>• Neuropathies</li> <li>• Neurological or orthopedic disorders</li> <li>• Musculoskeletal or cerebral lesions</li> </ul>	<ul style="list-style-type: none"> <li>• Stroke</li> <li>• Parkinson</li> <li>• Multiple sclerosis</li> <li>• Cerebral palsy</li> <li>• Spinal cord injury</li> </ul>	<ul style="list-style-type: none"> <li>• Stroke</li> <li>• Autism,</li> <li>• Paralysis</li> <li>• Brain injuries</li> </ul>	<ul style="list-style-type: none"> <li>• Stroke</li> <li>• Spinal cord injury</li> <li>• Neurological disorders</li> <li>• Musculoskeletal injuries</li> </ul>	<ul style="list-style-type: none"> <li>• Stroke</li> <li>• Neurological or orthopedic disorders</li> <li>• Musculoskeletal injuries</li> </ul>	<ul style="list-style-type: none"> <li>• Stroke</li> <li>• multiple sclerosis</li> <li>• neurological or orthopedic disorders</li> <li>• musculoskeletal injuries</li> </ul>

**Figure 2. 26** Characteristics of Robots for Upper Limb Rehabilitation

(SOURCE: Robotics for Rehabilitation: A State of the Art, In Exoskeleton Robots for Rehabilitation and Healthcare Devices, Springer, 2020)

As shown in Figure 2.27, the MIT-Manus (Krebs et al., 2004) was one of the first robots to be created. Due to its two degrees of freedom, this robot can move in a horizontal plane without being affected by gravity. A visual feedback system encourages patient participation in the therapeutic process. To assist the user with movement, the robot also offers assistive torque.



**Figure 2. 27** MIT-MANUS

(SOURCE: ZeroG: Overground gait and balance training system. Journal of Rehabilitation Research and Development, 48(4), 2005)

A seven DoF robotic arm called the UL-EXO7 is also available, and Figure 2.28 depicts it. It offers assistive forces and a full range of motion. A similar interactive game is played by this robot, the MIT-Manus. Patient outcomes from the initial trial have been demonstrated to be functional.

The T-WREX is a different rehab arm exoskeleton. The T-WREX has the advantage of large non-linear forces with low onboard bulk because it is pneumatically powered (Sanchez et al., 2005) in contrast to some of the other systems. A favorable rehabilitation outcome for this approach has also been demonstrated (Housman et al., 2007). Table 2.4 shows the classifications of upper-limb exoskeletons according to actuation and kinematic.



**Figure 2. 28** UL-EXO7

(SOURCE: A systematic review of bilateral upper limb training devices for poststroke rehabilitation. Stroke Research and Treatment, June 2014)

**Table 2. 4** Classifications of upper-limb exoskeletons according to actuation and kinematic

Exoskeleton	Actuation solution	Control	Anatomical districts	Number DOFs
L-Exos	Tendon drive	Impedance control	Shoulder and elbow	4
Exo-UL7	Cable-driven, tendon, and pulley	Impedance control	Shoulder, elbow, and wrist	7
Masia et al.	Soft exoskeleton with sheathed tendons	Friction compensation	Elbow and shoulder	1
MGAXOS	Gear drive	Force closed-loop control	Shoulder-elbow	4
ABLE	Ball screws and cable	Impedance control	Shoulder-elbow-wrist	7
Rehab-Exos	Gear drive	Closed-loop interaction joint control	Shoulder-elbow	4

Armin III	Gear drive		Impedance control	Shoulder-elbow-wrist	7
T-WREX	Passive exoskeleton		Spring passive	Shoulder-elbow-wrist	5
Pneu-WREX	Pneumatic		Nonlinear force control	Shoulder-elbow	4
BONES	Pneumatic		Nonlinear force control	Shoulder-elbow	4
Salford exoskeletons	Artificial pneumatic muscle		Force closed-loop control	Shoulder-elbow	7
Sarcos	Hydraulic		Admittance control	Shoulder-elbow	7
NEUROExos	Variable-impedance actuation		Torque control	Elbow	1

(SOURCE: Robotics for Rehabilitation: A State of the Art, In Exoskeleton Robots for Rehabilitation and Healthcare Devices. Springer, 2020)

#### 2.4.2.5 Actuator for Exoskeleton

The action that is created by the controller is transferred to functional movement by the actuator, which is typically coupled to the exoskeleton frame. The actuator's primary role is to perform this function. There are some technological decisions to be made when building robotic exoskeletons, one of which is the actuation principle (Colombo & Sanguineti, 2018). An overview map of the various technical options available to the design is shown in Figure 2.29. First and foremost, selecting an actuation concept is a crucial decision. Figure 2.30 and Figure 2.31 respectively show the principles of exoskeleton actuation and list of existing rehabilitation robots along with their actuator type (Hasan & Dhingra, 2020). While Table 2.5 compares actuator types implemented on the robot assisted gait trainer (X. Zhang et al., 2017).

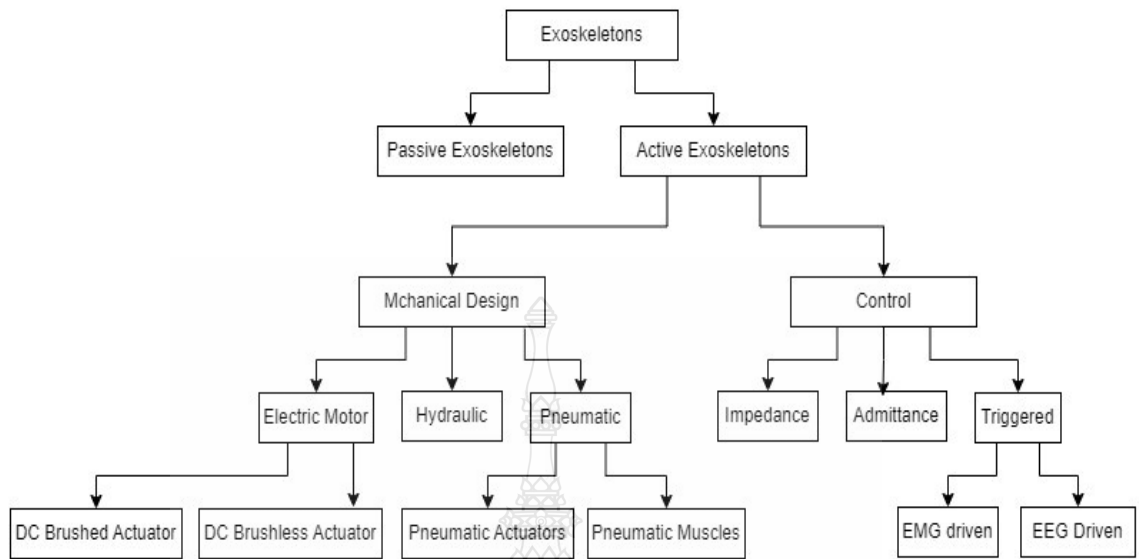


**Figure 2. 29** Exoskeleton concept solutions for actuation and power.

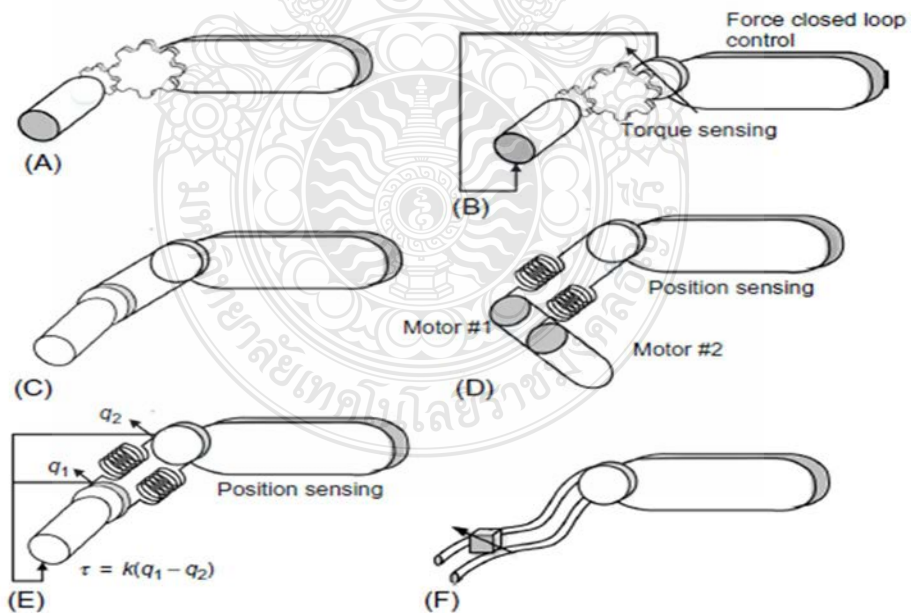


**Figure 2. 30** Exoskeleton actuation principles. (A) Transmission of gears. (B) A joint with a force sensor. Tendon transmission (C). Variable impedance (D). Elastic in the (E) sequence. Hydraulic-pneumatic (F).

(SOURCE: Rehabilitation Robotics : Technology and Application. Elsevier, 2018)

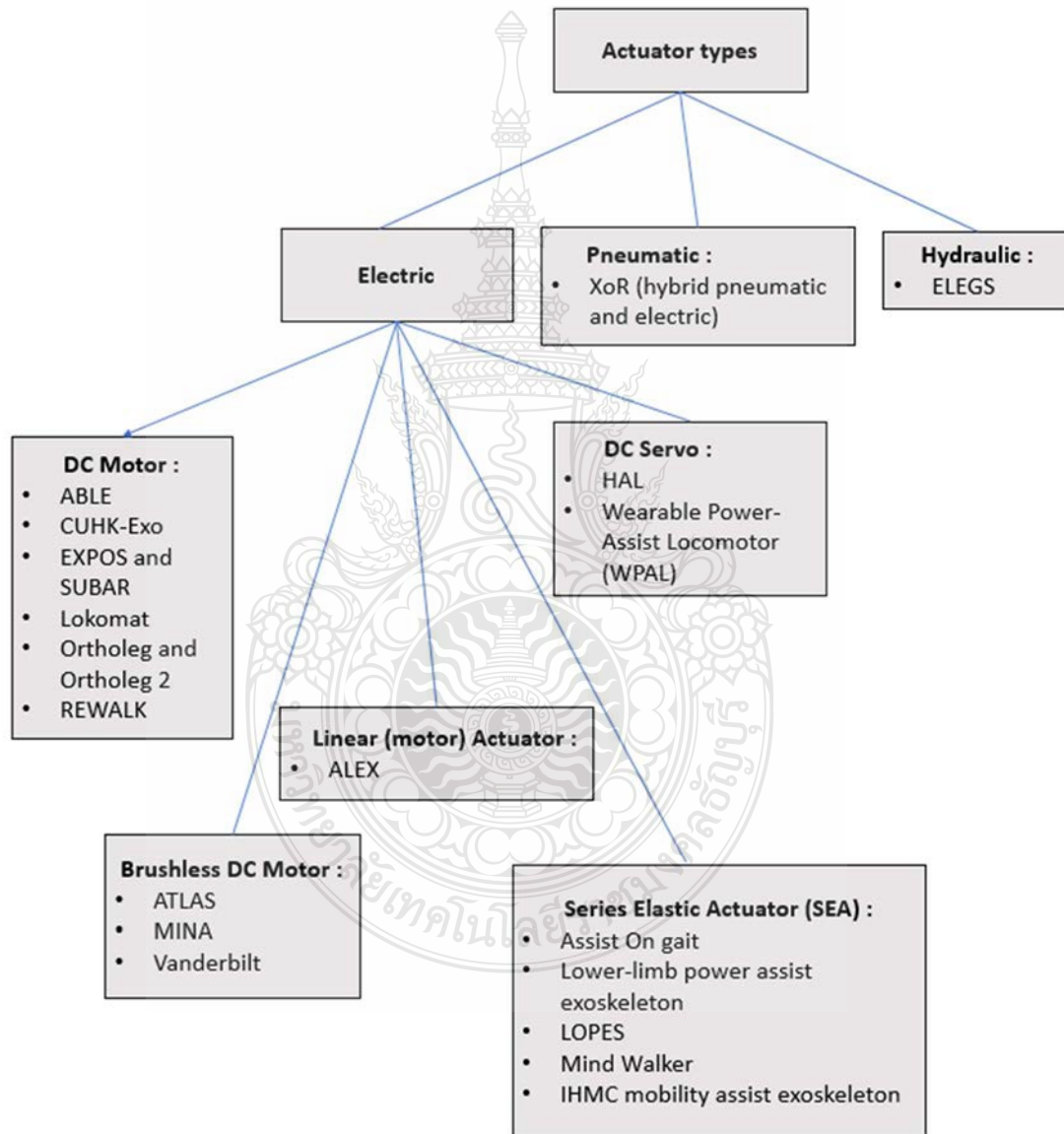


**Figure 2. 31** List of existing rehabilitation robot with their actuator type



**Table 2. 5** Comparison of actuator types implemented on robot assisted gait trainer

Actuator types	Advantages	Disadvantages
Hydraulic	<ul style="list-style-type: none"> <li>• Simple structure</li> <li>• Reliable</li> <li>• Stable</li> <li>• Low inertia</li> <li>• Protection of overload</li> </ul>	<ul style="list-style-type: none"> <li>• Easily to leak</li> <li>• Noisy</li> <li>• Slow</li> <li>• Low efficiency</li> <li>• Sensitive to temperature change</li> <li>• temperature change</li> <li>• Oil can be compressed</li> </ul>
Pneumatic	<ul style="list-style-type: none"> <li>• Low cost</li> <li>• Simple structure</li> <li>• Nonpolluting</li> <li>• Work in high temperature</li> <li>• High flow rate</li> </ul>	<ul style="list-style-type: none"> <li>• Non suitable for high temperature system</li> <li>• Difficult to precise control</li> <li>• Speed can change because of load</li> <li>• Can be compressed and leak</li> </ul>
Electric motor	<ul style="list-style-type: none"> <li>• Simple structure</li> <li>• Has advantages of convenient energy transfer</li> <li>• Nonpolluting</li> <li>• Easily to be controlled</li> </ul>	<ul style="list-style-type: none"> <li>• Large volume</li> <li>• Heavy</li> <li>• Influenced by external load</li> </ul>
Serial Elastic Actuator	<ul style="list-style-type: none"> <li>• High security</li> <li>• High control precision</li> <li>• Reduce of friction losses</li> </ul>	<ul style="list-style-type: none"> <li>• Complicated structure</li> <li>• High power</li> <li>• Large volume</li> <li>• Heavy</li> </ul>

#### 2.4.2.6 Powering for exoskeletons

Based on mobility, exoskeletons can be classified as either portable or nonportable. Due to its ability to allow its wearer to move freely wherever they like, the portable category is also known as mobile exoskeletons. In contrast, the mobility of non-portable exoskeletons is constrained by their high-power needs, which necessitate the usage of direct power sources. As a result, these exoskeletons are connected to the power source by wires, which restricts their workspace. Table 2.6 lists the most popular exoskeletons, their power source, and how they are powered. Below are some instances from both categories:

**Table 2. 6** Powering source and methods of various exoskeletons

Exoskeleton model	Developer	Power source
BLEEX	DARPA.	Rechargeable Li-ion battery
Power effector	MMSE project team	Direct power supply
Walking assist device	Honda	Rechargeable lithium-ion battery
Hybrid assistive limb	University of Tsukuba, Japan	AC100V Charged battery
Power assist suit for nursing car	Kanagawa Institute of Technology	NiMH batteries
HRP-2promet	Kawada Industries	Ni- IH Battery DC 48V,18Ah
HRP-1S	Honda	Ni-Zn battery
KHR-3(HUBO)	KAIST	300W NiMh battery

(SOURCE: Lower-limb exoskeletons: Research trends and regulatory guidelines in medical and non-medical applications. *International Journal of Advanced Robotic Systems*, 14(6), 2017)

#### 2.3.2.7 Portable Exoskeletons

Lower Extremity Exoskeleton of Berkeley (BLEEX) Exoskeletons for Human Performance Augmentation (EHPA), a DARPA program, produced this exoskeleton as one of its results. It carries a battery that serves as a power source for the actuators at various joints. Seven degrees of freedom (DOFs) are present in BLEEX, with three DOFs at the hip

joint, one at the knee, and three at the ankle. High DOFs result in BLEEX's high power consumption. Hydraulic actuators, different electronics, and control systems use about 1.3 kW of power (A. Zoss et al., 2005). It belongs to the class of powerful portable exoskeletons that use rechargeable batteries and may be charged by an AC power source. A full-body exoskeleton known as Sarcos has also been created by the DARPA program, as depicted in Fig. 2b. Sarcos has rotating hydraulic actuators as opposed to BLEEX's linear hydraulic actuators. Compared to BLEEX, this exoskeleton performs noticeably better (Huo et al., 2016). With a weight of about 70 kg, the wearer of this exoskeleton can walk at a pace of 1.6 m/s.

### 2.4.3 Robot assisted walk trainers





As with active and passive solutions, robots used for gait recovery can be split into two groups (Ceccarelli et al., 2014). The motion that robotic devices for gait recovery add to the patient's body may also be graded. According to the definition "Exoskeletons are active anthropomorphic mechanical device that is 'used' by an operator and suits tightly to his or her body and operates in compliance with movements of the operator's movements"(Federici & Scherer, 2018). Table 2.7 shows comparison of these devices (Morone et al., 2017). These are some of the commercial robots assisted walk trainers:

**Table 2. 7** Commercial robot assisted walk trainers

Developer	Product
Argo Medical Technology (Israel)	ReWalk
Hocoma (Switzerland)	Lokomat
Reha Technology AG (Switzerland)	G-EO
RehaStim (Germany)	Gait Trainer
Rex Bionics (New Zealand)	REX

Tibion Bionic Technology (USA)	Bionic Leg
University of California Berkeley (USA)	eLEGS

The end-effector robot G-EO System is made by Rehab Technology AG in Switzerland. It simulates symmetrical foot trajectory in gait by just moving the stationary feet on a moving support. The treadmill-based exoskeleton robot Lokomat (produced by Hocoma AG, Switzerland) employs predetermined trajectories to check hip and knee joints(Yeung & Tong, 2018). Figure 2.32 shows different approaches to robotic gait trainers.

Robotic devices (examples)	“Static” (training in place)	“Dynamic”
Exoskeletons	Lokomat 	Rewalk 
End effectors	Gait Trainer 	i-Walker 

**Figure 2. 32** Different approaches to robotic gait trainers  
(SOURCE: Robot-assisted gait training for stroke patients: Current state of the art and perspectives of robotics. In Neuropsychiatric Disease and Treatment, Vol. 13, 2017)

### 2.4.3.1 Characteristics of robot-assisted therapy

A robot-assisted therapy system's mechanical architecture should follow a common principle:

- (i) simple
- (ii) easy to control
- (iii) lightweight

A variety of robots for lower limb rehabilitation have been created recently. There are two types of these robots, as previously stated: exoskeleton and end-effector robots (J. fan Zhang et al., 2010). Exoskeleton robots include Lokomat (Duschau-Wicke et al., 2010), BLEEX(Kazerooni et al., 2006), and LOPES(Veneman et al., 2007)(Asseldonk et al., 2007), while end-effector robots include Rutgers Ankle(Girone et al., 2001) and Haptic Walker(Hesse et al., 2003). Exoskeleton robots are classified as treadmill-based machines (Lokomat, LokoHELP(Freivogel & Schmalohr, 2008), LOPES, ALEX(Banala et al., 2005)(Banala et al., 2008) or orthosis-based robots based (AAFO(Blaya & Herr, 2004), KAFO(Sawicki & Ferris, 2009), HAL(Paper & Sankai, 2014), BLEEX (A. B. Zoss et al., 2006)(Schmidt et al., 2007) on their mechanisms and recovery concepts, whereas end-effector robots are classified as footplate-based (Gait Trainer GT1)(*GT II - Reha-Stim*, n.d.), Haptic Walker(Hesse et al., 2003), G-EO-Systems(Hesse et al., 2016) or platform-based (Rutgers Ankle(Girone et al., 2001), ARBOT(Saglia et al., 2009b)(Saglia et al., 2013), Parallel Ankle robots(Tsoi et al., 2009)(Xie & Jamwal, 2011). The features of recent therapy robots are summarized in Figure 2.33 and Table 2.4.

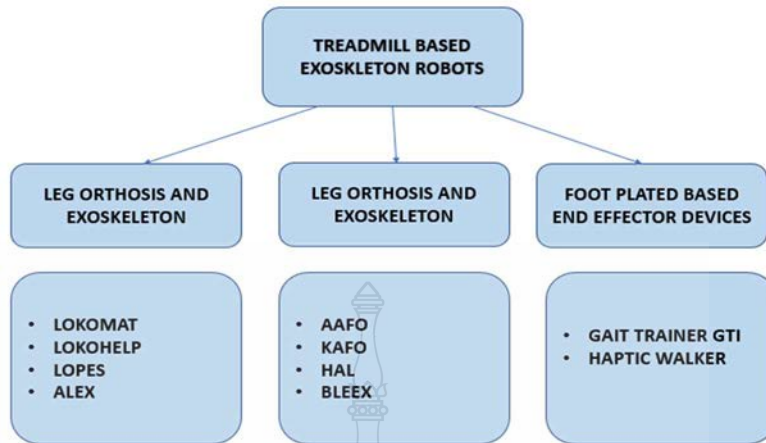


**Figure 2. 33** Most recent lower-limb therapy robots and their category



**Table 2. 8** Actuated DOF and characteristics of the most recent lower limb therapy robots

<b>Device</b>	<b>Company/ Institution</b>	<b>Country</b>	<b>Degree of Freedom</b>	<b>Characteristic</b>
Lokomat	Hocoma	Switzerland	2 DoF (leg)	<ul style="list-style-type: none"> <li>• Treadmill walking</li> <li>• Body weight support</li> <li>• Powered knee and hip support</li> </ul>
LokoHELP	Woodway & LokoHELP Group	Germany	2 DoF	<ul style="list-style-type: none"> <li>• Walking with levers on treadmill</li> <li>• Possible to use a treadmill with a weight support device.</li> <li>• Allows patients to track treadmill movement using levers</li> </ul>
LOPES	University of Twente	Netherlands	3 rotational DoF (each leg)	<ul style="list-style-type: none"> <li>• For walking on a treadmill</li> <li>• Each leg containing actuated rotational joints</li> <li>• Two joints at the one joint at the knee</li> <li>• When walking on a treadmill, can move parallel to the legs.</li> </ul>
ALEX	University of Delaware	USA	7 DoF	<ul style="list-style-type: none"> <li>• For leg rotations and translations</li> <li>• An electric leg orthosis</li> <li>• Actuators in the knee and hip joints</li> <li>• Help the patient use a treadmill by assisting them.</li> </ul>

AAFO	Massachusetts Institute of Technology	USA	2 DoF (ankle joints)	<ul style="list-style-type: none"> <li>• An active ankle-foot orthosis that activates using SEA</li> <li>• An ankle joint was made to fit. Enables unrestricted sagittal plane movements</li> </ul>
KAFO	University of Michigan	USA	Free motion DOFs in sagittal plane for ankle and knee	<ul style="list-style-type: none"> <li>• A foot, ankle, and knee orthosis</li> <li>• To power ankle and knee motions, six artificial pneumatic muscles are linked to the orthosis.</li> </ul>
HAL	Tsukuba University & Cyberdyne	Japan		<ul style="list-style-type: none"> <li>• Full-body exoskeleton for the torso, limbs, and legs</li> <li>• A full-body exoskeleton for assistance during rehabilitation and heavy lifting</li> <li>• To map the intention of patients, EMG signals are used.</li> </ul>
BLEEX	University of California	USA	7 DoFs of each leg in hip, knee, and ankle joints	<ul style="list-style-type: none"> <li>• A set of wearing robotic legs</li> <li>• Created to improve the wearer's capabilities</li> <li>• Supply power to support heavy loads</li> </ul>



Gait Trainer GTI	Reha-Stim	Germany	Two footplates for foot/leg movement	<ul style="list-style-type: none"> <li>• Footplates are in place for the patient's feet.</li> <li>• Controlled movements are used to replicate the action of the feet during stance and swing.</li> </ul>
Haptic Walker	Charite University Hospital	Germany	Arbitrary movement DoFs for two feet	<ul style="list-style-type: none"> <li>• Different gait patterns and walking speeds can be simulated.</li> <li>• Each footplate has a force/torque sensor.</li> </ul>
G-EO-Systems	Reha Technology AG	Switzerland	Two footplates for walking and climbing DOFs	<ul style="list-style-type: none"> <li>• A footplate that may be flexibly programmed on an end-effector gait robot.</li> <li>• Controllable to simulate walking and stair climbing</li> </ul>
Rutgers Ankle	Rutgers University	USA	6 DoFs for ankle and foot based on a Stewart platform	<ul style="list-style-type: none"> <li>• Delivers 6 DoFs of resistive pressures to the ankle of patients using VR</li> <li>• Upgraded to a dual platform for the purpose of gait rehabilitation</li> </ul>
ARBOT	Instituto Italiano di Tecnologia	Italy	2 ankle DoFs in plantar/dorsi flexion, inversion/eversion	<ul style="list-style-type: none"> <li>• An ankle rehabilitation parallel robot with the patient's foot fastened to the moving platform</li> <li>• Specifically designed linear actuator</li> </ul>

Parallel Ankle robot	The University of Auckland	New Zealand	3 ankle DoFs	<ul style="list-style-type: none"> <li>• 4 links</li> <li>• Driven by dc motors</li> <li>• A parallel robot with four axes powered by pneumatic muscles</li> <li>• Made for the rehabilitation of the ankle</li> </ul>
----------------------	----------------------------	-------------	--------------	--

(SOURCE: Recent developments and challenges of lower extremity exoskeletons. Journal of Orthopaedic Translation, 5, 26–37)

#### 2.4.3.2 Control modes

Passive mode and active training/control modes are described in Figures 2.34, 2.35, and Table 2.9. The ability to keep the patient moving in varying modes, based on their respective states of healing, is crucial to the success of robot-assisted rehabilitation and therapy (Akdoğan & Adli, 2011). The prescribed training regimen should be assessed by the physiotherapist's experience as well as the severity of the topic's disability. According to the study (Saglia et al., 2009a) the recovery phase can be split into preliminary, intermediate, and advanced stages. At these steps, the patient eventually regains freedom of motion and power in the wounded leg or joint. As a result, at various stages of rehabilitation, the patient should engage in both passive and active activities. Passive care, for example, should be provided in the recovery's early phases to assist patients in following predetermined routes to increase strength and minimize muscle atrophy (Jamwal et al., 2014). Active mode should be used after a training period, once the patient has developed a certain level of strength, to encourage patients to activate the robot help through their own active efforts.

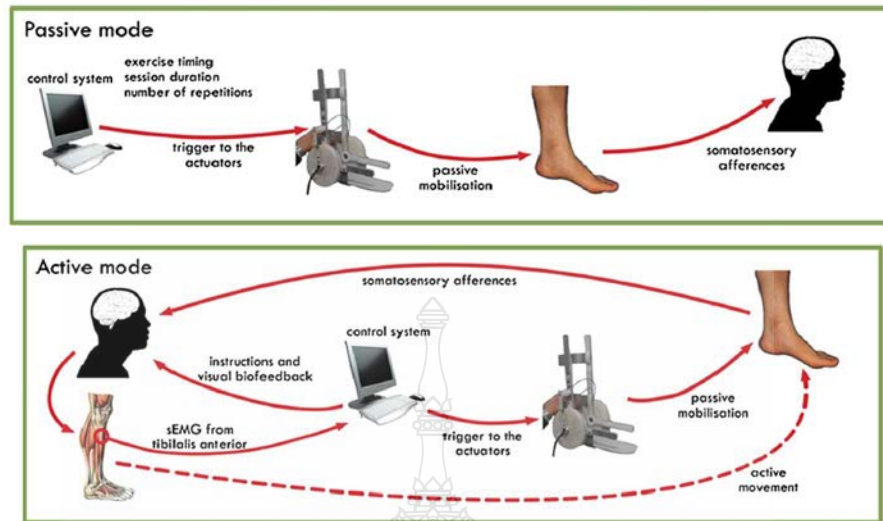


Figure 2. 34 Passive mode and active mode

(SOURCE: An EMG-controlled SMA device for the rehabilitation of the ankle joint in post-acute stroke. Journal of Materials Engineering and Performance, 20(4-5), 2011)

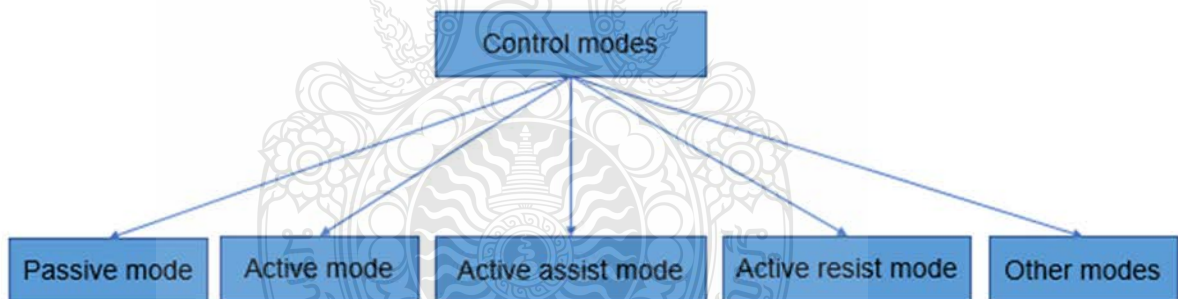


Figure 2. 35 Classification of control modes

**Table 2. 9** Some of the most common training modes for robots that help with lower limb rehabilitation.

Control modes	Outcomes
Passive mode	<ul style="list-style-type: none"> <li>• Repetitive, intense exercise can minimize muscle atrophy and aid in the rehabilitation of limb motor function.</li> <li>• Lacks patient’s motivation</li> </ul>

Active mode	<ul style="list-style-type: none"> <li>• Change the trajectory based on the patient's intent.</li> <li>• It is possible to significantly increase the initiative motivation.</li> </ul>
Active assist mode	<ul style="list-style-type: none"> <li>• Let the patient move without the robot at first.</li> <li>• The capacity for independent mobility can be enhanced.</li> </ul>
Active resist mode	<ul style="list-style-type: none"> <li>• Suitable for patients who are recovering quickly.</li> <li>• Resistance increases difficulty and can help muscles get stronger during the movement.</li> </ul>
Other modes	<ul style="list-style-type: none"> <li>• Developed based on a therapist's perspective.</li> <li>• Try to offer the user a specific level of support or resistance.</li> </ul>

#### 2.4.3.3 Control strategies

Robotic lower limb recovery aims to improve a patient's muscle activity in the lower limbs by using a variety of control techniques to restore nerve flexibility. As a result, robotic control systems that make direct contact with a patient's lower limbs are a significant source of concern. Researchers have been searching for further information about a patient's biological signals in recent years, especially those that can accurately represent the purpose of the patient's action and muscle activation. As a result, one of the most common fields is combining hybrid data blending (location, weight, and bio signals) and adaptive tuning to make it fit for individual patients. Depending on the intent of controller training and development, the control techniques outlined in this section may be categorized into these groups: force and impedance, position, tracking, bio-signals based, and adaptive. Figure 2.36 and Table 2.10 show the of overview recent control strategies and types of control algorithm for robot-assisted rehabilitation.

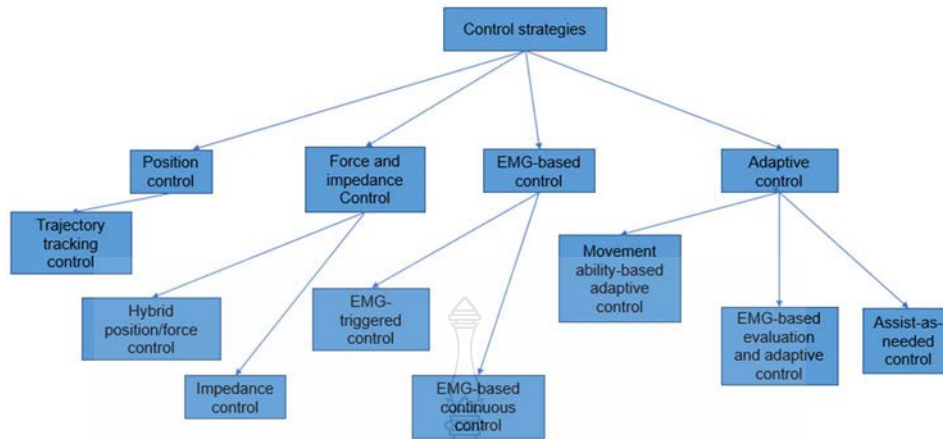


**Figure 2. 36** Summary of robot-assisted rehabilitation control strategies and their outcomes

**Table 2. 10** A summary of robot-assisted gait trainer control algorithm

No.	Device name	Control algorithm
1	AAFO	-
2	ABLE	PD Control
3	ALEX	Force, impedance control
4	Assist ON- Gait	Manual start/stop and speed varying operation
5	ATLAS	Finite state machine/PD control
6	Berkeley Exoskeleton System (BLEEX)	Force position hybrid controller
7	Body Extender	-
8	CUHK-Exo	PD Controller
9	ELEGS	Finite state machine
10	EXPOS and SUBAR	Fuzzy logic control, Impedance control
11	HAL	Proportional, myoelectric control

12	IHMC mobility assist exoskeleton	Position, force/torque control
13	Lokomat	Hybrid force-position control
14	Lopes	Impedance control
15	Lower-limb power assist exoskeleton	PI velocity control loop nested in a torque control loop
16	MINA	PD control
17	Mind walker	Model predictive control-based gait pattern generation
18	Nurse robot suit	PID control
19	Ortholeg and Ortholeg 2.0	Brain wave control
20	REWALK	Proportional, myoelectric control
21	Soft Exosuit	Trajectory based position control
22	Vanderbilt	Proportional control, myoelectric
23	Walking Assistance lower limb exoskeleton	Center of Pressure Control
24	Wearable Power-Assist Locomotor (WPAL)	PD control
25	XoR	-

#### 2.4.3.4 Improvement of the controller and hardware

Some control algorithms such as PID are linear control algorithms, however the pattern of people movement is not linear. There are some hybrid control algorithm methods that can be used to solve those cases. But there are only a few studies of hybrid control algorithms already implemented in lower limb gait trainer. Table 2.11 shows the comparison of the studies.

**Table 2. 11** Comparison of Hybrid Controller for robot assisted gait trainer

<b>Researcher</b>	<b>Type of Hybrid Control</b>	<b>Advantages</b>	<b>Disadvantages</b>
(D. Zhang & Wei, 2017)	PID with MRAC (Model Reference Adaptive Control)	Speed and performance are better than PID	Overshoot and then gradually returns to the desired position
(Majid et al., 2021)	PD with PSO (Particle Swarm Optimization)	Better joint tracking performance	-

Technological advances have made it possible to create exoskeletons feasible technology in the market. The advancement of electronics, actuators, batteries, and sensors propelled the use and acceptance of the exoskeleton. The device's drawbacks are calibration and setup time(Kittisares et al., 2020). However, many computer manufacturers now claim that their new devices need just a few minutes to put on. There are also issues with the user's ease and user experience. However, as more exoskeletons are evaluated on a larger user base, they improve. The question of how to efficiently monitor exoskeletons and optimize the benefits of these robotic devices remains unanswered.

The controllers differ significantly from one exoskeleton to the next. Several studies compare different controllers on the same computer. Furthermore, most exoskeletons depend solely on built-in mechanical sensors. Additional information about the user's status, while helpful, can be very useful for enforcing control choices that the user has over the system. We'll look at some promising research concepts that could be useful for exoskeleton technology.

Aside from controllers, exoskeleton hardware also has space for development. The frame (comfort and energy transmission) and the actuators are the most labor-intensive elements. Another common complaint among robotic exoskeleton users is that the device's soft tissue interface with the user's body is uncomfortable. Muscles attached directly to the

bones normally control the human skeleton. The situation is ideal for efficiently and painlessly moving torque and energy to the skeletal system.

Because humans who have skin, fat, and muscle between the exoskeleton and their skeletal system, when using a powered exoskeleton, compressed soft tissue can cause pain. When a robotic exoskeleton doesn't have enough space to travel about, the pain worsens. There are many things we can do to change the structure. We may upgrade the hardware and/or optimize the control algorithm (mechanism). As shown in Figure 2.37, a higher precision mechanism entails a higher cost. However, if we use low-cost mechanisms or electronic components, the device can become unstable. As a result, we must optimize using a different process, namely, optimization using a control algorithm.

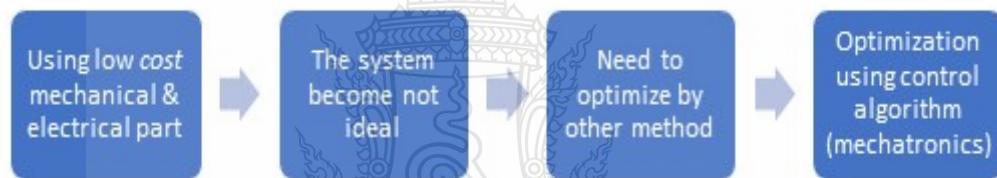


**Figure 2. 37** Mechanical compensation using control algorithm

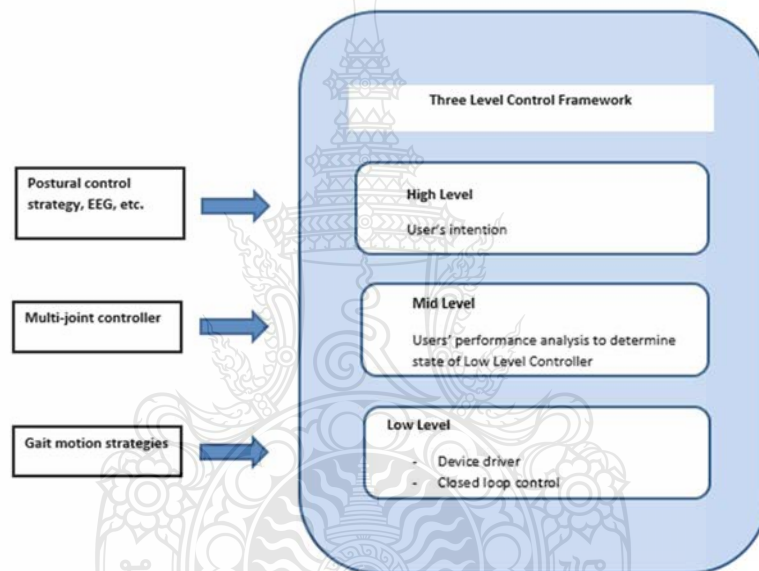


## CHAPTER 3

### RESEARCH METHODOLOGY

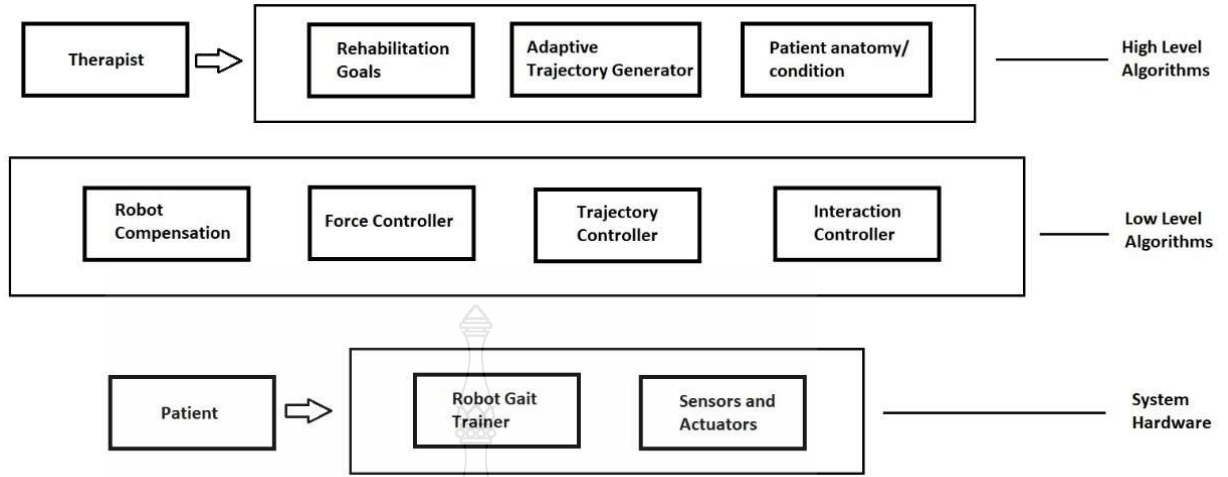
#### 3.1 System Design

Figure 3.1's representation of the three-level architecture of the basic control methods for the Robot Assisted Gait Trainer relates to how the human nervous system is set up and functions. These levels can function alone or in tandem with one another (Tucker et al., 2015).



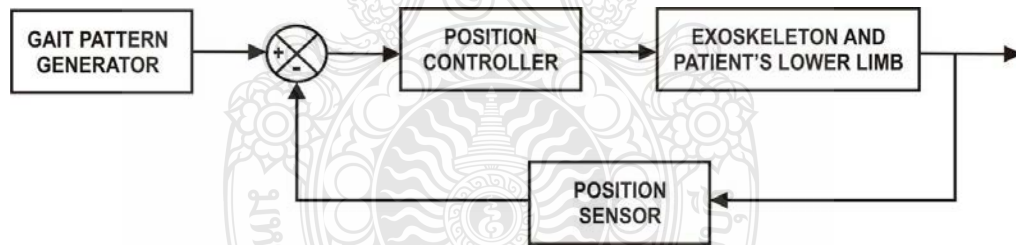
**Figure 3. 1** Framework for hierarchical control in the robotic gait trainer

Figure 3.2 depicts a common configuration of a gait rehabilitation control system, as presented by McDaid (McDaid et al., 2015). The hardware and multi-level control architecture of the rehabilitation system can be divided into two main groups: high-level physiotherapy algorithms and low-level feedback control algorithms. The low-level hardware and controller components that have a major influence on the overall performance of lower limb exoskeletons will be the focus of this study.



**Figure 3. 2** The gait rehabilitation control system's architecture

Figure 3.3 depicts the simplified closed-loop control that was specified for the Robot-Assisted Gait Trainer.



**Figure 3. 3** General closed-loop control of Robotic Gait Trainer

### 3.2 The lower limb exoskeleton's kinematics

A two-link planar RR arm is exactly like the lower link exoskeleton. Examine Figure 3.4, where the link masses are thought to be concentrated at the links' ends to determine its dynamics (Lewis, Frank L.; Dawson, Darren M.; Abdallah, 2004). The joint variable is

$$q = [\theta_1 \quad \theta_2]^T \quad (3.1)$$

where the vector of generalized force is

$$\tau = [\tau_1 \quad \tau_2] T \quad (3.2)$$

with  $\tau_1$  and  $\tau_2$  torques supplied by the actuators.

The kinetic and potential energies for link 1 are

$$K_1 = \frac{1}{2} m_1 a_1^2 \dot{\theta}_1^2 \quad (3.3)$$

$$P_1 = m_1 g a_1 \sin \theta_1 \quad (3.4)$$

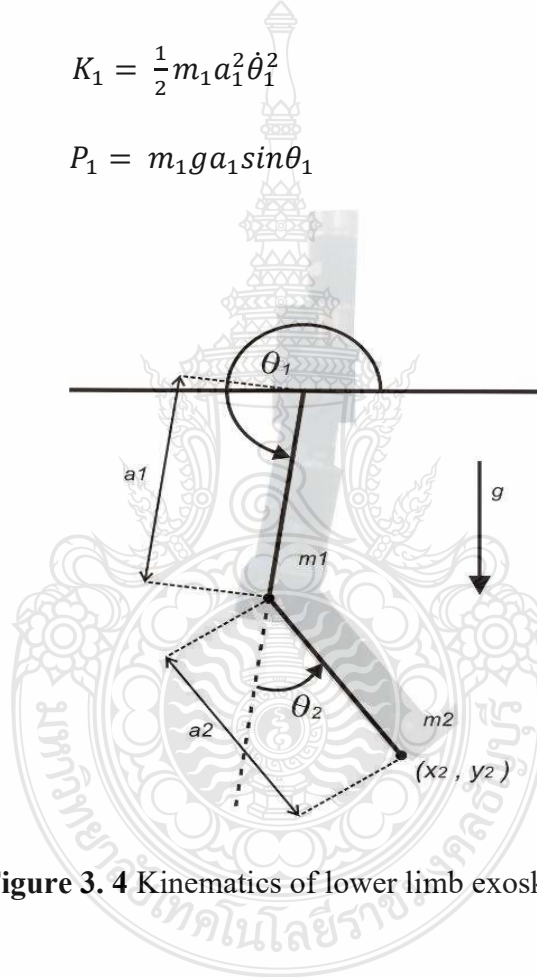


**Figure 3. 4** Kinematics of lower limb exoskeleton

For link 2 we have

$$X_2 = a_1 \cos \theta_1 \cos \theta_2 + a_2 \cos (\theta_1 + \theta_2) \quad (3.5)$$

$$Y_2 = a_1 \sin \theta_1 \sin \theta_2 + a_2 \sin (\theta_1 + \theta_2) \quad (3.6)$$

$$\dot{X}_2 = -a_1 \dot{\theta}_1 \sin \theta_1 \sin \theta_2 - a_2 \cos \theta_2 (\dot{\theta}_1 + \dot{\theta}_2) \sin (\theta_1 + \theta_2) \quad (3.7)$$

$$\dot{Y}_2 = -a_1 \dot{\theta} \sin \theta_1 - a_2 \cos (\dot{\theta}_1 + \dot{\theta}_2) \cos (\theta_1 + \theta_2) \quad (3.8)$$

So that the velocity squared is

$$v_2^2 = \dot{X}_2^2 + \dot{Y}_2^2 = a_1^2 \dot{\theta}_1^2 + a_2^2 (\dot{\theta}_1 + \dot{\theta}_2)^2 + 2a_1 a_2 (\dot{\theta}_1 + \dot{\theta}_1 \dot{\theta}_2) \cos \theta_2 \quad (3.9)$$

Consequently, link 2's kinetic energy is

$$K_2 = \frac{1}{2} m_2 v_2^2 = \frac{1}{2} m_2 a_1^2 \dot{\theta}_1^2 + \frac{1}{2} m_2 a_2^2 (\dot{\theta}_1 + \dot{\theta}_2)^2 + 2a_1 a_2 (\dot{\theta}_1 + \dot{\theta}_1 \dot{\theta}_2) \cos \theta_2 \quad (3.10)$$

Link 2's potential energy is

$$P_2 = m_2 g y_2 = m_2 g [a_1 \sin \theta_1 + a_2 \sin (\theta_1 + \theta_2)] \quad (3.11)$$

For the entire arm, the Lagrangian is

$$\begin{aligned} L &= K - P = K_1 + K_2 - P_1 - P_2 \\ &= \frac{1}{2} (m_1 + m_2) a_1^2 \dot{\theta}_1^2 + \frac{1}{2} m_2 a_2^2 (\dot{\theta}_1 + \dot{\theta}_2)^2 + m_2 a_1 a_2 (\dot{\theta}_1^2 + \dot{\theta}_1 \dot{\theta}_2) \cos \theta_2 \\ &\quad - (m_1 + m_2) g a_1 \sin \theta_1 - m_2 g a_2 \sin (\theta_1 + \theta_2) \end{aligned} \quad (3.12)$$

The terms needed for equation (3.14) are

$$\frac{\partial L}{\partial \dot{\theta}_1} = (m_1 + m_2) a_1^2 \dot{\theta}_1 + m_2 a_2^2 (\dot{\theta}_1 + \dot{\theta}_2) + m_2 a_1 a_2 (2\dot{\theta}_1 + \dot{\theta}_2) \cos \theta_2$$

$$\frac{d}{dt} \frac{\partial L}{\partial \dot{\theta}_1} = (m_1 + m_2) a_1^2 \ddot{\theta}_1 + m_2 a_2^2 (\ddot{\theta}_1 + \ddot{\theta}_2) + m_2 a_1 a_2 (2\ddot{\theta}_1 + \ddot{\theta}_2) \cos \theta_2 -$$

$$m_2 a_1 a_2 (2\dot{\theta}_1 \dot{\theta}_2 + \dot{\theta}_2^2) \sin \theta_2$$

$$\frac{\partial L}{\partial \theta_1} = -(m_1 + m_2)ga_1 \cos \theta_1 - m_2ga_2 \cos(\theta_1 + \theta_2) \quad \frac{\partial L}{\partial \dot{\theta}_2} = m_2a_2^2(\dot{\theta}_1 + \dot{\theta}_2) +$$

$$m_2a_1a_2\dot{\theta}_1 \cos \theta_2$$

$$\frac{d}{dt} \frac{\partial L}{\partial \dot{\theta}_2} = m_2a_2^2(\ddot{\theta}_1 + \ddot{\theta}_2) + m_2a_1a_2\ddot{\theta}_1 \cos \theta_2 - m_2a_1a_2\dot{\theta}_1\dot{\theta}_2 \sin \theta_2$$

$$\frac{\partial L}{\partial \theta_2} = -m_2a_1a_2(\dot{\theta}_1^2 + \dot{\theta}_1\dot{\theta}_2) \sin \theta_2 - m_2ga_2 \cos(\theta_1 + \theta_2)$$

Finally, according to Lagrange's equation, linked nonlinear differential equations provide the arm dynamics.

$$\begin{aligned} \tau_1 = & [(m_1 + m_2)a_1^2 + m_2a_2^2 + 2m_2a_1a_2 \cos \theta_2] \ddot{\theta}_1 \\ & + [m_2a_2^2 + m_2a_1a_2 \cos \theta_2] \ddot{\theta}_2 - m_2a_1a_2(2\dot{\theta}_1\dot{\theta}_2 + \dot{\theta}_2^2) \sin \theta_2 \\ & + (m_1 + m_2)ga_1 \cos \theta_1 + m_2ga_2 \cos(\theta_1 + \theta_2) \end{aligned} \quad (3.13)$$

$$\begin{aligned} \tau_2 = & [m_2a_2^2 + m_2a_1a_2 \cos \theta_2] \ddot{\theta}_1 + m_2a_2^2 \ddot{\theta}_2 + m_2a_1a_2 \dot{\theta}_1^2 \sin \theta_2 \\ & + m_2ga_2 \cos(\theta_1 + \theta_2) \end{aligned} \quad (3.14)$$

### 3.3 Lower limb exoskeleton dynamics

When the dynamics are expressed as vectors, the following results are

$$\begin{aligned} \text{obtained.} & [(m_1 + m_2)a_1^2 + m_2a_2^2 + 2m_2a_1a_2 \cos \theta_2] \ddot{\theta}_1 + m_2a_2^2 \ddot{\theta}_2 + m_2a_1a_2 \dot{\theta}_1^2 \sin \theta_2 \\ & + m_2ga_1 \cos \theta_1 + m_2ga_2 \cos(\theta_1 + \theta_2) \end{aligned} \quad (3.15)$$

$$+[-m_2 a_1 a_2 (2 \dot{\theta}_1 \dot{\theta}_2) \sin \theta_1 \sin \theta_2 \ m_2 a_1 a_2 \dot{\theta}_2^2 \sin \theta_1 \cos \theta_2] + [(m_1 m_2) g a_1 \cos \theta_1 \cos \theta_2 + m_2 g a_1 \cos(\theta_1 + \theta_2) \ m_2 g a_1 \cos(\theta_1 + \theta_2)]$$

$$= [\tau_1 \ \tau_2]$$

Standard form of these manipulator dynamics:

$$M(q)\ddot{q} + V(q, \dot{q}) + G(q) = \tau_3 \quad (3.16)$$

### 3.4 Mechanical Design

The human knee has similarities with manufactured robotic joint, as depicted in Figure 3.5. Figure 3.5 (a) (Hamill et al., 2015) illustrates the flexion, extension, internal rotation, and exterior rotation movements at the knee joint. Only sagittal plane mobility (flexion and extension) is used by the exoskeleton being built.

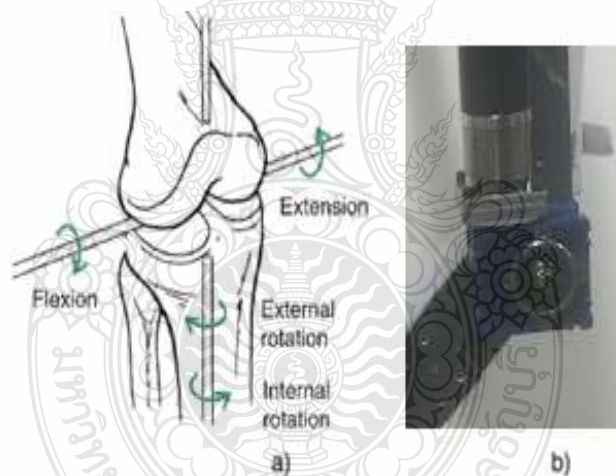


**Figure 3. 5** Knee joints from human(a) and exoskeleton(b) are compared.

It is made to be as light as possible. Four actuators on a four-DoF system are positioned at the knee and hip joints. To accommodate for reduced weight and mechanical resistance, the mechanical framework uses aluminum(Moreno et al., 2008). Figure 3.6 and 3.7 depict the exoskeleton's mechanical drawing. For user protection, the allowed joint-angle

range is limited mechanically. The data for the knee and hip kinematics are displayed in Table 3.1 (Low, 2011).

**Table 3. 1** Kinematics of the Hip and Knee

<b>Joints</b>	<b>Motion</b>	<b>Range of Motion (degree)</b>	<b>Average Torque</b>
Hip	Flexion	100-140	140
	Extension	15-30	120
Knee	Flexion	120-150	140
	Extension	0-10	15

The performance requirements for a tiny solution for a portable device are met by DC motors. One practical way to increase torque and decrease speed is by connecting the gearbox (Figure 3.8 b) to the shaft of PG56 brushless DC motor (Figure 3.8 a). Because skeletal joints require more torque and slower speeds than what direct current (DC) motors can deliver (Hollerbach et al., 1992).

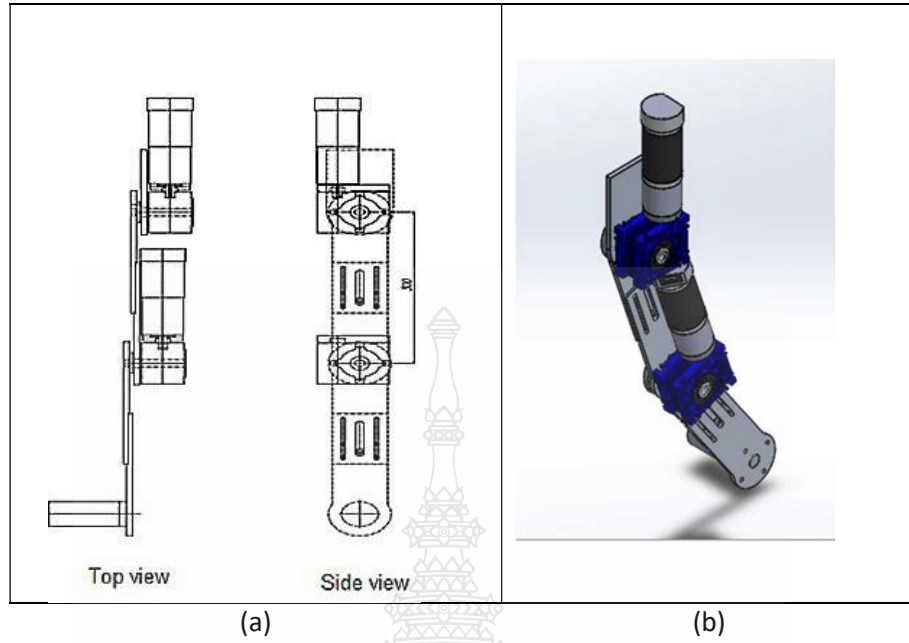


**Figure 3. 6** Exoskeleton of the lower limb in mechanical illustration  
 (a) 2D drawing (b) 3D drawing

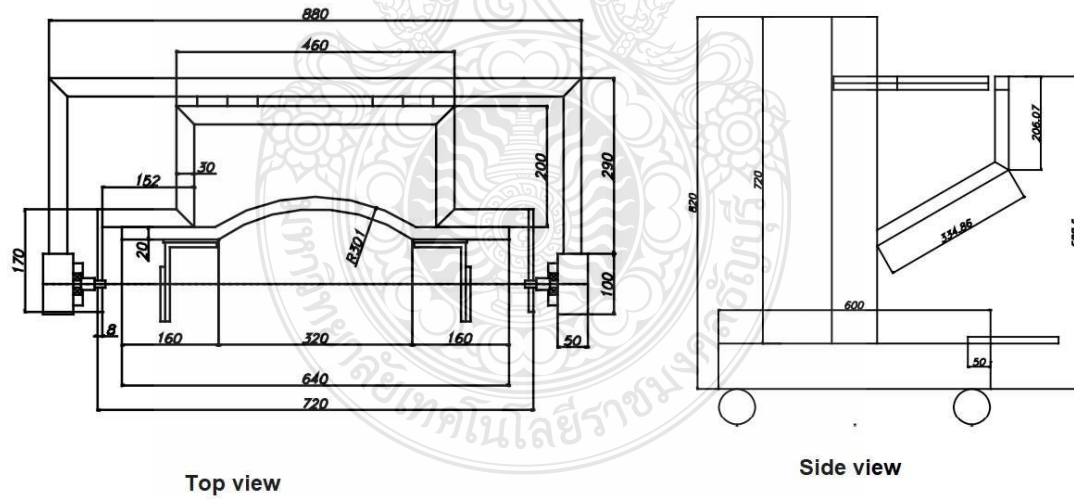


**Figure 3. 7** Exoskeleton support (top and side mechanical illustration)





**Figure 3. 8** a) PG56 brushless DC motor with encoder b) Gearbox Shaft Ratio 1:50

Figure 3.9 shows that this lower limb exoskeleton has four dc motors that move four joints, two on the right and two on the left side. Pulse width modulation signals from the microcontroller outputs are used by the motor drivers to drive the direct current motor.

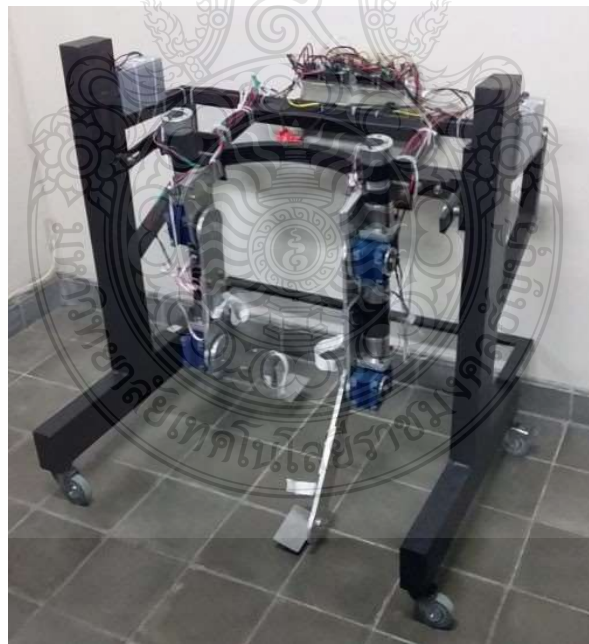


**Figure 3. 9** The physical appearance of the gait trainer

This lower limb exoskeleton has 4 dc motors that operate 4 joints, 2 motors for each side. A PWM (Pulse Width Modulation) dc servo motor drives the joint motors (PG56).

### 3.5 Actuator Selection

An electronic control system may include an actuator, which is a functional device that connects the information processing portion of the system with a process that may be technical or nontechnical, such as biological. Controlling the flow of energy, mass, or volume can be accomplished through the utilization of actuators (Janocha, 2004). Within the larger system that makes up the exoskeleton, actuators and sensors are essential components that make up the exoskeleton. Actuators are essential components of active devices, and the technological decisions that are made have a substantial impact on the overall performance of the device (Tiboni et al., 2022). Energy is transferred to a load by a direct current (DC) motor, a type of power actuator (Dorf & Bishop, 2022). A DC motor's schematic is shown in Figure 3.10(b). The motor's rotor (armature) can provide enough torque to drive an external load in a sizable proportion. due to traits including strong torque, wide speed controllability, portability, good speed-torque characteristics, and versatility.

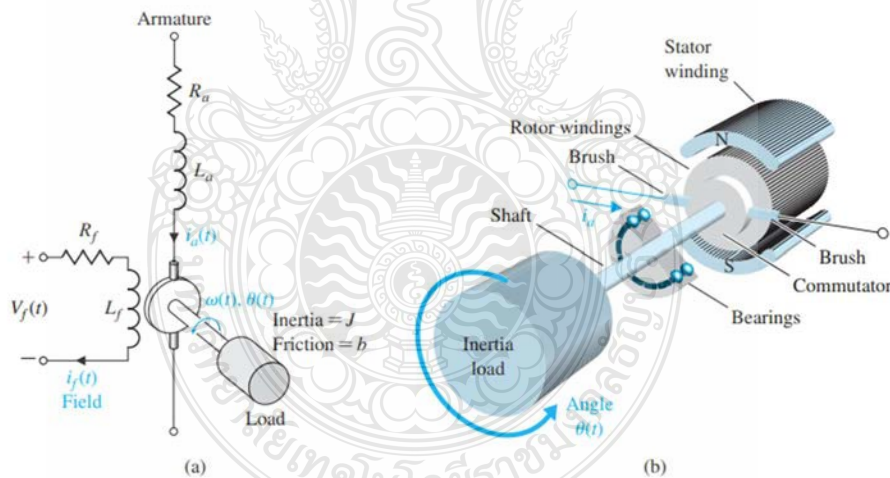


**Figure 3. 10** A dc motor (a) electrical schematic (b) sketch of the parts  
(SOURCE: Modern Control Systems (14th ed.). Pearson, 2002)

If the field is not saturated, the motor's air-gap flux  $\phi(t)$  is proportional to the field current, indicating that

$$\phi(t) = K_f i_f(t) \quad (3.17)$$

According to this theory, the torque of the motor is linearly related to the armature current and flux  $\phi(t)$ :

$$T_m(s) = K_1 \phi(t) i_a(t) = K_1 K_f i_f(t) i_a(t) \quad (3.18)$$

The Laplace transform notation for this equation is then displayed:

$$T_m(s) = (K_1 K_f I_a) I_f(s) = K_m I_f(s) \quad (3.19)$$

where  $K_m$  is the motor constant and  $i_a = I_a$  is the armature current constant. As shown below, the field voltage is:

$$V_f(s) = (R_f + L_f s) I_f(s) \quad (3.20)$$

The torque  $T_m(s)$  of the motor is the same as the torque applied to the load. The following diagram illustrates this relationship:

$$T_m(s) = T_L(s) + T_d(s) \quad (3.21)$$

$T_d(s)$  is torque of the disturbance, whereas  $T_L(s)$  is the torque of load. Figure 3.11 depicts the torque under load for rotating inertia as

$$T_L(s) = Js^2 \theta(s) + bs \theta(s) \quad (3.22)$$

We can get Equations (3.19) – (3.21) by rearranging them.

$$T_L(s) = T_m(s) - T_d(s) \quad (3.23)$$

$$T_m(s) = K_m I_f(s) \quad (3.24)$$

$$I_f(s) = \frac{V_f(s)}{R_f + L_f s} \quad (3.25)$$

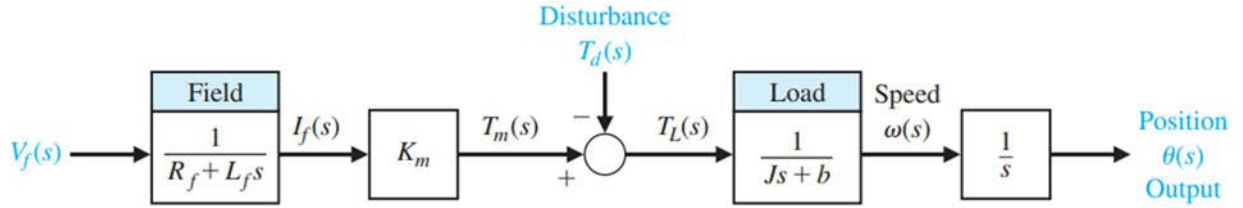


**Figure 3. 11** DC motor field-controlled type

(SOURCE: Modern Control Systems (14th ed.). Pearson, 2002)

Therefore, the motor-load pair transfer function is when  $T_d(s) = 0$ :

$$\frac{\theta(s)}{V_f(s)} = \frac{K_m}{s(Js+b)(L_f s + R_f)} = \frac{K_m / (JL_f)}{s(s+b/J)(s+R_f/L_f)} \quad (3.26)$$

Figure 3.11 illustrates a model of a field-controlled direct current motor. The transfer function can also be stated in another way, which is as follows:

$$\frac{\theta(s)}{V_f(s)} = G(s) = \frac{K_m / (bR_f)}{s(\tau_f s + 1)(\tau_L s + 1)} \quad (3.27)$$

Where  $\tau_f = \frac{L_f}{R_f}$  and  $\tau_L = \frac{J}{b}$ ,  $\tau_L > \tau_f$ , in many cases, the field time constant is often overlooked.

In an armature-controlled DC motor, the control parameter is the armature current,  $i_a$ . A field coil, a permanent magnet, and electricity work together to produce the stator field.

$$T_m(s) = (K_1 K_f I_f) I_a(s) = K_m I_a(s) \quad (3.28)$$

With a permanent magnet, we obtain:

$$T_m(s) = K_m I_a(s)$$

$K_m$  correlates with the magnetic substance's permeability, while the input voltage of the armature determines how much current flows through it.

$$V_a(s) = (R_a + L_a s)I_a(s) + V_b(s) \quad (3.29)$$

The motor speed is correlated with the back electromotive force voltage,  $V_b(s)$ .

Consequently, we have

$$V_b(s) = K_b \omega(s) \quad (3.30)$$

where the angular speed transform is  $\omega(s) = s\theta(s)$  and the armature current is

$$I_a(s) = \frac{V_a(s) - K_b \omega(s)}{R_a + L_a s} \quad (3.31)$$

The load torque is represented by equations (3.22) and (3.23).

$$T_L(s) = Js^2\theta(s) + bs\theta(s) = T_m(s) - T_d(s) \quad (3.32)$$

Figure 3.12 depicts the armature-controlled DC motor's relationships schematically. Solving for the transfer function using Equations (3.28), (2.31), and (2.32) with  $\tau_d(s) = 0$ .

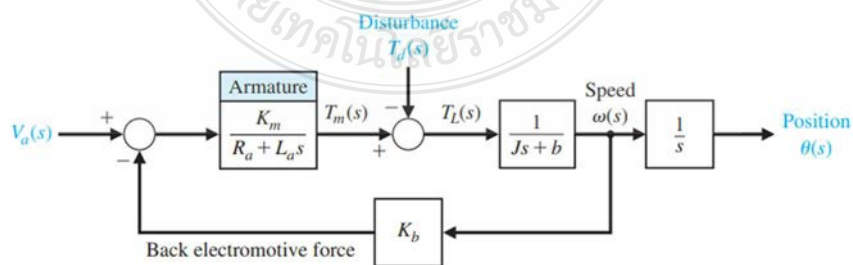


**Figure 3. 12** DC motor (armature-controlled type)

(SOURCE: Modern Control Systems (14th ed.). Pearson, 2002)

$$G(s) = \frac{\theta(s)}{V_a(s)} = \frac{K_m}{s[(R_a + L_a s)(Js + b) + K_b K_m]} \quad \dots \quad (3.33)$$

$$= \frac{K_m}{s(s^2 + 2\zeta\omega_n s + \omega_n^2)}$$

The armature time constant for many DC motors,  $\tau_a = \frac{L_a}{R_a}$ , is insignificant, as a result,

$$G(s) = \frac{\theta(s)}{V_a(s)} = \frac{K_m}{s[(R_a + L_a s)(Js + b) + K_b K_m]} = \frac{K_m / (R_a b + K_b K_m)}{s(\tau_1 s + 1)} \quad (3.34)$$

where  $\tau_1 = \frac{R_a J}{(R_a b + K_b K_m)}$  is the equivalent time constant. It's important to note that  $K_m$  is the same as  $K_b$ .  $K_b \omega(t) i_a(t)$  is the rotor's power input, and  $T(t) \omega(t)$  represents the force applied to the shaft. The input power and output power transmitted to the shaft are equal in a steady state, therefore  $K_b \omega(t) i_a(t) = T(t) \omega(t)$ ; since  $T_t = K_m i_a(t)$ . (Equation 3.28), we conclude that  $K_b = K_m$ .

The concept and technique of transfer function are critical because they provide a usable mathematical representation of the system parts to the analyst and designer. The transfer function will prove to be an invaluable tool in our efforts to model dynamic systems.

### 3.6 Control Theory

In the history of control theory, there have been three different kinds of control algorithms: intelligent, modern, and classical. Though essential, traditional methods like PID linear control and basic PD control are useless for nonlinear systems. Due to its excellent control performance and straightforward design, motion control is becoming a more and more popular modern control method. Intelligent control can provide optimal performance,

but it is difficult to design and needs extensive expertise. For nonlinear mechanical systems, numerous creative and complex control schemes have recently been created.(Martynyuk, 2000). Among the most advanced control methods created for nonlinear mechanical systems are adaptive control, computed torque control, fuzzy control, neural network control, and sliding mode control. (Yang et al., 2008).

### 3.6.1 PID Control

The acronym PID stands for proportional, integral, and derivative, which are the three components that make up a PID controller. Because of the ease with which it may be implemented, as well as its durability and versatility in terms of tuning (Niu et al., 2013). The PID is attempting to adjust the system by first correcting the error that was computed based on the difference between the angle that was measured and the angle that was desired, and then computing the proper action. The PID controller combines the proportional, integral, and derivative parameters into a single set of control inputs. It can be shown that the transfer function of PID is as follows:

$$u(t) = K_c e(t) + \frac{K_c}{\tau_I} \int_0^t e(\tau) d\tau + K_c \tau_D \frac{de(t)}{dt} \quad (3.35)$$

Between the reference signal  $r(t)$  and the output  $y(t)$ , there is a signal called the feedback error signal,  $e(t)$ . This signal is calculated as the difference between  $r(t)$  and  $y(t)$ , and  $D$  refers to the derivative control gain.

$$\frac{U(s)}{E(s)} = K_c \left( 1 + \frac{1}{\tau_I s} + \tau_D s \right) \quad (3.36)$$

The output of most applications merely uses a derivative filter to implement the derivative control. Because of this, the control signal  $U(s)$  is expressed in the following way:

$$U(s) = K_c \left( 1 + \frac{1}{\tau_I s} \right) (R(s) - Y(s)) - \frac{K_c \tau_D s}{\beta \tau_D s + 1} Y(s) \quad (3.37)$$

Figure 3.13 provides a visual representation of the block diagram for the PID controller. Calculating the control signal makes use of

$$u(t) = -K_c y(t) + \frac{K_c}{\tau_I} \int_0^t (r(\tau) - y(\tau)) d\tau - K_c \tau_D \frac{dy_f(t)}{dt} \quad (3.38)$$

Accordingly, the control signal can be expressed in Laplace transform as

$$\begin{aligned} U(s) &= -K_c Y(s) + \frac{K_c}{\tau_I s} \int_0^t (R(s) - Y(s)) - \frac{K_c \tau_D}{\beta \tau_D s + 1} Y(s) \\ &= \frac{K_c}{\tau_I s} (R(s) + Y(s)) - \frac{K_c (\tau_D (\beta + 1) s + 1)}{\beta \tau_D s + 1} Y(s) \end{aligned} \quad (3.39)$$

Figure 3.14 presents the block diagram of the alternative PID controller, which is referred to as the IPD controller.

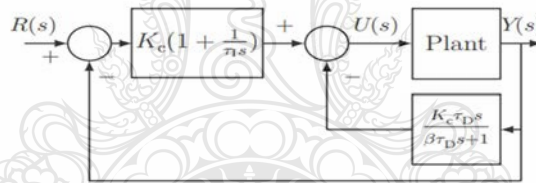


**Figure 3. 13** PID controller structure.

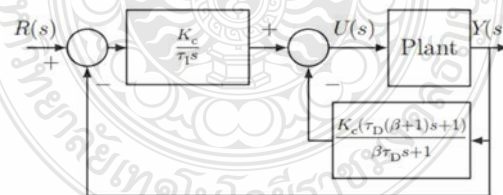


**Figure 3. 14** IPD controller structure.

(SOURCE: Fuzzy PID control for passive lower extremity exoskeleton in swing phase. ICEIEC 2013 - Proceedings of 2013 IEEE 4th International Conference on Electronics Information and Emergency Communication)



### 3.6.2 Hybrid Feedback Control

A hybrid system is one that is made up of two dissimilar components that contains both analog and digital components. A system of this sort generates a blend of continuous and discrete signals, as well as numerous forms of control mechanisms. As shown in Figure 3.15, hybrid systems are quite widespread in the fields of research and engineering because they make it possible to capture the complex, interconnected continuous and discrete behavior of a wide variety of systems. Figure 3.16 displays the hybrid control system's general block diagram.

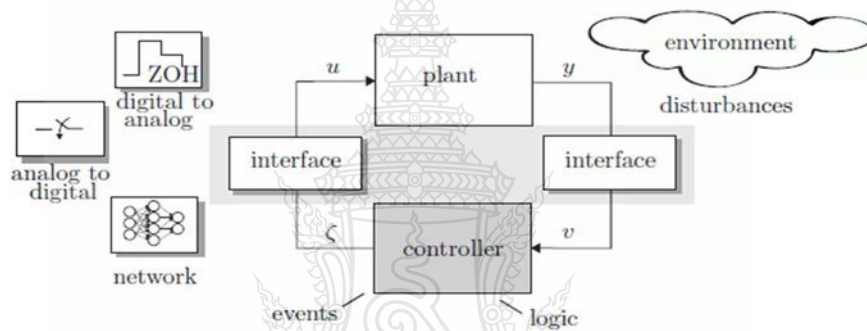


**Figure 3. 15** Hybrid control system illustration

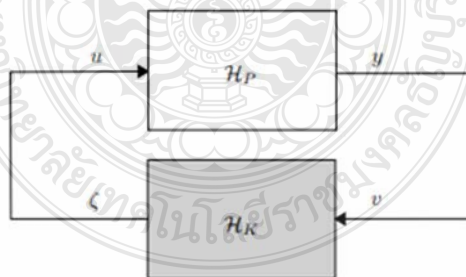


**Figure 3. 16** A generalized hybrid closed loop system block diagram

(SOURCE: Hybrid Feedback Control, Princeton, 2021)

### 3.6.3 Feedback Linearization and Computed torque control

After a sufficient modification to the state space coordinates, a transformation called "inner-loop control" in feedback linearization accurately linearizes the nonlinear system. The basic requirements for control design, such as disturbance rejection, tracking, and so on, can be achieved by a second stage of control or an outer-loop control in the new coordinates. Computed torque control is a technique for applying feedback linearization to nonlinear systems (Khatib, 2016). Figure 3.17 shows the block diagram of computed torque control

Look at the input.

$$\tau = H(q)v + C(q, \dot{q})\dot{q} + \tau_g(q)$$

When this control law is inserted into the robot manipulator's dynamical model, the outcome is  $k_p = \alpha k_v$ .

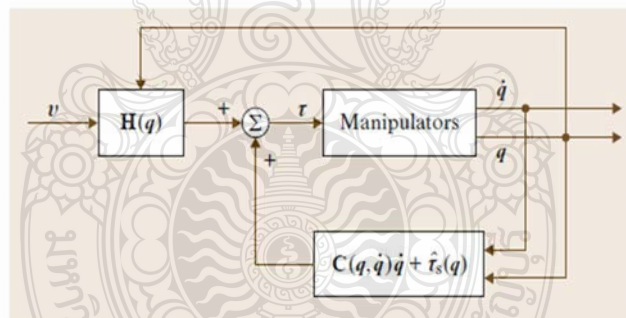


**Figure 3. 17** Computed torque control

(SOURCE: Springer Handbook of Robotics (2nd ed.). Springer, 2016)

Proportional-derivative (PD) feedback is one method for outer-loop control.

$$v = \ddot{q}_d + K_v \dot{e}_q + K_p e_q$$

As a result, the entire control input becomes

$$\tau = H(q)(\ddot{q}_d + K_v\dot{e}_q + K_p e_q) + C(q, \dot{q})\dot{q} + \tau_g(q)$$

The dynamics of linear error that arise are as follows:

$$\ddot{e}_q + K_v\dot{e}_q + K_p e_q = 0$$

The tracking error is guaranteed to go away altogether over time according to the linear systems theory.

### 3.7 Microcontroller and motor driving system

#### 3.7.1 Arduino

According to the official Arduino website, Arduino is an open-source electronic device that is frequently used to build and manufacture user-friendly software and electronic products. Arduino is made to make it easier to use electronic equipment in a variety of settings. Pins, microcontrollers, and connectors are only a few of the key parts of Arduino that will be covered in more detail in the future. In addition, Arduino also makes use of the programming language known as Arduino Language, which is somewhat like C++. Processing and the Wiring-based Arduino Programming Language are the foundations upon which the Arduino Software (IDE) is constructed.

Throughout its existence, Arduino has been the brains of thousands of different machines. These projects span the spectrum of difficulty, from simple home appliances to complicated scientific instruments. Students, amateurs, artists, and programmers from all **around the world take advantage of this open-source platform. Because of their efforts, a large body of knowledge has accumulated. This body of knowledge is simple to access, and it has the potential to be of great help to users with varying degrees of experience.**

The Arduino was created at the Ivrea Interaction Design Institute to give students who lacked experience with electronics or programming a simple tool for quick prototyping. With a larger audience and a movement in product options from straightforward 8-bit boards to parts for Internet of Things (IoT) applications, wearable technology, 3D printing, and embedded settings, the Arduino board started to develop.

### 3.7.1.1 Advantages of using Arduino

- **Affordable** – In comparison to other microcontroller platforms, Arduino boards are reasonably priced.
- **Cross-platform**  
Linux, Windows, and Macintosh OSX are all supported by the Arduino Software (IDE). Windows is the only operating system that can run microcontrollers.
- **Simple and understandable programming environment**  
Beginners will find the Arduino Software (IDE) to be simple to use, but advanced users will also find it to be flexible.
- **Extensible software that is open source**  
Open-source technologies that can be extended by knowledgeable programmers are made accessible with the Arduino software. People who are interested in the technical specifics can switch from Arduino to the AVR C programming language, which is the language on which it is based, and the language can be expanded through C++ libraries.
- **Hardware that is extendable and open source**  
Circuit designers with experience can build, expand, and develop their own versions of the module because Arduino board designs are available under a Creative Commons license. To test a form's functionality and save money, even beginners can make a dummy version of it.

### 3.7.1.2 Types of Arduino Devices

Over time, the board designs produced by the designers at arduino.cc have varied. In 2007 saw the release of the Diecimila, the first Arduino board that was widely utilized. The Arduino family has expanded during the intervening years to gain from the numerous Atmel AVR MCU products. In 2012, the Due joined the lineup, setting itself apart from the rest of the series with its superior processing capability and unique board pinout configuration. This type of Arduino is the first device to utilize the 32-bit ARM Cortex-M3 central processing

unit. The pinouts of some boards, like as the Nano and LilyPad, are different from those of the other members of the family. They were created with a variety of applications in mind, such as wearable technology in the case of the Nano and the LilyPad, portable technology in the case of the Esplora, and compact form factors in the case of the Mini, Micro, and the Nano.

New varieties of Arduino boards are introduced every year. Current add-on boards known as shields and a range of add-on components like sensors, relays, and actuators are compatible with the most recent models because they use the same pinout configurations. The more recent models also include more modern CPUs with more memory and greater input/output (I/O) functions. The Arduino variants that have arisen since 2005 are listed in Table 3.2. Most designs created for earlier iterations of the Arduino will still function on more recent models of the hardware, albeit with a few minor modifications and newer libraries.

Table 3.2 also provides background information about the Arduino. In the years 2007 and 2008, numerous technological advancements were made, including the introduction of the LilyPad, compact form-factor boards like as the Nano, Mini, and Mini Pro, and the Duemilanove, which was a logical progression based on the Diecimila. Both the Diecimila and the Duemilanove have the same physical design, but the Duemilanove has several improvements to the power supply. One of these improvements is a feature that automatically switches between an external DC (direct current) power source and power supplied by a USB port on the board. The Duemilanove uses the ATmega328 MCU, which has additional programme memory, in later iterations.

**Table 3. 2** Timeline of Arduino products

<b>Year</b>	<b>Microcontroler</b>	<b>Board name.</b>
2001	ATmega 168	Diecimila
	ATmega168/ATmega328V	LilyPad

2008	ATmega328/ATmega168	Nano
	ATmega168	Mini
	ATmega.328 ATmega.328	Mini Pro Duemilanove
2009	AT mega2560	Mega ADK
2010	ATmega328P	Fio
	ATmega2560	ATmega2560
	ATmega328P	Uno
20H	ATmega328	Ethemet
	ATmega2560	Mega ADK
2012	ATmega32U4	Leonardo
	ATmega.32U4 ATmega32U4	Esplora Micro
	ATmega32U4 + Linino	Yun
2013	ATmega32U4 + Linino	Yun
2015	Intel Curie	101

The Arduino UNO board is shown in Figure 3.18. The low-level controller used to manage the leg's joint angles is Arduino UNO. There are 4 degrees of freedom for the gait trainer. Its four joints can be manipulated; therefore, this means. Two joint angles are managed by one Arduino UNO. As a result, the system includes 4 Arduino UNOs. From the Arduino Mega2560, which serves as the gait generator, they receive positional commands.



**Figure 3. 18** Arduino UNO

An ATmega328 chip serves as the controller in the Arduino UNO. It contains a 16 MHz quartz crystal, 6 analog inputs, and 6 PWM outputs among its 14 digital input/output ports.

**Table 3. 3** Hardware specification of Arduino UNO (Arduino)

<b>Microcontroller</b>	<b>ATmega328P</b>
Operating Voltage	5v
Input Voltage (recommended)	7-12V
Input Voltage (limit)	6-20V
Digital I/O Pins	14 (of which 6 provide PWM output)
PWM Digital I/O Pins	6
Analog Input Pins	6
DC Current per I/O Pin	20 mA
DC Current for 3.3V Pin	50 mA

Flash Memory	32 KB (ATmega328P) of which 0.5 KB used by bootloader
SRAM	2 KB (ATmega328P)
EEPROM	1KB (ATmega328P)
Clock Speed	16 MHz
Length	68.6 mm
Width	53.4 mm

The gait generator is an Arduino Mega 2560. To determine the angle location of each joint, inverse kinematic was used to generate all the gait data. After that, Arduino UNO receives this information.



**Figure 3. 19** Arduino Mega 2560

Based on the ATmega2560, the Arduino Mega 2560 is a microcontroller board. It contains a 16 MHz crystal oscillator, 4 UARTs (hardware serial ports), 16 analog inputs, and 54 digital input/output pins, 15 of which can be utilized as PWM outputs.

**Table 3. 4** Hardware specification of Arduino MEGA2560 (Arduino)

<b>Microcontroller</b>	ATmega2560
<b>Weight</b>	37 g
<b>Operational voltage</b>	5 volts
<b>Voltage at Input (recommended)</b>	7.12 volts



<b>Max.Input Voltage</b>	6-20 volts
<b>Pins for digital I/O</b>	54
<b>Analog Input Pins</b>	16
<b>110 Pin DC Current</b>	20 mA
<b>3.3V Pin DC Current</b>	50 mA
<b>Flash Memory</b>	256 kB

### 3.7.1.3 Communication between Arduino Mega 2560 and Arduino Uno

The Arduino Mega 2560 and Arduino Uno can connect in a variety of ways. The UART protocol, a serial communication technique that uses the RX (receive) and TX (transmit) pins, is one option. Both boards have hardware serial ports or use the SoftwareSerial library to build virtual serial ports on additional pins<sup>1</sup>.

Another option is to use the I2C protocol, a synchronous communication technique that makes use of two pins: SDA for serial data and SCL for serial clock. Data transfer between the boards using I2C can be done with the Wire library. Each board must be given a distinct address, using one as the controller (master), and the other as the peripheral (slave).

Figure 3.20 shows the wiring diagram for one side of the exoskeleton's microcontroller and motor driving system. The exoskeleton's DC motor and electrical circuits are powered by a 24 V battery. The battery's 24 DC volts are then reduced to 5 volts by the switching regulators so that the electronic control circuits can be powered. The memory of the microcontroller, an Atmel ATmega2560 running on the Arduino Mega, contains the gait trajectories. The transmission of data on the position of the motor drivers will be made periodically by the microcontroller. To provide enough current to drive the DC motors (PG56 DC motors), the BTS7960 High Current Motor Driver H-Bridge module will amplify the currents. Each motor can operate one joint. The encoder will give the microcontroller inputs based on the actual positions of the joints. The microcontroller then determines the voltage value that must be given to the driving circuits.

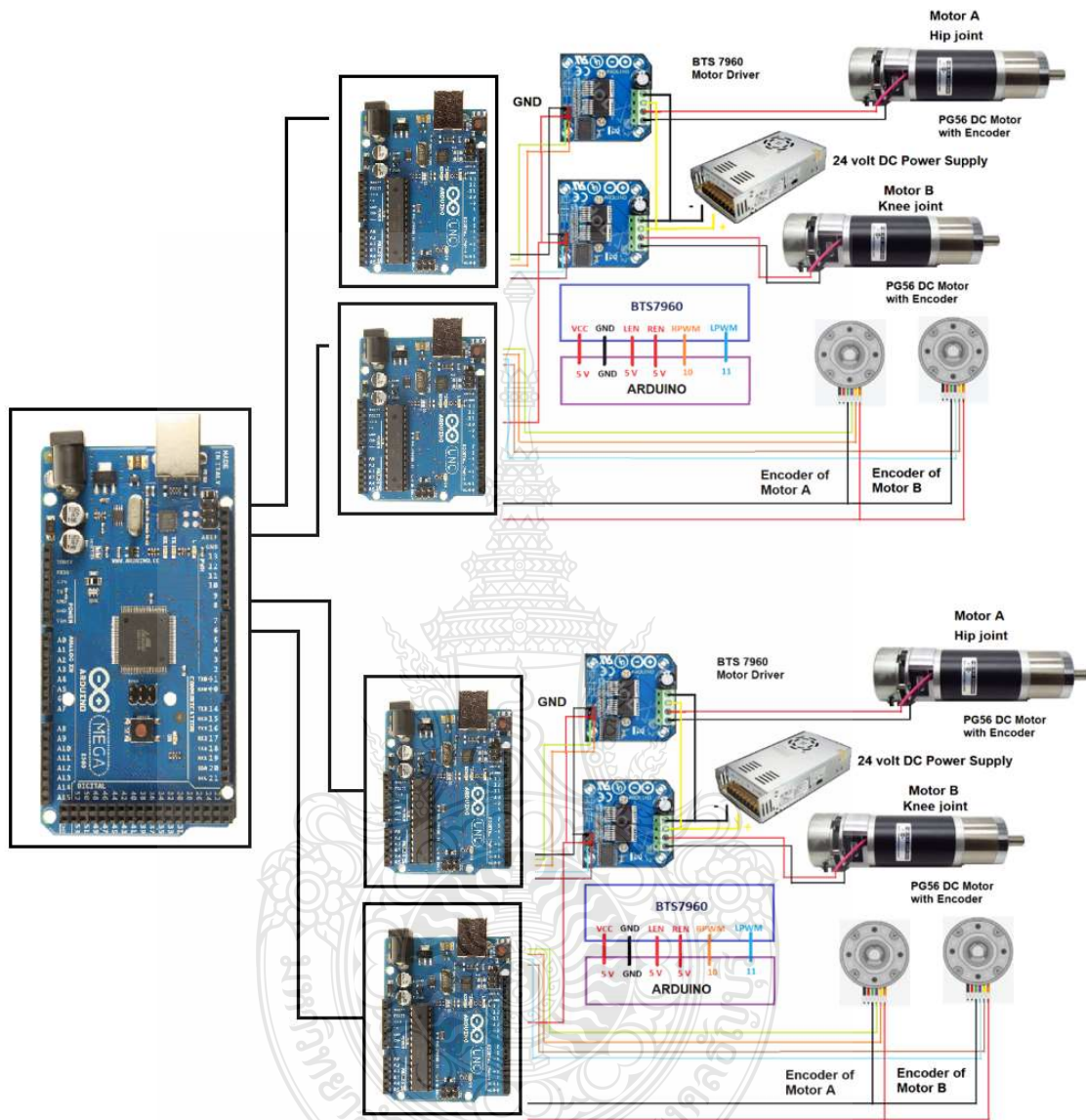


**Figure 3. 20** Diagram of the system for driving a motor and a microcontroller

### 3.7.2 Motor Driver

To drive the motors, BTS7960 H-Bridge DC Motor Drive High Current Motor Driver Board are used. For motor driving applications, the BTS7960 is a fully integrated high current H bridge module. The integrated driver IC makes it easy to connect it to a microcontroller since it provides logic level inputs, current sense diagnosis, slew rate adjustment, dead time generation, and

protection against overheating, overvoltage, undervoltage, overcurrent, and short circuit. With little board area consumption, the BTS7960 driver offers a cost-optimized solution for protected high current PWM motor drives. The BTS7960 driver is made up of 5 semiconductor parts: a microcontroller, 2 BTS7960 mosfets, a TLE4278G voltage regulator, and an SPD50P03L mosfet for reverse polarity protection. Figure 3.21 and 3.22 respectively show the BTS7960 H-Bridge DC Motor Driver and its schematic. While Table 3.5 and 3.6 respectively show its brief data and pin function.



**Figure 3. 21** BTS7960 H-Bridge DC Motor Driver

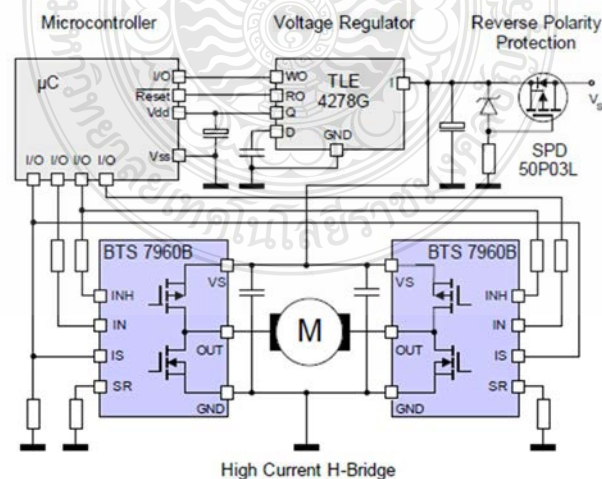


**Figure 3. 22** Schematic of BTS7960 H-Bridge DC Motor Drive

**Table 3. 5** Brief data of BTS7960

<b>Voltage at Input</b>	6-27Vdc
<b>Driver</b>	Dual BTS7960 H Bridge Configuration.
<b>Peak current:</b>	43-Amp
<b>P\VM capability</b>	up to 25 kHz
<b>Control Input Level</b>	3.3-5V
<b>Control Mode</b>	P\VM or level
<b>Working Duty Cycle</b>	0....100%.
<b>Over-voltage Lock Out</b>	Under-voltage Shut Down
<b>Board Size (L x W x H)</b>	50mm x 50mm x 43mm
<b>Weight</b>	66g

**Table 3. 6** Pin function and description

<b>Pin No</b>	<b>Function</b>	<b>Description</b>
1	RPWM	Forward Level or PWM signal (Active High)
2	LPWM	Reverse Level or PWM signal (Active High)
3	R EN	Forward Drive Enable Input (Active High/ Low Disable)
4	L-EN	Reverse Drive Enable Input (Active High/Low Disable)
5	R IS	Forward Drive, Side current alarm output
6	L-IS	Reverse Drive, Side current alarm output
7	Vee	Microcontroller +5V Power Supply
8	Gnd	Microcontroller Ground Power Supply

The MOSFET BTS 7960 shown in Figure 3.23 is a fully integrated high current half bridge used in motor driving applications. It offers a solution that is optimized for affordability and provides protection for high current PWM motor drives while consuming a relatively modest amount of board area. The key elements of this MOSFET is shown in Table

3.7. While Figure 3.24 and 3.25 respectively the inside block diagram and inside of this MOSFET.

**BTS 7960B**  
**P-TO-263-7**

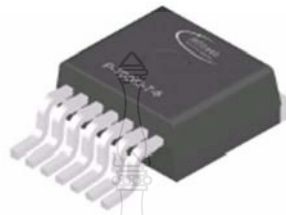


**Figure 3. 23** BTS 7960B MOSFET

**Table 3. 7** Key elements of BTS 7960B

Key Elements
16 m path resistance typical at 25 °C
A typical quiescent current at 25 °C
Active freewheeling in conjunction with PWM if capability up to 25 kHz
Power dissipation in overcurrent is <u>minimized</u> via Switched mode current limitation.
43 A typical of current limitations.
Cwrent sensory capacity and status flag diagnosis
Overtemperature shut off with latching behavior
Voltage overload lockout
Shutdown due to low voltage

Driver circuit with inputs for logic levels
Flexible slew rates for EMI optimization

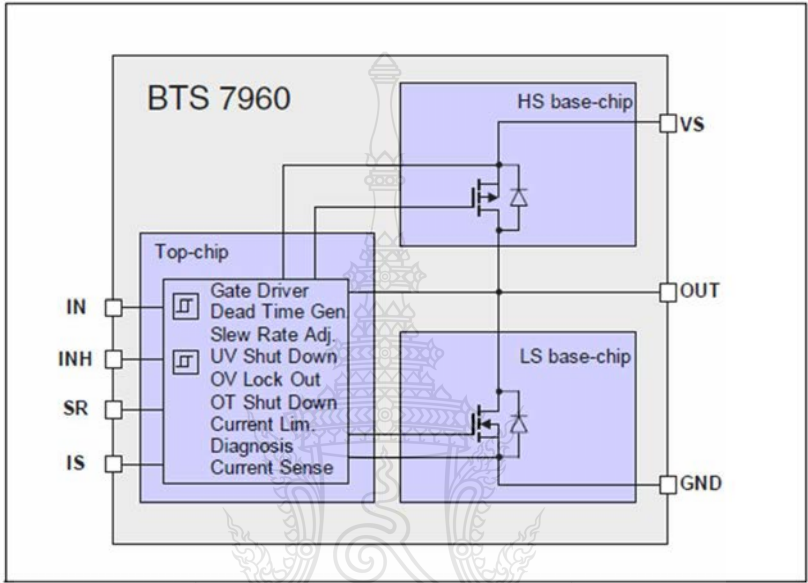


**Figure 3. 24** Inside BTS 7960 IC

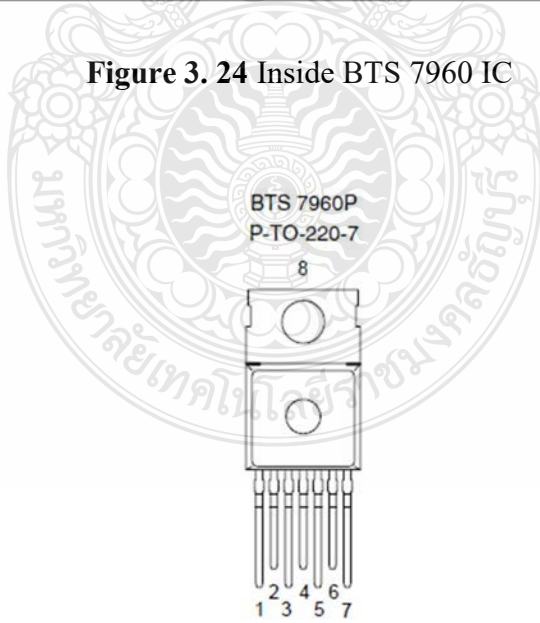


**Figure 3. 25** Pinout BTS 7960P MOSFET

An adjustable 5 V low drop voltage regulator shown in Figure 3.26 is the TLE4278. It is a 200mA load-supplying monolithic integrated low-drop voltage regulator.  $V_{Q_{nom}} = 5$  V is regulated with an accuracy of 2% from an input voltage  $V_I$  in the range of 5.5 V  $V_I$  45 V. The gadget can function across a wide range of temperatures,  $T_j = -40^{\circ}\text{C}$  to  $150^{\circ}\text{C}$ . The TLE4278 includes two additional features: a load-dependent watchdog feature and a sophisticated reset feature that includes power-on reset, under-voltage reset, adjustable reset delay time, and adjustable reset switching threshold. Both of these features are load-dependent.

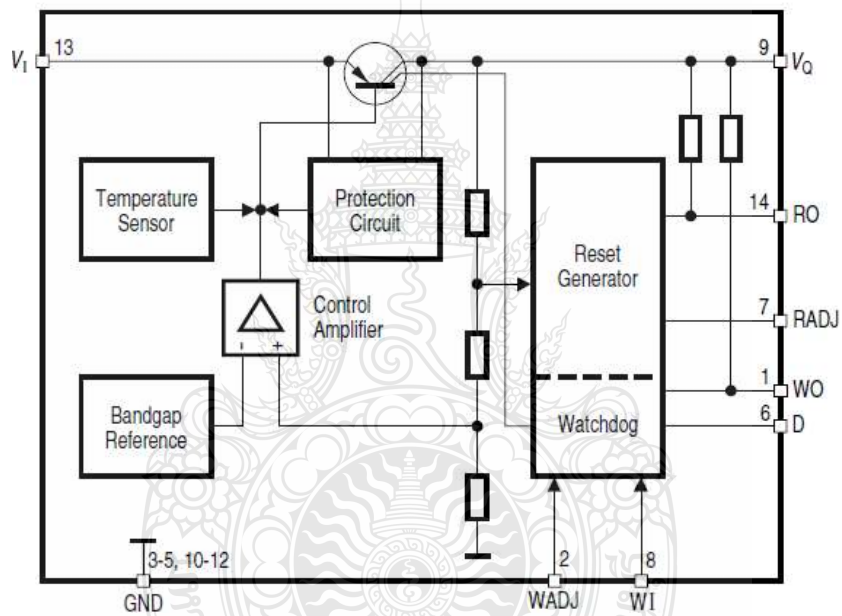


**Figure 3. 26** Block Diagram of TLE4278G

### 3.7.3 DC Motor

This gait trainer uses 4 PG 56 DC motors, one motor for each joint. A PG 56 motor is a type of electric motor that has a power rating of 56 watts and uses a gearbox with a planetary gear system. The motors are commonly used in a variety of applications due to their compact size and high efficiency. The sideview of this motor is shown in Figure 3.27. While Table 3.8 and 3.9 respectively show the gearbox data of the motor

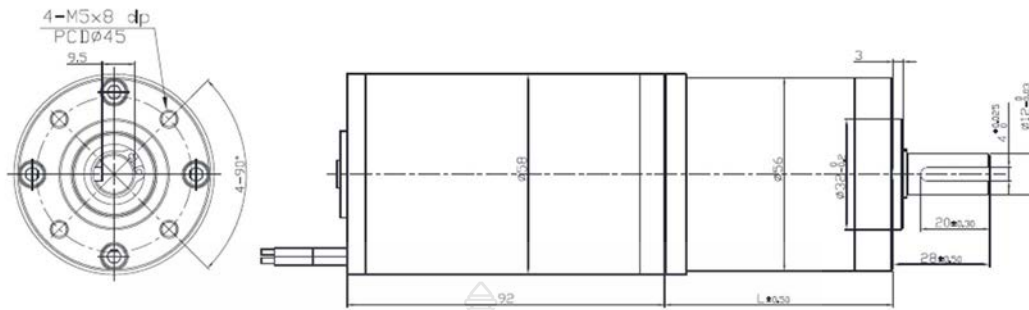


Figure 3. 27 Sideview of PG 56 motor

Table 3. 8 Gearbox data

Gearbox data:					
Number of stages	1 stages reduction	2 stages reduction	3 stages reduction	4stages reduction	5stages reduction
Reduction ratio	3.6, 4.3	13, 19.2, 22.7	46.7, 69, 102, 121,	198, 276, 326, 409, 513,	843, 995, 1567, 1966, 2321, 3439,
Gearbox length "L" mm	38.3	52.2	66.1	80.0	96.4
Max. Running torque	100Kgf · cm	200Kgf · cm	400Kgf · cm	400Kgf · cm	400Kgf · cm
Max. Gear breaking torque	300Kgf · cm	600Kgf · cm	600Kgf · cm	600Kgf · cm	1200Kgf · cm
Gearing efficiency	90%	81%	73%	65%	59%

Table 3. 9 Motor data

Motor data:									
Motor name	Rated Volt. V	No load		Load torque				Stall torque	
		Current	Speed	Current	Speed	Torque	Output power	Torque	Current
		mA	r/min	mA	r/min	gf · cm	W	gf · cm	A
ZY58123000	12	≤480	3000	≤4600	2418	1508	38.1	7594	21.1
ZY58243000	24	≤260	3000	≤2620	2412	1562	39.5	8392	12.4

1、 After connecting motor and gearbox which is named gearmotor the output torque: motor torque X reduction ratio X gearing efficiency; output speed: motor speed / reduction ratio.



### 3.7.4 Gearbox

The additional gearbox connected to the motor is NMRV 030 HOLLOW SHAFT RATIO 1:75 -1:100 GEARBOX YUEMA. Shown in Figure 3.28 is the mechanical drawing of this gearbox.

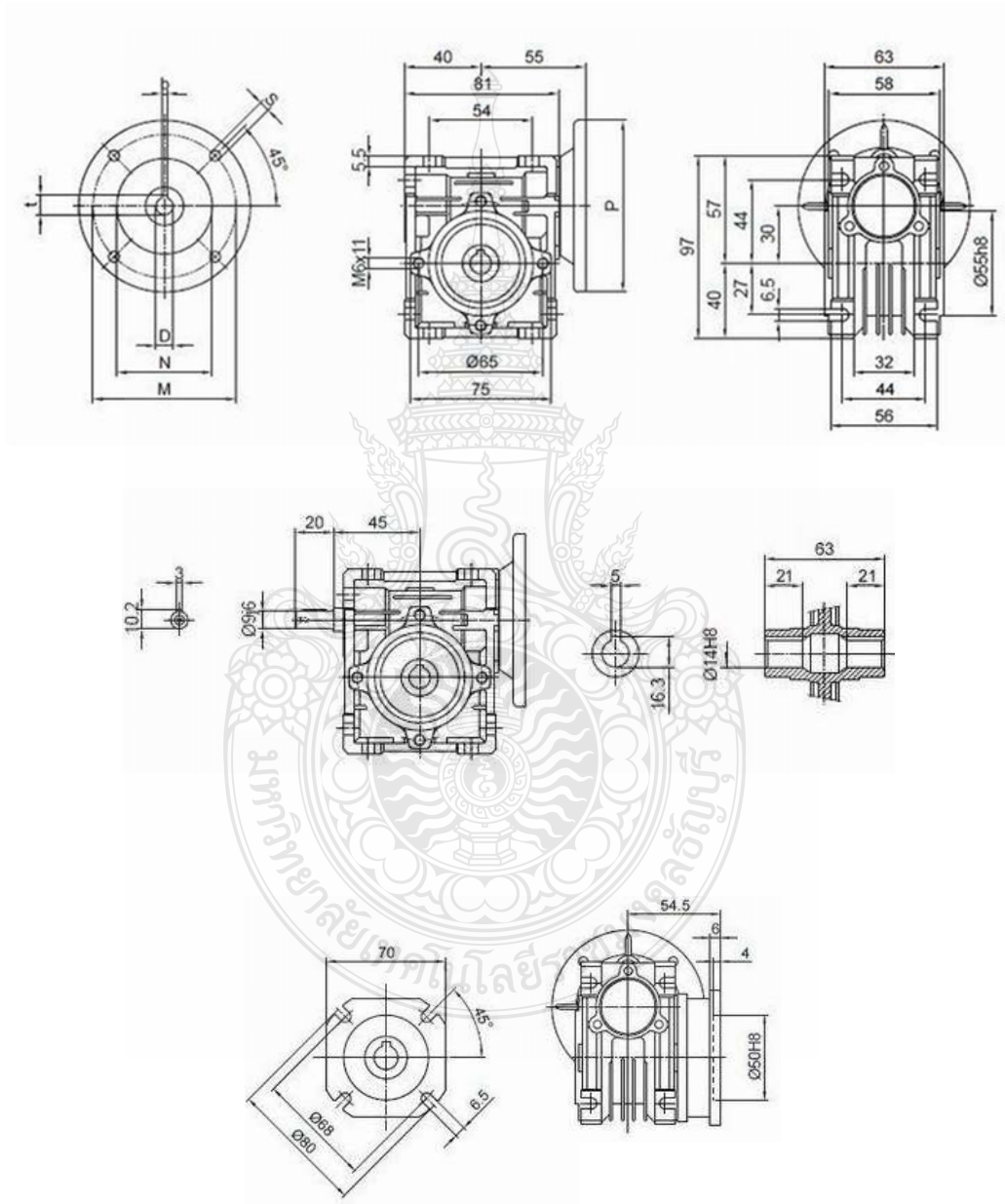


Figure 3.28 Yuema Gearbox

## CHAPTER 4

### RESULTS AND DISCUSSION

#### 4.1 Hybrid Proportional Integral Derivative Iterative Learning Control for Robot-Assisted Gait Trainer

##### 4.1.1 Advantage of Iterative Learning Control (ILC)

Indefinitely repeatable process control is possible via iterative learning control, or ILC for short (Owens, 2016). The exoskeleton robot has dynamic properties such as high nonlinearity, strong coupling, and time-varying features. Instability in system performance may result from the planned controller if the mathematical model used to create it is unclear. Iterative learning-based control stands out due to its fundamental learning mechanism, which is independent of the system's detailed model. It is suitable for a movable object under control that travels in a predetermined amount of time. A lower limb exoskeleton robot's dynamics model is used to modify the tracking error to the learning signal in order to refine control over a desired trajectory (Ke et al., 2017). 4.1 depicts the block diagram of the combined PID and ILC control system, where:

$u_j$ : value of ILC control signal

$k_p$ : value of proportional gain

$k_d$ : value of derivative gain

$k_i$ : value of integral gain

$e_j$ : value of error between desired and actual outputs ( $y_d - y_j$ )

$j$ : number of iterations

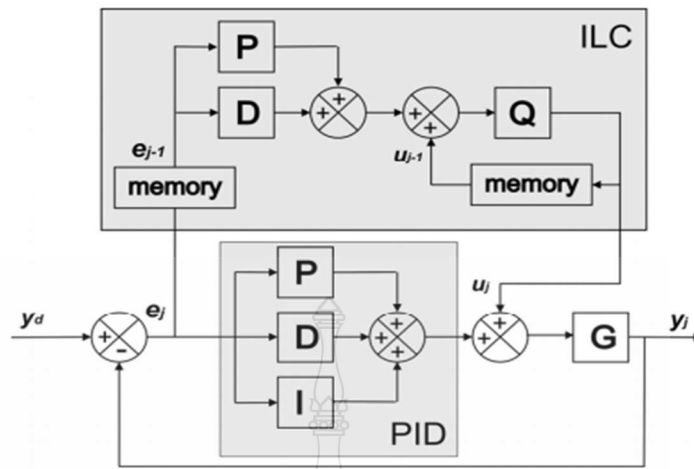


**Figure 4. 1** Schematic representation of a hybrid PID-ILC system

#### 4.1.2 Dataset of normal gait

A typical walking pattern that was used as the reference trajectory in this study was obtained from a dataset of healthy people that was taken from earlier investigations (Bovi et al., 2011). The data was used to create graphs depicting hip and knee flexion and extension (figures 4.2 and 4.3, respectively). Hip flexion and extension can occur between -18 and 25 degrees, as shown in Figure 4.2. Figure 4.3 illustrates that the knee can flex and extend anywhere between 0 and 60 degrees.

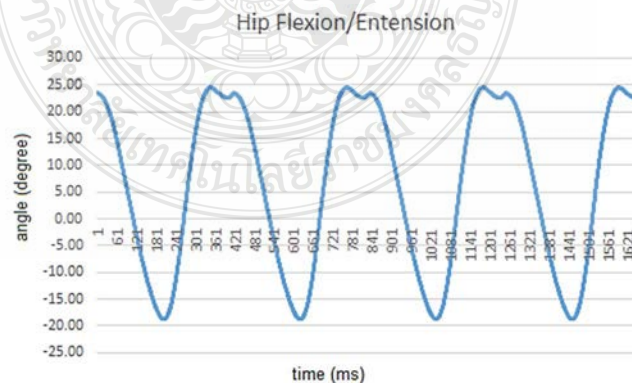


**Figure 4. 2** Hip flexion and extension based on the dataset

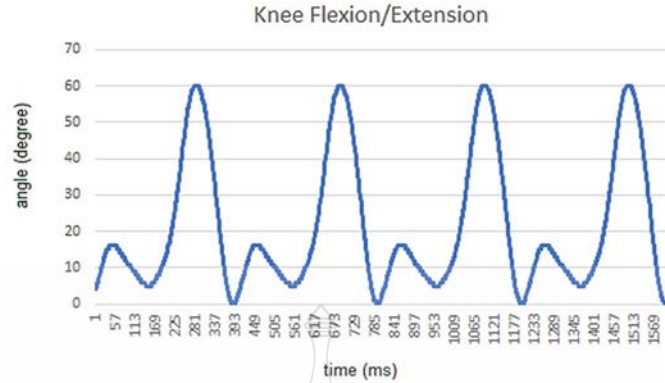


**Figure 4.3** Knee flexion and extension depending on the dataset

#### 4.1.3 Result and discussion

The DC motor is guided along the programmed path by the microcontroller's control algorithm after receiving the gait data from the drivers. The hybrid PID-ILC method is implemented in two stages. In the first place, the ILC can be skipped and achieve stability by setting the PID control's  $K_p$ ,  $K_i$ , and  $K_d$  parameters. The PID adjustment can be done using Table 4.1 as a guide. The ILC learning method can be activated once the PID response has stabilized.

**Table 4.1** PID controller tuning parameters

RESPONSE	RISE TIME	OVERSHOOT	SETTLING TIME	S-S ERROR
<b><math>K_p</math></b>	Decrease	Increase	Small Change	Decrease
<b><math>K_i</math></b>	Decrease	Increase	Increase	Decrease
<b><math>K_d</math></b>	Small Change	Decrease	Decrease	No Change

(SOURCE:<https://ctms.engin.umich.edu/CTMS/index.php?example=Introduction&section=ControlPID>)

The exoskeleton's hip and knee joints are depicted in Figures 4.4–4.7. Figures 4.4 and 4.6 show that, despite the large steady-state error introduced by PID, the system maintains stability. As can be seen in Figure 4.4, hip motion is being regulated by a PID-only controller. The exoskeleton shifted as the weight was transferred from the leg. Hip flexion/extension

can occur between -15 and 20 degrees. Although the system is reliable, there are 0-10 degree steady-state errors.

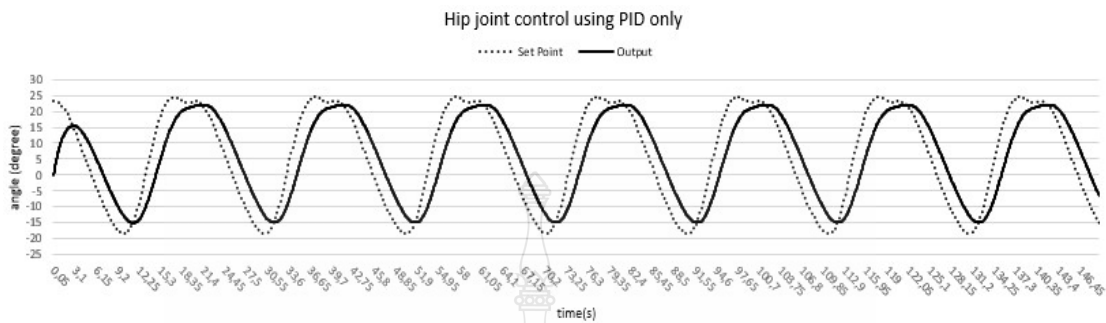


**Figure 4. 4** PID-only hip flexion and extension in an exoskeleton

The hip's motion is controlled using a hybrid PID-ILC controller, as shown in Figure 4.5. Even with no changes to the controller's gain or load, the initial 0–5-degree rotation performs noticeably better. The hip range is approximately the same as the set point, yet steady-state errors after more than ten iterations can be less than 1 degree.

In Figure 4.6, we see that knee motion is being controlled by a PID-only controller. With the same controller gain, the exoskeleton followed the lower limb while carrying the same load. Eighty-five degrees of knee flexion and extension is possible. There are errors in the steady state of 0 to 10 degrees, but the system is stable elsewhere.

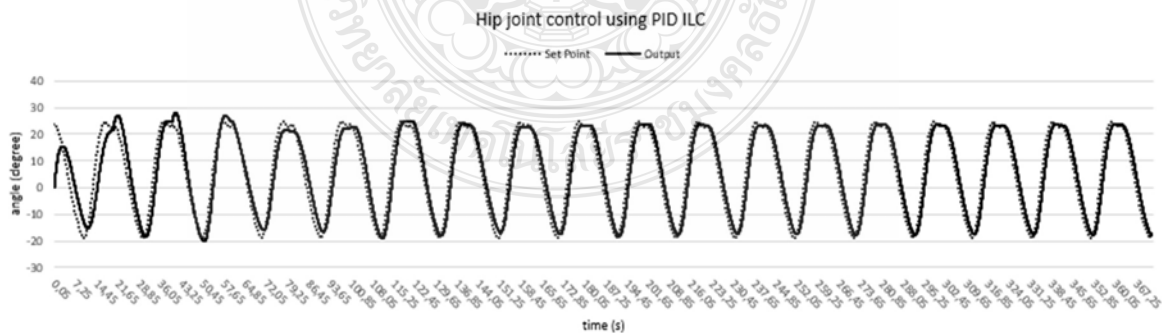


**Figure 4. 5** PID-ILC control of exoskeleton hip flexion and extension

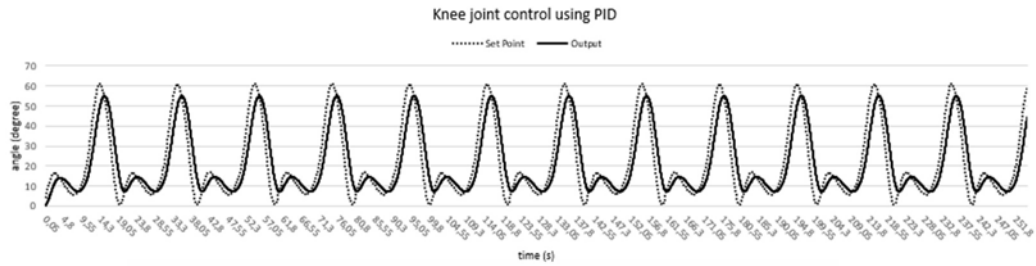


**Figure 4. 6** PID-only control of knee flexion and extension in an exoskeleton

The hybrid PID-ILC controller is shown in action in Figure 4.7, regulating knee motion. Even with no changes to the controller's gain or load, the initial 0–10-degree rotation performs noticeably better. However, after more than 10 repetitions, the steady-state errors can be minimized to a range of 1 degree. Figures 4.5 and 4.7 show that before the required trajectory set point is attained, PID-ILC needs to do more than ten iterations. The output is precise, with a negligible steady-state error.

A system's performance index can be measured or calculated. Here, it is helpful to use measures like mean square error (MSE) and mean square error (MSE). The accuracy with which a model predicts future events is quantified by its root-mean-squared error (RMSE) (Salkind et al., 2010). Table 4.2 displays the results of a numerical analysis that compares the RMSE and MSE of PID and PID-ILC responses. Errors in the steady state are cut by half.

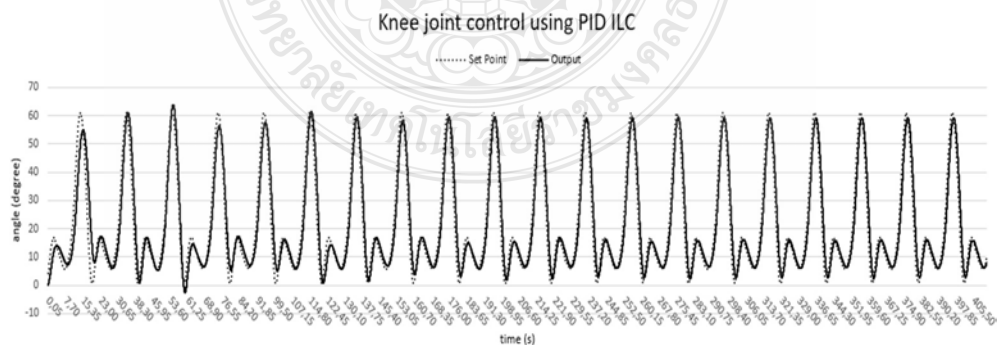


**Figure 4. 7** PID-ILC control of knee flexion and extension in an exoskeleton

Mean square error is characterized as follows:

$$MSE = \frac{\sum_{j=1}^V E_j^2}{V}$$

V: number of data

Root mean square error is characterized as follows:

$$RMSE = \sqrt{\frac{\sum_{j=1}^V E_j^2}{V}}$$

**Table 4. 2** A numerical comparison of the PID-ILC and PID responses

	<b>Control type</b>	<b>RMSE</b>	<b>MSE</b>
<b>Hip</b>	PID	0.141532	0.020031
	PID-ILC	0.080999698	0.01
<b>Knee</b>	PID	0.162832	0.026514
	PID-ILC	0.09	0.01

In spite of unmodeled dynamics, uncertainty, and disruption, the recommended PID-ILC hybrid controller enables an exoskeleton to track the gait trajectory. Using a certain load and controller gain, the experiment demonstrated that although being reliable, the PID-controlled system shows steady-state errors of up to 10 degrees. Despite an early steady-state error, the suggested hybrid PID-ILC controller proved to be stable.. An error of less than 1 degree at steady state can be achieved with more than ten iterations. At steady sate, errors are reduced by half.

## 4.2 Enhancing the lower limb exoskeleton using computed torque.

### 4.2.1 Computed torque control

As time goes on, more and more control systems for robots are being proposed as alternatives. Research in the 1970s led to the development of the first computed torque controller (Paul, 1972). However, as a result of further investigation, there are issues with its real-world implementation (e.g. computational complexity and faulty models).(Lynch & Park, 2017). Computed torque control (CTC) is a non-linear feedback linearization approach. Also known as inverse dynamics control (IDC), the computed torque control is dependent on

the inversion of the robot dynamics (Sharkawy et al., 2019). Introducing the concept of a servo, modeled as a PD controller, computed torque controls provide a linearization to address the non-linearities present in the dynamics of the manipulator. Figure 4.8 displays the block diagram for the computed torque control method. Implementing feedback linearization can be demanding in terms of time and resources, making it challenging to universally transform a nonlinear system into a linear one. The experiment shows that calculated torque controllers demonstrate strong and resilient performance characteristics (R. Murray et al., 1994)(Oriolo et al., 2002)(Meddahi et al., 2020)(Belda-Lois et al., 2011)(Sutyasadi, 2022). Several successful studies utilizing the computed torque control algorithm have been conducted (Meddahi & Meguenni, 2019)(Atit Shah & Rattan, 2016)(Abdel-Salam & Jleta, 2020). However, a drawback of computed torque controls is the necessity for real-time computation of system dynamics related to tracking (Jarzebowska, 2012). Take into account the control input provided below:

$$\tau = H(q)v + \dot{C}(q, \dot{q})\dot{q} + \tau_g(q) \quad (4.1)$$

Known as computed torque control, this system is made up of:

1. A feedback loop to address nonlinearity
2. A secondary loop that takes an input from an outside source

If these control concepts are incorporated into the dynamic model of the robotic arm,

$$\ddot{q} = v$$

The utilisation of this control input simplifies the intricate task of developing a nonlinear controller by reducing it to the straightforward task of creating a linear system with  $n$  subsystems.

The utilisation of Propositional Derivative feedback represents a technique for regulating the outer loop  $v$ .



$$v = \ddot{q}_d + K_V \dot{e}_q + K_P e_q \quad (4.2)$$

This results in the overall dominant input into

$$\tau = H(q) + (\ddot{q}_d + K_V \dot{e}_q + K_P e_q) + C(q, \dot{q})\dot{q} + \tau_g(q) \quad (4.3)$$

resulting in linear error dynamics that are

$$\ddot{e}_q + K_V \dot{e}_q + K_P e_q = 0 \quad (4.4)$$

According to the theory of linear systems, it is predicted that the error in tracking would ultimately converge to zero.

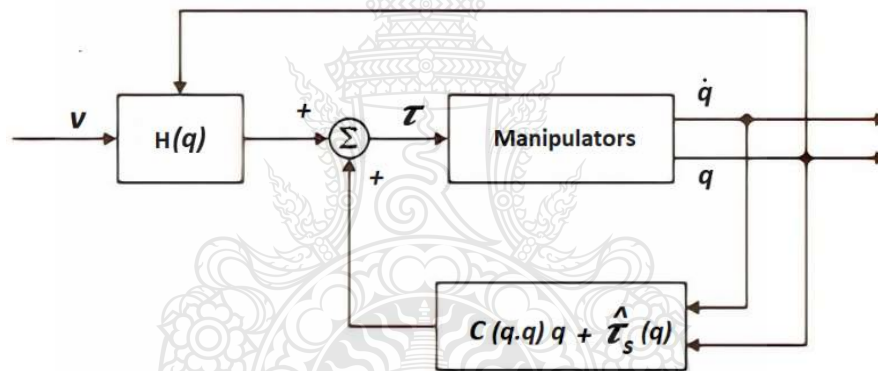


**Figure 4.8** Control technique utilizing computed-torque

(SOURCE: Springer Handbook of Robotics (2nd ed.). Springer, 2016)

Computed Torque Control (CTC) is a highly reliable motion control technique used in robot control systems. It ensures global asymptotic stability. However, a traditional closed-loop trajectory control (CTC) system can only be effectively utilised if an accurate and comprehensive dynamic model of a manipulator is available (C. Chen et al., 2018). Figure 4.9 presents a comparison between the Lokomat, a low-cost gait trainer, and the 2 links model. The parameters of a two-link model are displayed in Table 4.3.

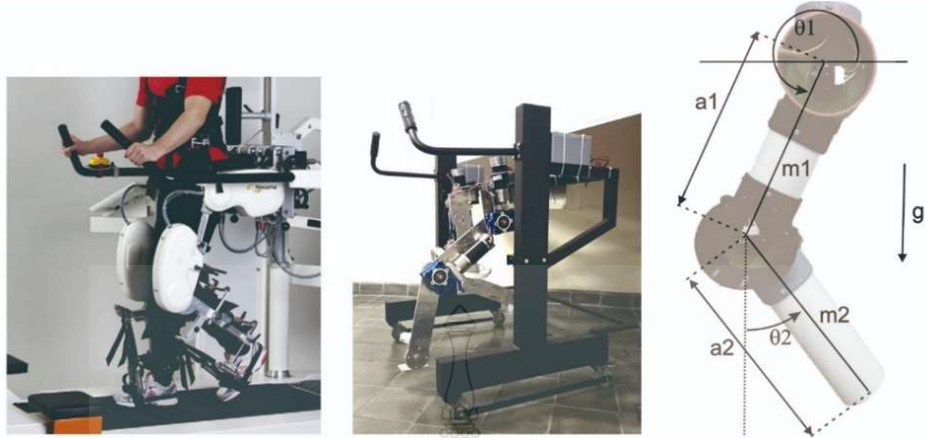


**Figure 4.9** Robot assisted gait trainers (a) Lokomat® from Hocoma; (b) the low-cost version of gait trainer;(c)2 links kinematics model

**Table 4.3** Parameters with two links

Parameters	Units	Values
Link 1 (L1)	m	0.2
Link 2 (L2)	m	0.215
L1 mass (m1)	kg	0.2
L2 mass (m2)	kg	0.2
Gravity (g)	m/s <sup>2</sup>	9.8

#### 4.2.2 Microcontroller and motor driving circuit

A miniature prototype was utilised in this experiment. Figure 4.10 illustrates the utilisation of two DC motors to drive the two links in the mechanism, with encoders employed as position sensors. The motor control is achieved by utilizing the Monster Moto Shield VNH30SP DC motor driver circuit and Arduino Uno microcontroller. Arduino is the main controller, which is built around the ATmega 328 microcontroller. The VNH30SP motor controller part amplifies the electric current being supplied to the motor. The encoder will deliver information about the current position of the link with a sample interval of 10

ms. The microcontroller will employ the computed torque control method to determine the suitable PWM value for transmission to the drive circuit.

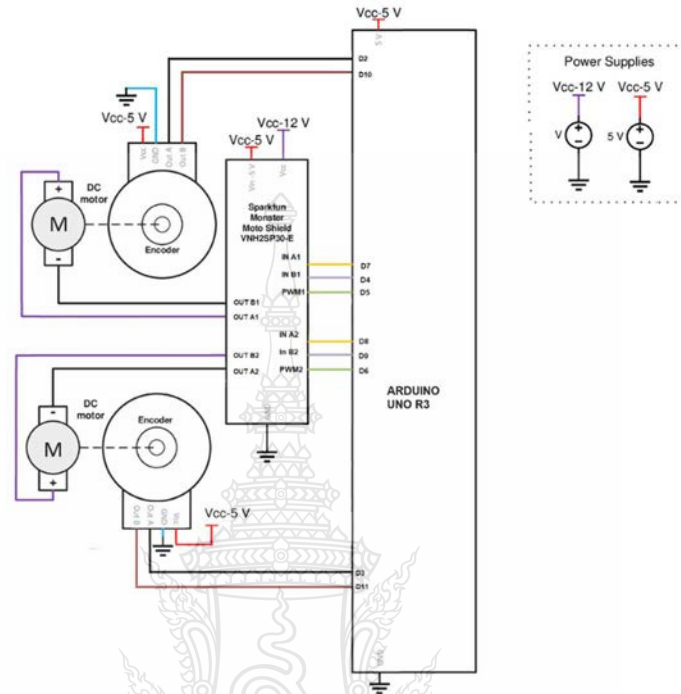


**Figure 4. 10** Diagram illustrating the experimental setup

#### 4.2.2.1 Monster Moto Shield VNH30SP driver

Figure 4.11 illustrates the utilisation of a Monster Motor shield (VNH2SP30) dual shield for motor propulsion. This motor shield contains a pair of VNH2SP30 full-bridge motor drivers. The VNH2SP30 twin monster motor shield can reliably support the operation of two motors with a maximum current of 12A, provided that adequate heat dissipation measures are in place. The Monster Motor shield (VNH2SP30) is capable of operating two DC motors within a voltage range of 5.5 to 16 volts. Additionally, it has the capability to deliver a maximum current of 30A and 6A without the need for a heat sink per channel. The system is capable of diagnosing the output and identifying thermal shutdown and other similar types of malfunctions. This board has the capability to function independently or as

an extension to any Arduino board. The operational ratings of this board are displayed in Table 4.4, and the schematic of the board may be found in Figure 4.12.

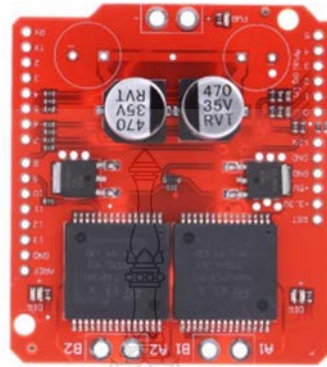


**Figure 4. 11** Monster Motor shield (VNH2SP30)

**Table 4. 4** Operating ratings of Monster Moto Shield

<b>Operating Ratings</b>	
Voltage Range	5.5-16V DC
Max current (peak)	30A
Max current (sustained)	12-14A (with heat sink)

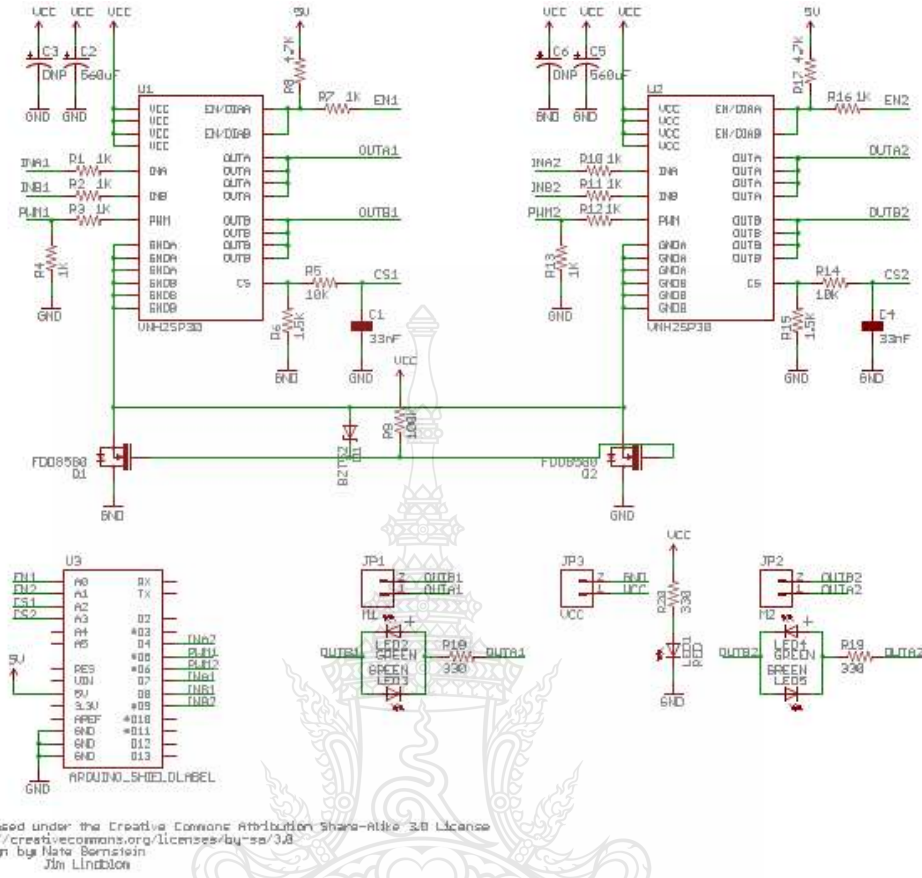


**Figure 4. 12** DC motor driver schematic (Sparkfun monster motoshield)

The crucial component of the Monster Motor shield is the VN125P30-E, a full bridge motor driver specifically engineered for a wide range of automotive uses. The component consists of two low side switches and a dual monolithic high side driver. The attribute of this component is displayed in Table 4.5.

**Table 4.5** Characteristics of VNH2SP30-E

Compatible inputs at the 5V logic level
Shutdowns caused by low voltage and high voltage
Exceeding voltage limit
Power off due to temperature
safeguarding against cross-conduction
Current limiter with linearity
Superb standby power efficiency
Operate at a pulse width modulation (PWM) of up to 20 kHz
Defense against falling below ground and losing VCC
Measurement of current as a function of motor current

#### 4.2.2.2 DC Geared Motor w/Encoder JG25-310

The geared motor utilises a gear set to transform the motor's initial high speed and low torque into a low speed and high torque configuration. Geared motors are commonly employed when a substantial amount of torque is required. Figure 4.13 and 4.14 depict the JG25-370 geared dc motor, illustrating its front view and side view, respectively. Figure 4.15 displays the wiring diagram, and Table 4.6 presents the datasheet of the encoder.

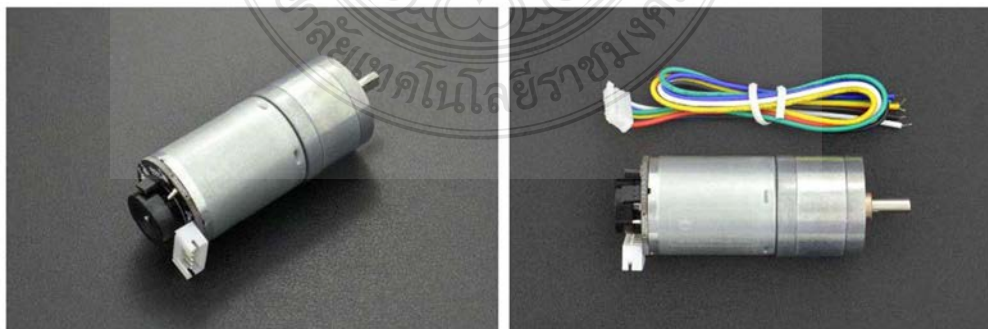


**Figure 4.13** JG25-370 Geared DC motor

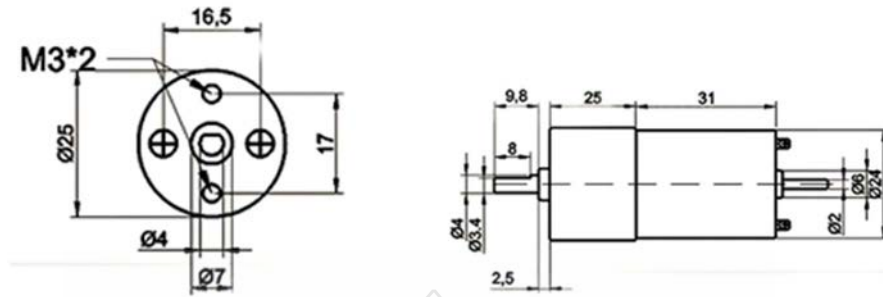


Figure 4.14 JG25-370 Geared DC motor (a) front view (b) side view

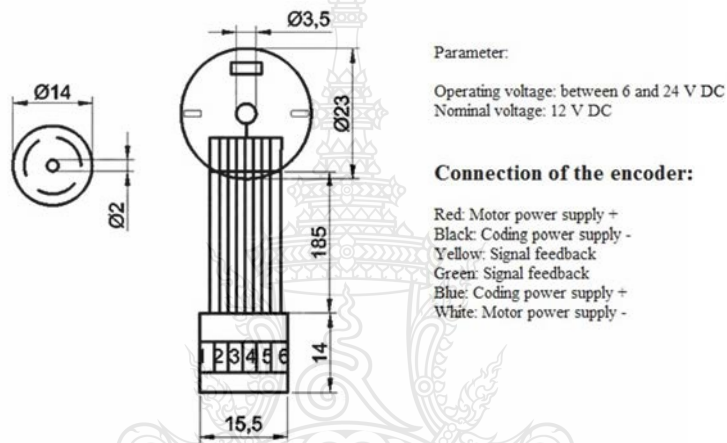


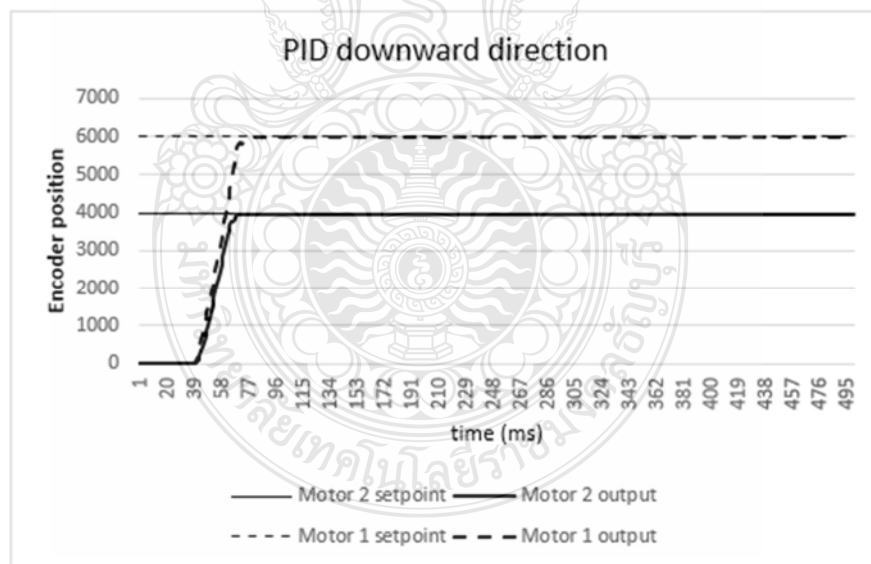
Figure 4.15 Wiring diagram of the encoder

Table 4.6 Datasheet of the encoder

Model JGA 25-371		Datasheet										
Voltage		No Load		Load				Stall		Reducer		Weight
Workable Range	Rated Voltage	Speed	Current	Speed	Current	Torque	Output	Torque	Current	Ratio	Size	Unit
		rpm	mA	rpm	mA	kg.cm	W	kg.cm	A	1:00	mm	g
6-24V	12	977	46	781	300	0.11	1.25	0.55	1	44	15	99
6-24V	12	463	46	370	300	0.23	1.25	1.1	1	9.28	17	99
6-24	12	201	46	168	300	0.53	1.25	2.65	1	21.3	19	99
6-24V	12	126	46	100	300	0.85	1.25	4.2	1	34	21	99
6-24	12	95	46	76	300	1.1	1.25	5.5	1	45	21	99
6-24V	12	55	46	44	300	1.95	1.25	9.7	1	78	23	99
6-24V	12	44	46	32	300	2.5	1.25	12.5	1	103	23	99
6-24	12	25	46	20	300	42	1.25	21	1	171	25	99
6-24	12	19	46	15	300	5.6	1.25	28	1	226	25	99
6-24V	12	11	46	8.8	300	9.45	ACO	47	1	378	27	99
6-24V	12	8.6	46	6.8	300	12	1.25	60	1	500	27	99

### 4.2.3 Results and discussion

Figures 4.16 and 4.17 depict the encoders position when a PID controller is employed, whereas Figures 4.18 and 4.19 illustrate the encoders position when the computed torque controller is utilised. The findings produced from both controllers are being compared. The graphs clearly demonstrate that both PID and CTC are effective in reducing overshoot. Both controllers exhibit satisfactory performance in downward movements but require improvement in upward movements due to the added gravitational force acting as a disturbance. Figure 4.16 depicts the graph illustrating the vertical movement of motor 1 and motor 2 when controlled by the PID controller. For motor 1, the parameters have the following values:  $K_p = 0.5$ ,  $K_i = 0.01$ , and  $K_d = 1.1$ . Similarly, for motor 2, the values are  $K_p = 0.5$ ,  $K_i = 0.01$ , and  $K_d = 1.1$ . Under those conditions, the PID controller worked well. Motor 1's steady-state error is 0.0167% and its rise time is 25 ms. The steady-state error is 0.75% and the rise time is 19 ms at motor 2.



**Figure 4.16** The graph displays the relationship between the setpoint and the PID output in the downward direction.



The diagram depicted in Figure 4.17 showcases the vertical displacement of motor 1 and motor 2 under the influence of the PID controller. The values of the parameters for motor 1 are as follows: the proportional gain ( $K_p$ ) is 0.5, the integral gain ( $K_i$ ) is 0.01, and the derivative gain ( $K_d$ ) is 1.1. Similarly, for motor 2, the values of  $K_p$ ,  $K_i$ , and  $K_d$  are also 0.5, 0.01, and 1.1 respectively. Motor 2 exhibited poor performance with the PID controller, resulting in a steady-state error above 5%. The PID controller is unable to manage a gravitational disturbance. Motor 1 has a rise time of 21 ms and a steady-state error of 0.1%. Motor 2 exhibits a rise time of 17 milliseconds, with a steady-state error of 5.6%.

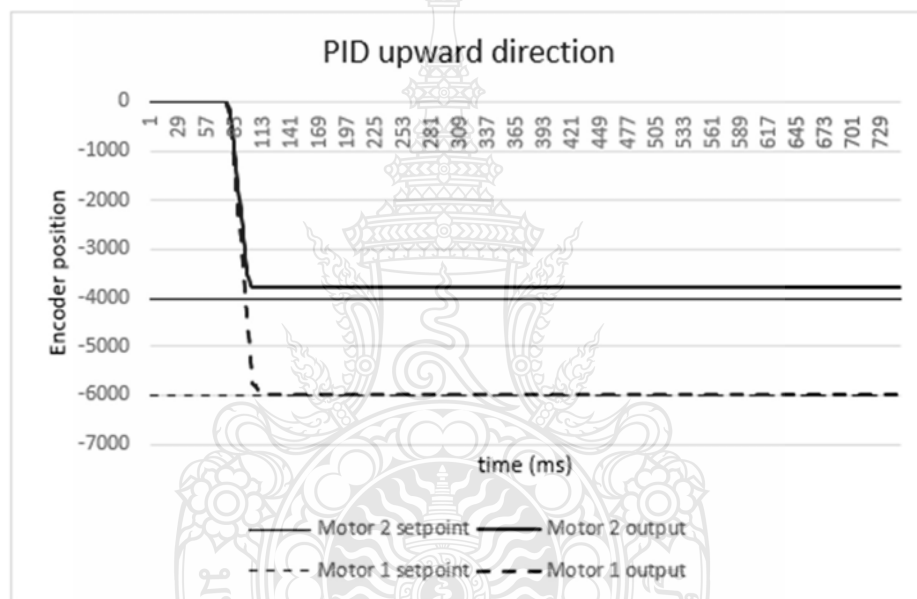


**Figure 4. 17** The graph displays the correlation between the setpoint and the PID output in the upward direction.

The plot in Figure 4.18 illustrates the downward movement of motor 1 and motor 2, controlled by the CTC controller. Motor 1 is characterized by a proportional gain ( $K_p$ ) set at 4, an integral gain ( $K_i$ ) at 0.001, and a derivative gain ( $K_d$ ) at 0.0005. On the other hand, for motor 2, the proportional gain ( $K_p$ ) is 0.35, the integral gain ( $K_i$ ) is 0.001, and the derivative gain ( $K_d$ ) is 0.0005. The CTC controller performed effectively in this scenario, although there was a minor residual error at motor 2 in the steady-state. Motor 1 has a rise time of 21

ms and a steady state error of 1.04%. Motor 2 has a rise time of 30 ms and a steady-state error of 2.175%.

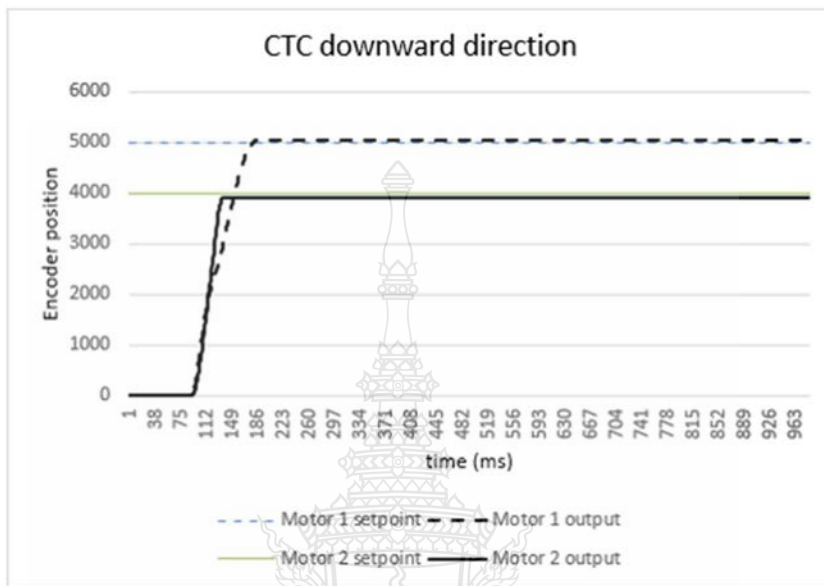


**Figure 4. 18** The graph displays the relationship between the setpoint and the output of the CTC in the downward direction.

Figure 4.19 displays the trajectory of motor 1 and motor 2 positions during upward motion using CTC. The values assigned to the parameters of motor 1 are as follows:  $K_p = 4$ ,  $K_i = 0.001$ , and  $K_d = 0.0005$ . On the other hand, the parameters of motor 2 have the following values:  $K_p = 0.35$ ,  $K_i = 0.001$ , and  $K_d = 0.0005$ . The CTC demonstrated exceptional performance in these circumstances. As previously stated, the computed torque controller approach compensates for the influence of gravity. Motor 1 exhibits a steady state error of 1.74% and a rise time of 44 ms. Simultaneously, motor 2 exhibited a rise time of 25 milliseconds and a steady-state error of 2.125%.

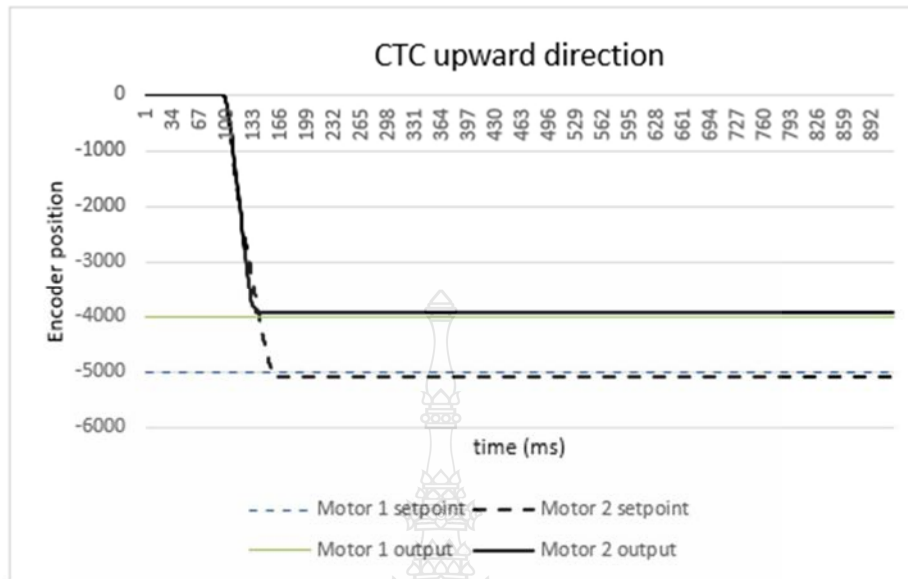


**Figure 4. 19** The graph displays the correlation between the setpoint and the output of the CTC in upward direction

The performance parameters, such as overshoot, rise time, and steady state error, for both PID and CTC controllers in both upward and downward motion are displayed in Tables 4.7 and 4.8, correspondingly. While the CTC controller outperforms the PID controller in handling disturbances, such as gravity, the PID controller exhibits a quicker rise time.

**Table 4. 7** Evaluation of the performance of PID controller in both the downward and upward directions

		rise time	steady state error	overshoot
<b>PID in downward motion</b>	M1	25 ms	0.0167%	-
	M2	19 ms	0.75 %	-
<b>PID in upward motion</b>	M1	21 ms	0.1 %	-
	M2	17 ms	5.6 %	-

**Table 4. 8** Evaluation of the performance of CTC controller in both the downward and upward directions

		rise time	steady state error	overshoot
<b>downward motion of CTC</b>	M1	64 ms	1.04 %	-
	M2	30 ms	2.175 %	-
<b>upward motion of CTC</b>	M1	44 ms	1.74 %	-
	M2	25 ms	2.125 %	-

In order to evaluate the performance, one can compute or assess the system performance index. Both the mean square error (MSE) and the root mean square error (RMSE) are applicable in this case. The abbreviation MSE stands for the mean squared error, which is calculated as the square of the root mean squared error (RMSE). The Root Mean Square Error (RMSE) is a statistical measure that compares the real values with the predictions produced by a theoretical framework (Salkind et al., 2010).

The representation of mean square error is as follows:

$$MSE = \frac{\sum_{j=1}^V E_j^2}{V}$$

V: quantity of data

The formula for root mean square error is as follows:

$$RMSE = \sqrt{\frac{\sum_{j=1}^V E_j^2}{V}}$$

Tables 4.9 and 4.10 present a quantitative comparison of the responses of the PID and CTC systems, as indicated by the RMSE and MSE.

**Table 4. 9** Numerical analysis is used to compare the responses of CTC and PID (upward direction).

<b>Joints</b>	<b>Type of control</b>	<b>RMSE</b>	<b>MSE</b>
<b>M1</b>	PID	35.83	861605.63
	CTC	31.22	895538.63
<b>M2</b>	PID	604.61	406298.42
	CTC	16.31	244404.95

**Table 4. 10** Numerical analysis is used to compare the reactions of CTC and PID (downward direction).

<b>Joints</b>	<b>Type of control</b>	<b>RMSE</b>	<b>MSE</b>
<b>M1</b>	PID	92.40	3944754.63
	CTC	54.44	2913817.40
<b>M2</b>	PID	61.11	1721801.91
	CTC	217.34	213643.10

The measurement of Root Mean Squared Error (RMSE) Mean Squared Error (MSE) clearly demonstrates that CTC consistently outperforms PID in terms of response quality during upward fluctuations. Nevertheless, when it comes to the downward direction, the performance of motor 2 (M2) utilising CTC is inferior to that of PID. The results show that the computed torque controller that is suggested for this two-link model has advantages in efficiently handling disturbances. However, in terms of rise time, the PID controller performs faster than the CTC method. The trials demonstrate that both the CTC and PID controller have the ability to effectively mitigate overshoot. The PID controller is unable to counteract the effects of gravity as a disturbance, however the CTC (Computed Torque Control) method is capable of doing so. As a result, the PID controller may display a downward steady-state error of up to 5.6%.. However, in the case of CTC, this error can be decreased to 2.125%.

The Mean Squared Error (MSE) and Root Mean Squared Error (RMSE) analyses consistently demonstrate that the CTC (Controlled Temperature Control) method consistently outperforms the PID (Proportional-Integral-Derivative) method in terms of response. Nevertheless, when it comes to descending motion, the performance of motor 2 (M2) employing CTC surpasses that of PID.



## CHAPTER 5

### CONCLUSIONS AND FUTURE WORKS

#### 5.1 Conclusions

Robots for gait therapy have the potential to improve patient safety, lessen the workload on therapists, and open up new training opportunities. It is crucial to patients' lower limb rehabilitation and assistance, and it can help them get in a better state of health. Although there are robot-powered walking trainers on the market, they are still somewhat expensive. The ability to "do more with less"—that is, to produce a significant increase in commercial and social benefit while utilizing less limited resources like electricity, money, and time—is referred to as frugal innovation. When faced with limited resources, medical professionals frequently come up with creative ways to treat patients effectively. Despite their shortcomings, these inexpensive, useful, and thrifty products have the potential to provide accessibility to wellness for all.

Proportional integral and derivative (PID) controllers are the most often used due to their excellent reliability and ease of installation, making them highly dependable. A PID-only controller, however, is not well suited to an exoskeleton robot due to variables such as load variations, friction, and external interference. It is hoped that greater performance will result from integrating PID control with other controls. A gait trainer with a lower limb exoskeleton has been created in this research. On these two links in the exoskeleton, two different controller types—the Hybrid PID-ILC and the Computed Torque Control algorithm—have previously been implemented and tested. The dynamics and kinematics of the two-link mechanism have been analyzed using the Lagrangian method.

##### 5.1.1 Hybrid PID ILC

A control method called Iterative Learning Control (ILC) is used to enhance the efficiency of systems that repeat an operation across a number of iterations. It is frequently used in motion control, manufacturing, and robotics applications. Even in situations where there are uncertainties or unmodeled dynamics in the system, the objective is to decrease mistakes and enhance control.

If there are unmodeled dynamics in a system, then there isn't a precise mathematical model of all the parts and interactions in the system that the control system is using. Because a typical control system depends on an accurate model for control, this might cause problems during the

design process. In order to solve this problem, ILC learns from prior iterations and gradually modifies the control input in light of the mistakes made in earlier cycles. By utilizing past data, it enhances control performance and efficiently makes up for uncertainties and unmodeled dynamics in the system. Iterative learning control, which makes use of the system's performance history to modify control inputs repeatedly and enhance overall control performance, is a helpful technique for systems with unmodeled dynamics.

The proposed hybrid PID-ILC controller allows a robot-assisted gait trainer to follow the gait trajectory in the presence of unmodeled dynamics, uncertainty, and disruption. The real experiment utilizing a specific load and controller gain revealed that the PID-controlled system is only stable with steady-state faults of up to 10 degrees. With its initial steady-state error, the suggested hybrid PID-ILC controller displayed stability. The steady-state error can be decreased to under 1 degree, though, after more than ten iterations. 50% is a significant reduction from the steady-state errors.

### **5.1.2 Computed Torque Control**

In robotics, computed torque control, sometimes referred to as computed torque modeling, is a control technique that is frequently used to raise the precision and efficiency of robot manipulators. Another name for it is the "inverse dynamics control" technique. Computed torque control's main concept is to calculate the torques, or forces, necessary to produce desired joint motions and then utilize that knowledge to control the robot.

The primary benefit of computed torque control is that it enables robotic manipulators to be precisely and flexibly controlled, enabling them to perform intricate tasks with exceptional accuracy. In addition, it has the ability to adjust to changes in load circumstances and the environment. When implementing computed torque control on robotic systems, researchers and engineers frequently utilize control methods and simulation tools. It is essential to increasing the adaptability and capability of robots in a variety of settings, such as automation, research, and production. This two-link model in this study benefits from a computed torque controller, which helps it deal with disturbances. When it comes to rising time, nevertheless, the PID controller remains ahead of CTC. Both the PID controller and the CTC are able to suppress overshoot, according to the experiments. While CTC is able to compensate for gravity as a disturbance, PID controllers are unable to do so. Consequently, the PID controller's steady-state error can reach



5.6% in the down direction, but it can be lowered to 2.125 % in the up direction using the CTC. A comparison of CTC vs PID using MSE and RMSE reveals that CTC consistently outperforms PID. On the other hand, motor 2 (M2) responds better to downward movement when CTC is used instead of PID.

## 5.2 Future Works

The exoskeleton needs to be entirely completed before it can be tested on real patients. This will ensure that the exoskeleton joints, as well as the structural parts and connections, are evaluated for comfort. After that, work on a thesis will continue to be done on the high/low level control of the exoskeleton regarding the scalability of the system. Because of this, it is necessary to adjust the trajectories of all the patients' joints considering their diseases, ages, sizes, and weights.

The following list provides recommendations for conducting supplementary studies and implementing necessary enhancements to ensure the device's readiness for clinical application:

- Conducting experiments involving diverse patient populations would be advantageous in order to gain insights into which populations are most suitable for utilizing the device.
- Further investigation can be conducted to establish a stronger connection between the design of the specific needs of therapy. This research has the potential to lead to the creation of software modules designed for addressing specific impairments.
- Different conceptualizations of support can be formulated and assessed within clinical trials involving patients. This assignment may include the integration of data from many methods, such as electromyography (EMG) and electroencephalography (EEG), or the implementation of algorithms that adapt assistance in response to a user's level of effort.

## List of Bibliography

- Abdel-Salam, A.-A. S., & Jleta, I. N. (2020). Fuzzy logic controller design for PUMA 560 robot manipulator. *IAES International Journal of Robotics and Automation (IJRA)*, *9(2)*, 73. <https://doi.org/10.11591/ijra.v9i2.pp73-83>
- Akdoğan, E., & Adli, M. A. (2011). The design and control of a therapeutic exercise robot for lower limb *rehabilitation*: Physiotherobot. *Mechatronics*, *21(3)*, 509–522. <https://doi.org/10.1016/j.mechatronics.2011.01.005>
- Alan T. Asbeck, R. J. D. (2013). **Biologically-inspired Soft Exosuit**. *2013 IEEE International Conference on Rehabilitation Robotics*.
- Aliman, N., Ramli, R., & Haris, S. M. M. (2017). Design and development of lower limb exoskeletons: A survey. *Robotics and Autonomous Systems*, *95*, 102–116. <https://doi.org/10.1016/j.robot.2017.05.013>
- Alouane, M. A., Huo, W., Rifai, H., Amirat, Y., & Mohammed, S. (2019). Hybrid FES-Exoskeleton Controller to Assist Sit-To-Stand movement. *IFAC-PapersOnLine*, *51(34)*, 296–301. <https://doi.org/10.1016/j.ifacol.2019.01.032>
- Amatachaya, S., Naewla, S., Srisim, K., Arrayawichanon, P., & Siritaratiwat, W. (2014). Concurrent validity of the 10-meter walk test as compared with the 6-minute walk test in patients with spinal cord injury at various levels of ability. *Spinal Cord*, *52(4)*, 333–336. <https://doi.org/10.1038/sc.2013.171>
- Aoyagi, D., Ichinose, W. E., Harkema, S. J., Reinkensmeyer, D. J., & Bobrow, J. E. (2005). **An assistive robotic device that can synchronize to the pelvic motion during human gait training**. *Proceedings of the 2005 IEEE 9th International Conference on Rehabilitation Robotics, 2005*, 565–568. <https://doi.org/10.1109/ICORR.2005.1502026>
- Aoyagi, D., Ichinose, W. E., Harkema, S. J., Reinkensmeyer, D. J., & Bobrow, J. E. (2007). A robot and control algorithm that can synchronously assist in naturalistic motion during body-weight-supported gait training following neurologic injury. *IEEE Transactions on Neural Systems and Rehabilitation Engineering*, *15(3)*, 387–400. <https://doi.org/>

- Artemiadis, P. K., & Krebs, H. I. (2010). **On the control of the MIT-Skywalker**. *2010 Annual International Conference of the IEEE Engineering in Medicine and Biology Society, EMBC'10, August 2010*, 1287–1291. <https://doi.org/10.1109/IEMBS.2010.5626407>
- Asseldonk, E. H. F. Van, Ekkelenkamp, R., Veneman, J. F., Helm, F. C. T. Van Der, & Kooij, H. Van Der. (2007). **Selective control of a subtask of walking in a robotic gait trainer ( LOPES )**. *IEEE 10th International Conference on Rehabilitation Robotics, 00(c)*, 841–848.
- Atit Shah, J., & Rattan, S. S. (2016). Dynamic Analysis of Two Link Robot Manipulator for Control Design Using PID Computed Torque Control. *International Journal of Robotics and Automation (IJRA)*, *5(4)*, 277–283. <https://doi.org/10.11591/ijra.v5i4.pp277-283>
- Auvray, M., & Duriez, C. (2014). **Haptics: Neuroscience, devices, modeling, and applications: 9th international conference, EuroHaptics 2014 Versailles, France, June 24-26, 2014 Proceedings, Part I. Lecture Notes in Computer Science (Including Subseries Lecture Notes in Artificial Intelligence and Lecture Notes in Bioinformatics)**, *8618*(June), 0–8. <https://doi.org/10.1007/978-3-662-44193-0>
- Awad, L. N., Kudzia, P., Revi, D. A., Ellis, T. D., & Walsh, C. J. (2020). Walking faster and farther with a soft robotic exosuit: Implications for post-stroke gait assistance and rehabilitation. *IEEE Open Journal of Engineering in Medicine and Biology*, *1*(December 2019), 108–115. <https://doi.org/10.1109/OJEMB.2020.2984429>
- Bai, Y., Li, F., Zhao, J., Li, J., Jin, F., & Gao, X. (2012). **A powered ankle-foot orthoses for ankle rehabilitation**. *IEEE International Conference on Automation and Logistics, ICAL, August*, 288–293. <https://doi.org/10.1109/ICAL.2012.6308213>
- Ball, S. J., Brown, I. E., & Scott, S. H. (2007). **MEDARM: A rehabilitation robot with 5DOF at the shoulder complex**. *IEEE/ASME International Conference on Advanced Intelligent Mechatronics, AIM, October*. <https://doi.org/10.1109/AIM.2007.4412446>
- Banala, S. K., Kim, S. H., Agrawal, S. K., & Scholz, J. P. (2008). **Robot assisted gait training**

**with active leg exoskeleton (ALEX).** *Proceedings of the 2nd Biennial IEEE/RAS-EMBS International Conference on Biomedical Robotics and Biomechatronics, BioRob 2008*, 17(1), 653–658. <https://doi.org/10.1109/BIOROB.2008.4762885>

Banala, S. K., Student, G., & Agrawal, S. K. (2005). **Gait Rehabilitation with An active Leg Orthosis.** *ASME 2005 International Design Engineering Technical Conferences and Computers and Information in Engineering Conference.*

Baratini, P., Federico, V., Virk, G. S., & Haidegger, T. (Eds.). (2019). **Human–Robot Interaction: Safety, Standardization, and Benchmarking.** CRC Press.

Barbeau, H., & Visintin, M. (2003). Optimal Outcomes Obtained With Body-Weight Support Combined With *Treadmill* Training in Stroke Subjects. *The Archives of Physical Medicine and Rehabilitation*, 84(October), 1458–1465. [https://doi.org/10.1053/S0003-9993\(03\)00361-7](https://doi.org/10.1053/S0003-9993(03)00361-7)

Bartlett, R. (2007). **Introduction to sports biomechanics: Analysing human movement patterns (2 nd).** Routledge.

Belda-Lois, J. M., Mena-Del Horno, S., Bermejo-Bosch, I., Moreno, J. C., Pons, J. L., Farina, D., Iosa, M., Molinari, M., Tamburella, F., Ramos, A., Caria, A., Solis-Escalante, T., Brunner, C., & Rea, M. (2011). Rehabilitation of gait after stroke: A review towards a top-down approach. In *Journal of NeuroEngineering and Rehabilitation (Vol. 8, Issue 1)*. <https://doi.org/10.1186/1743-0003-8-66>

Benjamin, E. J., Blaha, M. J., Chiuve, S. E., Cushman, M., Das, S. R., Deo, R., De Ferranti, S. D., Floyd, J., Fornage, M., Gillespie, C., Isasi, C. R., Jim'nez, M. C., Jordan, L. C., Judd, S. E., Lackland, D., Lichtman, J. H., Lisabeth, L., Liu, S., Longenecker, C. T., ... Muntner, P. (2017). Heart Disease and Stroke Statistics'2017 Update: A Report from the American Heart Association. In *Circulation (Vol. 135, Issue 10, pp. e146–e603)*. Lippincott Williams and Wilkins. <https://doi.org/10.1161/CIR.0000000000000485>

Bennett, J., Das, J. M., & Emmady, P. D. (2022). **Spinal Cord Injuries.** *StatPearls*. <https://www.ncbi.nlm.nih.gov/books/NBK560721/>

- Bhatnagar, T., Ben Mortensen, W., Mattie, J., Wolff, J., Parker, C., & Borisoff, J. (2017). **A survey of stakeholder perspectives on a proposed combined exoskeleton-wheelchair technology.** *IEEE International Conference on Rehabilitation Robotics*, 1574–1579. <https://doi.org/10.1109/ICORR.2017.8009472>
- Blaya, J. A., & Herr, H. (2004). Adaptive *Control* of a Variable-Impedance Ankle-Foot Orthosis to Assist Drop-Foot Gait. *IEEE Transactions on Neural Systems and Rehabilitation Engineering*, *April 2004*. <https://doi.org/10.1109/TNSRE.2003.823266>
- Bock, T., & Linner, T. (2016). *Construction Robots*. Cambridge University Press.
- Bortole, M., Venkatakrishnan, A., Zhu, F., Moreno, J. C., Francisco, G. E., Pons, J. L., & Contreras-Vidal, J. L. (2015). The H2 robotic exoskeleton for gait rehabilitation after stroke: Early findings from a clinical study Wearable robotics in clinical testing. *Journal of NeuroEngineering and Rehabilitation*, *12(1)*, 1–14. <https://doi.org/10.1186/s12984-015-0048-y>
- Boubaker, O. (Ed.). (2020). *CONTROL THEORY IN BIOMEDICAL ENGINEERING: Applications in Physiology and Medical Robotics (1th ed.)*. Elsevier.
- Bovi, G., Rabuffetti, M., Mazzoleni, P., & Ferrarin, M. (2011). A multiple-task gait analysis approach: Kinematic, kinetic and EMG reference data for healthy young and adult subjects. *Gait and Posture*, *33(1)*, 6–13. <https://doi.org/10.1016/j.gaitpost.2010.08.009>
- Bovolenta, F., Goldoni, M., Clerici, P., Agosti, M., & Franceschini, M. (2009). Robot therapy for functional recovery of the upper limbs: A pilot study on patients after stroke. *Journal of Rehabilitation Medicine*, *41(12)*, 971–975. <https://doi.org/10.2340/16501977-0402>
- Bovolenta, F., Sale, P., Dall'Armi, V., Clerici, P., & Franceschini, M. (2011). Robot-aided therapy for upper limbs in patients with stroke-related lesions. Brief report of a clinical experience. *Journal of NeuroEngineering and Rehabilitation*, *8(1)*, 1–6. <https://doi.org/10.1186/1743-0003-8-18>
- Burgess, J. K., Weibel, G. C., & Brown, D. A. (2010). Overground walking speed changes when subjected to body weight support conditions for nonimpaired and post stroke individuals.

*Journal of NeuroEngineering and Rehabilitation*, 7(1), 1–11. <https://doi.org/10.1186/1743-0003-7-6>

- Butler, R. J., Marchesi, S., Royer, T., & Davis, I. S. (2007). The Effect of a Subject-Specific Amount of Lateral Wedge on Knee. *Journal of Orthopaedic Research*, 25(June), 1121–1127. <https://doi.org/10.1002/jor>
- Calabrò, R. S., Russo, M., Naro, A., De Luca, R., Leo, A., Tomasello, P., Molonia, F., Dattola, V., Bramanti, A., & Bramanti, P. (2017). Robotic gait training in multiple sclerosis rehabilitation: Can virtual reality make the difference? Findings from a randomized controlled trial. *Journal of the Neurological Sciences*, 377, 25–30. <https://doi.org/10.1016/j.jns.2017.03.047>
- Cardona, M., Destarac, M., & Cena, C. G. (2020). Robotics for Rehabilitation: A State of the Art. In M. Cardona, V. K. Solanki, & C. E. G. Cena (Eds.), *Exoskeleton Robots for Rehabilitation and Healthcare Devices*. Springer.
- Casolo, F., Cinquemani, S., & Cocetta, M. (2008). **On active lower limb exoskeletons actuators.** *Proceeding of the 5th International Symposium on Mechatronics and Its Applications, ISMA 2008*, 25–30. <https://doi.org/10.1109/ISMA.2008.4648796>
- Castro, M. J., Apple, D. F., Rogers, S., & Dudley, G. A. (2000). Influence of complete spinal cord injury on skeletal muscle mechanics within the first 6 months of injury. *European Journal of Applied Physiology and Occupational Physiology*, 81(1–2), 128–131. <https://doi.org/10.1007/PL00013785>
- Ceccarelli, M., Copilusi, C., & Flores, P. (2014). Lab Experiences with a Linkage Exoskeleton for Walking Assistance. *New Trends in Mechanism and Machine Science From Fundamentals to Industrial Applications*. <https://doi.org/10.1007/978-3-319-09411-3>
- Chang, W. H., & Kim, Y.-H. (2013). Robot-assisted Therapy in Stroke Rehabilitation. *Journal of Stroke*, 15(3), 174–181. <https://doi.org/10.1143/jjap.38.4868>
- Chen, B., Ma, H., Qin, L. Y., Gao, F., Chan, K. M., Law, S. W., Qin, L., & Liao, W. H. (2016). Recent developments and challenges of lower extremity exoskeletons. *Journal of Orthopaedic Translation*, 5, 26–37. <https://doi.org/10.1016/j.jot.2015.09.007>

- Chen, C., Zhang, C., Hu, T., Ni, H., & Luo, W. C. (2018). Model-assisted extended state observer-based computed torque control for trajectory tracking of uncertain robotic manipulator systems. *International Journal of Advanced Robotic Systems*, *15*(5), 1–12. <https://doi.org/10.1177/1729881418801738>
- Chern, J. S., Chang, H. S., Lung, C. W., Wu, C. Y., & Tang, S. F. (2013). **Static ankle-foot orthosis improves static balance and gait functions in hemiplegic patients after stroke.** *Proceedings of the Annual International Conference of the IEEE Engineering in Medicine and Biology Society, EMBS, August 2015*, 5009–5012. <https://doi.org/10.1109/EMBC.2013.6610673>
- Chin, R., Hsiao-Wecksler, E. T., Loth, E., Kogler, G., Manwaring, S. D., Tyson, S. N., Shorter, K. A., & Gilmer, J. N. (2009). A pneumatic power harvesting ankle-foot orthosis to prevent foot-drop. *Journal of NeuroEngineering and Rehabilitation*, *6*(1), 1–11. <https://doi.org/10.1186/1743-0003-6-19>
- Chui, K. K., Jorge, M., Yen, S.-C., & Lusardi, M. M. (2020). *Orthotics and Prosthetics in Rehabilitation (4th ed.)*. Elsevier.
- Cifu, D. X., & Johns, J. S. (2021). *2021 Braddom 's Physical Medicine and Rehabilitation (6th ed.)*. Elsevier.
- Colombo, R., & Sanguineti, V. (Eds.). (2018). *Rehabilitation Robotics: Technology and Application*. Elsevier.
- Craven, C., Hitzig, S. L., & Mittmann, N. (2012). Impact of impairment and secondary health conditions on health preference among Canadians with chronic spinal cord injury. *Journal of Spinal Cord Medicine*, *35*(5), 361–370. <https://doi.org/10.1179/2045772312Y.0000000046>
- CTM: Control Tutorial.** (n.d.). Retrieved April 6, 2021, from <https://ctms.engin.umich.edu/CTMS/index.php?example=Introduction&section=ControlPID>
- del-Ama, A. J., Koutsou, A. D., Moreno, J. C., de-los-Reyes, A., Gil-Agudo, Á., & Pons, J. L. (2012). Review of hybrid exoskeletons to restore gait following spinal cord injury. *Journal of Rehabilitation Research and Development*, *49*(4), 497–514.

<https://doi.org/10.1682/JRRD.2011.03.0043>

Díaz, I., Gil, J. J., & Sánchez, E. (2011). Lower-Limb Robotic Rehabilitation: Literature Review and Challenges. *Journal of Robotics*, **2011(1)**, 1–11. <https://doi.org/10.1155/2011/759764>

Dorf, R. C., & Bishop, R. H. (2022). *Modern Control Systems (14th ed.)*. Pearson.

Duschau-Wicke, A., Caprez, A., & Riener, R. (2010). Patient-cooperative control increases active participation of individuals with SCI during robot-aided gait training. *Journal of Neuroengineering and Rehabilitation*, **7**, 43.

Elliott, G., Marecki, A., & Herr, H. (2014). Design of a clutch-spring knee exoskeleton for running. *Journal of Medical Devices, Transactions of the ASME*, **8(3)**, 1–11. <https://doi.org/10.1115/1.4027841>

Esquenazi, A. (2018). Comment on “Assessing Effectiveness and Costs in Robot-Mediated Lower Limbs Rehabilitation: A Meta-Analysis and State of the Art.” *Journal of Healthcare Engineering*. <https://doi.org/10.1155/2018/7634965>

Esquenazi, A., Talaty, M., Packel, A., & Saulino, M. (2012). The Rewalk powered exoskeleton to restore ambulatory function to individuals with thoracic-level motor-complete spinal cord injury. *American Journal of Physical Medicine and Rehabilitation*, **91(11)**, 911–921. <https://doi.org/10.1097/PHM.0b013e318269d9a3>

Farris, R. J., Quintero, H. A., Withrow, T. J., & Goldfarb, M. (2009). **Design and simulation of a joint-coupled orthosis for regulating FeS-aided gait.** *Proceedings - IEEE International Conference on Robotics and Automation*, 1916–1922. <https://doi.org/10.1109/ROBOT.2009.5152634>

Federici, S., & Scherer, M. J. (Eds.). (2018). *Assistive Technology Assessment Handbook (2 nd)*. CRC Press.

Flores, G. (2020). *Design and construction of robotic device for rehabilitation* Master in Optomechatronic Adviser : Dr . Gerardo Flores Colunga Student : Ing . José Alberto Sánchez Santis November of 2018. July.

Freivogel, S., & Schmalohr, D. (2008). Gait training with the newly developed ' LokoHelp ' -



system is feasible for non-ambulatory patients after stroke , spinal cord and brain injury . A feasibility study. *Brain Injury*, **22(August)**, 625–632. <https://doi.org/10.1080/02699050801941771>

Frey, M., Colombo, G., Vaglio, M., Bucher, R., Jörg, M., & Riener, R. (2006). A novel mechatronic body weight support system. *IEEE Transactions on Neural Systems and Rehabilitation Engineering*, **14(3)**, 311–321. <https://doi.org/10.1109/TNSRE.2006.881556>

Garcia, E., Arevalo, J. C., Muñoz, G., & Gonzalez-de-Santos, P. (2011). On the biomimetic design of agile-robot legs. *Sensors*, **11(12)**, 11305–11334. <https://doi.org/10.3390/s111211305>

Gardner, A. D., Potgieter, J., & Noble, F. K. (2017). *A review of commercially available exoskeletons' capabilities*. 2017 24th International Conference on Mechatronics and Machine Vision in Practice, M2VIP 2017, 2017-Decem, 1–5. <https://doi.org/10.1109/M2VIP.2017.8211470>

Gasser, B. W., Bennett, D. A., Durrrough, C. M., & Goldfarb, M. (2017). **Design and preliminary assessment of Vanderbilt hand exoskeleton**. *IEEE International Conference on Rehabilitation Robotics*, 1537–1542. <https://doi.org/10.1109/ICORR.2017.8009466>

Gassert, R., & Dietz, V. (2018). Rehabilitation robots for the treatment of sensorimotor deficits: A neurophysiological perspective. *Journal of NeuroEngineering and Rehabilitation*, **15(1)**, 1–16. <https://doi.org/10.1186/s12984-018-0383-x>

Giangregorio, L., & McCartney, N. (2006). Bone loss and muscle atrophy in spinal cord injury: epidemiology, fracture prediction, and rehabilitation strategies. *The Journal of Spinal Cord Medicine*, **29(5)**, 489–500. <https://doi.org/10.1080/10790268.2006.11753898>

Girone, M., Burdea, G., Bouzit, M., Popescu, V., & Deutsch, J. E. (2001). A Stewart Platform-Based System for Ankle Telerehabilitation \*. *Autonomous Robots*, **10**, 203–212.

Glasper, A., Aylott, M., & Battrick, C. (2010). *Developing Practical Skills for Nursing Children and Young People*. Hodder Arnold.

Goemaere, S., Van Laere, M., De Neve, P., & Kaufman, J. M. (1994). Bone mineral status in

paraplegic patients who do or do not perform standing. *Osteoporosis International*, 4(3), 138–143. <https://doi.org/10.1007/BF01623058>

**GT II - Reha-Stim.** (n.d.). Retrieved May 23, 2023, from <https://reha-stim.com/gt-ii/>

Ha, K. H., Quintero, H. A., Farris, R. J., & Goldfarb, M. (2012). **Enhancing stance phase propulsion during level walking by combining fes with a powered exoskeleton for persons with paraplegia.** *Proceedings of the Annual International Conference of the IEEE Engineering in Medicine and Biology Society, EMBS*, 344–347. <https://doi.org/10.1109/EMBC.2012.6345939>

Haisma, J. A., van der Woude, L. H., Stam, H. J., Bergen, M. P., Sluis, T. A., Post, M. W., & Bussmann, J. B. (2007). Complications following spinal cord injury: Occurrence and risk factors in a longitudinal study during and after inpatient rehabilitation. *Journal of Rehabilitation Medicine*, 39(5), 393–398. <https://doi.org/10.2340/16501977-0067>

Hamill, J., Knutzen, K. M., & Derrick, T. R. (2015). *Biomechanical Basis of Human Movement (4th ed.)*. Lippincott Williams & Wilkins.

Hankey, G. J., Macleod, M., Gorelick, P. B., Chen, C., Caprio, F. Z., & Mattle, H. (Eds.). (2019). *Warlow's Stroke Practical Management (4th ed.)*. Wiley-Blackwell.

Hasan, S. K., & Dhingra, A. K. (2020). State of the Art Technologies for Exoskeleton Human Lower Extremity Rehabilitation Robots. *Journal of Mechatronics and Robotics*, 4(1), 211–235. <https://doi.org/10.3844/jmrsp.2020.211.235>

Hesse, S., Schmidt, H., Werner, C., & Bardeleben, A. (2003). Upper and lower extremity robotic devices for rehabilitation and for studying motor control. *Current Opinion in Neurology*, 705–710. <https://doi.org/10.1097/01.wco.0000102630.16692.38>

Hesse, S., Tomelleri, C., Bardeleben, A., Werner, C., & Waldner, A. (2016). Robot-assisted practice of gait and stair climbing in nonambulatory stroke patients. *The Journal of Rehabilitation Research and Development*, February. <https://doi.org/10.1682/JRRD.2011.08.0142>

Hidler, J., Brennan, D., Black, I., Nichols, D., Brady, K., & Nef, T. (2011). ZeroG: Overground

gait and balance training system. *Journal of Rehabilitation Research and Development*, **48(4)**, 287–298. <https://doi.org/10.1682/JRRD.2010.05.0098>

Hitzig, S. L., Campbell, K. A., McGillivray, C. F., Boschen, K. A., & Craven, B. C. (2010). Understanding age effects associated with changes in secondary health conditions in a Canadian spinal cord injury cohort. *Spinal Cord*, **48(4)**, 330–335. <https://doi.org/10.1038/sc.2009.135>

Ho, N. S. K., Tong, K. Y., Hu, X. L., Fung, K. L., Wei, X. J., Rong, W., & Susanto, E. A. (2011). **An EMG-driven exoskeleton hand robotic training device on chronic stroke subjects: Task training system for stroke rehabilitation.** *IEEE International Conference on Rehabilitation Robotics*. <https://doi.org/10.1109/ICORR.2011.5975340>

Hollerbach, J. M., Hunter, I. W., & Ballantyne, J. (1992). A Comparative Analysis of Actuator Technologies for Robotics. In O. Khatib, J. J. Craig, & T. Lozano-Pérez (Eds.), *The Robotics Review 2* (pp. 299–342). The MIT Press.

Housman, S. J., Le, V., Rahman, T., Sanchez, R. J., & Remkensmeyer, D. J. (2007). **Arm-training with T-WREX after chronic stroke: Preliminary results of a randomized controlled trial.** *2007 IEEE 10th International Conference on Rehabilitation Robotics, ICORR'07*, 00(c), 562–568. <https://doi.org/10.1109/ICORR.2007.4428481>

Hsu, J. D., Michael, J. W., & Fisk, J. R. (Eds.). (2008). *AAOS Atlas of Orthoses and Assistive Devices (4th ed.)*. MOSBY Elsevier.

Huo, W., Mohammed, S., Moreno, J. C., & Amirat, Y. (2016). Lower Limb Wearable Robots for Assistance and Rehabilitation: A State of the Art. *IEEE Systems Journal*, **10(3)**, 1068–1081. <https://doi.org/10.1109/JSYST.2014.2351491>

Hussein, S., Schmidt, H., Hesse, S., & Krüger, J. (2009). **Effect of different training modes on ground reaction forces during robot assisted floor walking and stair climbing.** *2009 IEEE International Conference on Rehabilitation Robotics, ICORR 2009*, 845–850. <https://doi.org/10.1109/ICORR.2009.5209488>

Ichinose, W. E., Reinkensmeyer, D. J., Aoyagi, D., Lin, J. T., Ngai, K., Edgerton, V. R., Harkema, S. J., & Bobrow, J. E. (2003). **A robotic device for measuring and controlling pelvic**

**motion during locomotor rehabilitation.** *Annual International Conference of the IEEE Engineering in Medicine and Biology - Proceedings*, 2(June 2014), 1690–1693. <https://doi.org/10.1109/iembs.2003.1279715>

Jamwal, P. K., Xie, S. Q., Hussain, S., & Parsons, J. G. (2014). An adaptive wearable parallel robot for the treatment of ankle injuries. *IEEE/ASME Transactions on Mechatronics*, **19**(1), 64–75. <https://doi.org/10.1109/TMECH.2012.2219065>

Janocha, H. (2004). *Actuators: Basics and Applications (Issue 1)*. Springer-Verlag.

Jarzebowska, E. (2012). Model-Based Tracking Control of Nonlinear Systems. In *Model-Based Tracking Control of Nonlinear Systems*. CRC Press. <https://doi.org/10.1201/b12262-8>

Jeffrey, J. S., DeLuca, J., & Caplan, B. (Eds.). (2018). *Encyclopedia of Clinical Neuropsychology (2nd ed.)*. Springer International Publishing.

Jensen, M. P., Molton, I. R., Groah, S. L., Campbell, M. L., Charlifue, S., Chiodo, A., Forchheimer, M., Krause, J. S., & Tate, D. (2012). Secondary health conditions in individuals aging with SCI: Terminology, concepts and analytic approaches. *Spinal Cord*, **50**(5), 373–378. <https://doi.org/10.1038/sc.2011.150>

Kasina, H., Raju Bahubalendruni, M. V. A., & Botcha, R. (2017). Robots in medicine: Past, present and future. *International Journal of Manufacturing, Materials, and Mechanical Engineering*, **7**(4), 44–64. <https://doi.org/10.4018/IJMMME.2017100104>

Kazerooni, H., Steger, R., & Huang, L. (2006). Hybrid control of the Berkeley Lower Extremity Exoskeleton (BLEEX). *International Journal of Robotics Research*, **25**(5–6), 561–573. <https://doi.org/10.1177/0278364906065505>

Ke, D., Ai, Q., Meng, W., Zhang, C., & Liu, Q. (2017). **Fuzzy PD-type Iterative Learning Control of A Single Pneumatic Muscle Actuator.** *International Conference on Intelligent Robotics and Applications: ICIRA 2017*.

Khatib, S. (2016). *Springer Handbook of Robotics (2nd ed.)*. Springer.

Kittisares, S., Nabae, H., Endo, G., Suzumori, K., & Sakurai, R. (2020). Design of knee support

device based on four-bar linkage and hydraulic artificial muscle. *ROBOMECH Journal*, **7(1)**. <https://doi.org/10.1186/s40648-020-00165-2>

Klamroth-Marganska, V., Blanco, J., Campen, K., Curt, A., Dietz, V., Ettl, T., Felder, M., Fellinghauer, B., Guidali, M., Kollmar, A., Luft, A., Nef, T., Schuster-Amft, C., Stahel, W., & Riener, R. (2014). Three-dimensional, task-specific robot therapy of the arm after stroke: A multicentre, parallel-group randomised trial. *The Lancet Neurology*, **13(2)**, 159–166. [https://doi.org/10.1016/S1474-4422\(13\)70305-3](https://doi.org/10.1016/S1474-4422(13)70305-3)

Krebs, H. I., Ferraro, M., Buerger, S. P., Newbery, M. J., Makiyama, A., Sandmann, M., Lynch, D., Volpe, B. T., & Hogan, N. (2004). Rehabilitation robotics: Pilot trial of a spatial extension for MIT-Manus. *Journal of NeuroEngineering and Rehabilitation*, **1**, 1–15. <https://doi.org/10.1186/1743-0003-1-5>

Kumar, D., Subburaj, K., Lin, W., Karampinos, D. C., McCulloch, C. E., Li, X., Link, T. M., Souza, R. B., & Majumdar, S. (2013). Quadriceps and hamstrings morphology is related to walking mechanics and knee cartilage MRI relaxation times in young adults. *Journal of Orthopaedic and Sports Physical Therapy*, **43(12)**, 881–890. <https://doi.org/10.2519/jospt.2013.4486>

Levine, P. G. (2018). *Stronger After Stroke: Your Roadmap to Recovery (3th ed.)*. Demos Health.

Lewis, Frank L.; Dawson, Darren M.; Abdallah, C. T. (2004). *Manipulator Control Theory and Practice*. Marcel Dekker.

Lo, H. S., & Xie, S. Q. (2012). Exoskeleton robots for upper-limb rehabilitation: State of the art and future prospects. *Medical Engineering and Physics*, **34(3)**, 261–268. <https://doi.org/10.1016/j.medengphy.2011.10.004>

*LokoHelp - Electromechanical Gait Trainer* | Woodway. (n.d.). Retrieved May 23, 2023, from <https://www.woodway.com/products/loko-help/>

Low, K. H. (2011). *Robot-Assisted Gait Rehabilitation: From Exoskeletons to Gait Systems*. Defense Science Research Conference and Expo (DSR).

Luu, T. P., Low, K. H., Qu, X., Lim, H. B., & Hoon, K. H. (2014). Hardware development and locomotion control strategy for an over-ground gait trainer: NaTure-gaits. *IEEE Journal*

*of Translational Engineering in Health and Medicine*, 2(January). <https://doi.org/10.1109/JTEHM.2014.2303807>

Lynch, K. M., & Park, F. C. (2017). *Modern Robotics : Mechanics, Planning, and Control (Vol. 48)*. Cambridge University Press.

Majid, M., Chin, B. L. F., Jawad, Z. A., Chai, Y. H., Lam, M. K., Yusup, S., & Cheah, K. W. (2021). Particle swarm optimization and global sensitivity analysis for catalytic co-pyrolysis of *Chlorella vulgaris* and plastic waste mixtures. *Bioresource Technology*, 329(December 2020), 124874. <https://doi.org/10.1016/j.biortech.2021.124874>

Mao, Y. R., Lo, W. L., Lin, Q., Li, L., Xiao, X., Raghavan, P., & Huang, D. F. (2015). The Effect of Body Weight Support Treadmill Training on Gait Recovery, Proximal Lower Limb Motor Pattern, and Balance in Patients with Subacute Stroke. *BioMed Research International*, 2015. <https://doi.org/10.1155/2015/175719>

Martínez, A., Lawson, B., & Goldfarb, M. (2018). A Controller for Guiding Leg Movement during Overground Walking with a Lower Limb Exoskeleton. *IEEE Transactions on Robotics*, 34(1), 183–193. <https://doi.org/10.1109/TRO.2017.2768035>

Martynuk, A. A. (2000). A survey of some classical and modern developments of stability theory. *Nonlinear Analysis, Theory, Methods and Applications*, 40(1–8), 483–496. [https://doi.org/10.1016/S0362-546X\(00\)85027-0](https://doi.org/10.1016/S0362-546X(00)85027-0)

Matarić, M. J. (2008). **The robotics primer**. In *Massachusetts Institute of Technology* (Vol. 45, Issue 06). <https://doi.org/10.5860/choice.45-3222>

McDaid, A. J., Lakkhananukun, C., & Park, J. (2015). **Paediatric robotic gait trainer for children with cerebral palsy**. *IEEE International Conference on Rehabilitation Robotics, 2015-Septe*, 780–785. <https://doi.org/10.1109/ICORR.2015.7281297>

McDonald, J. W., & Sadowsky, C. (2002). Spinal cord injury. *The Lancet*, 359(9304), 417–425.

Meadows, M. S. (2011). *We, Robot*. Lyons Press.

Meddahi, Y., & Meguenni, K. Z. (2019). PD-computed torque control for an autonomous airship. *IAES International Journal of Robotics and Automation (IJRA)*, 8(1), 44.

<https://doi.org/10.11591/ijra.v8i1.pp44-51>

- Meddahi, Y., Meguenni, K. Z., & Aoued, H. (2020). The nonlinear computed torque control of a quadrotor. *Indonesian Journal of Electrical Engineering and Computer Science*, **20**(3), 1221–1229. <https://doi.org/10.11591/ijeecs.v20.i3.pp1221-1229>
- Mehrholz, J., Thomas, S., & Elsner, B. (2017). Treadmill training and body weight support for walking after stroke. *Cochrane Database of Systematic Reviews*, **2017**(8). <https://doi.org/10.1002/14651858.CD002840.pub4>
- Mertz, L. (2012). The next generation of exoskeletons: Lighter, cheaper devices are in the works. *IEEE Pulse*, **3**(4), 56–61. <https://doi.org/10.1109/MPUL.2012.2196836>
- Meuleman, J. (2015). *Design of a Robot-Assisted Gait Trainer: LOPES II*. Twente.
- Mohr, J. P., Wolf, P. A., Grotta, J. C., Moskowitz, M. A., Mayberg, M. R., & von Kummer, R. (Eds.). (2011). *Stroke : Pathophysiology, Diagnosis and Management (5th ed., Issue 1)*. Elsevier.
- Monaco, V., Galardi, G., Coscia, M., Martelli, D., & Micera, S. (2012). Design and evaluation of NEUROBike: A neurorehabilitative platform for bedridden post-stroke patients. *IEEE Transactions on Neural Systems and Rehabilitation Engineering*, **20**(6), 845–852. <https://doi.org/10.1109/TNSRE.2012.2212914>
- Moreno, J. C., Brunetti, F., Rocon, E., & Pons, J. L. (2008). Immediate effects of a controllable knee ankle foot orthosis for functional compensation of gait in patients with proximal leg weakness. *Medical and Biological Engineering and Computing*, **46**(1), 43–53. <https://doi.org/10.1007/s11517-007-0267-x>
- Morone, G., Paolucci, S., Cherubini, A., De Angelis, D., Venturiero, V., Coiro, P., & Iosa, M. (2017). Robot-assisted gait training for stroke patients: Current state of the art and perspectives of robotics. In *Neuropsychiatric Disease and Treatment (Vol. 13, pp. 1303–1311)*. Dove Medical Press Ltd. <https://doi.org/10.2147/NDT.S114102>
- Munawar, H. (2017). *Design, Implementation and Control of an Overground Gait and Balance Trainer with an Active Pelvis-Hip Exoskeleton*. Sabanci University.

- Murray, R., Li, Z., & Sastry, S. (1994). *A Mathematical Introduction to Robotic Manipulation*. CRC Press.
- Murray, S. A., Ha, K. H., Hartigan, C., & Goldfarb, M. (2015). An assistive control approach for a lower-limb exoskeleton to facilitate recovery of walking following stroke. *IEEE Transactions on Neural Systems and Rehabilitation Engineering*, *23*(3), 441–449. <https://doi.org/10.1109/TNSRE.2014.2346193>
- Nef, T., & Riener, R. (2005). ARMin - **Design of a novel arm rehabilitation robot**. *Proceedings of the 2005 IEEE 9th International Conference on Rehabilitation Robotics, 2005*(June 2014), 57–60. <https://doi.org/10.1109/ICORR.2005.1501051>
- Niu, J., Song, Q., & Wang, X. (2013). **Fuzzy PID control for passive lower extremity exoskeleton in swing phase**. *ICEIEC 2013 - Proceedings of 2013 IEEE 4th International Conference on Electronics Information and Emergency Communication*, 185–188. <https://doi.org/10.1109/ICEIEC.2013.6835483>
- Noreau, L., & Shephard, R. J. (1995). Spinal Cord Injury, Exercise and Quality of Life. *Sports Medicine*, *20*(4), 226–250. <https://doi.org/10.2165/00007256-199520040-00003>
- Okamoto, T., & Okamoto, K. (2007). *Development of Gait by Electromyography*. Walking Development Group.
- Onwubolu, G. C. (2005). *Mechatronics: Principles and applications*. Elsevier Butterworth-Heinemann.
- Oriolo, G., De Luca, A., & Vendittelli, M. (2002). WMR control via dynamic feedback linearization: Design, implementation, and experimental validation. *IEEE Transactions on Control Systems Technology*, *10*(6), 835–852. <https://doi.org/10.1109/TCST.2002.804116>
- Owens, D. (2016). *Iterative Learning Control An Optimization Paradigm*. Springer London.
- Palermo, A. E., Maher, J. L., Baunsgaard, C. B., & Nash, M. S. (2017). Clinician-focused overview of bionic exoskeleton use after spinal cord injury. *Topics in Spinal Cord Injury Rehabilitation*, *23*(3), 234–244. <https://doi.org/10.1310/sci2303-234>



- Pandy, M. G., & Andriacchi, T. P. (2010). Muscle and joint function in human locomotion. In *Annual Review of Biomedical Engineering* (Vol. 12). <https://doi.org/10.1146/annurev-bioeng-070909-105259>
- Paper, C., & Sankai, Y. (2014). *HAL : Hybrid Assistive Limb based on Cybernics HAL : Hybrid Assistive Limb based on Cybernics. January 2007*. <https://doi.org/10.1007/978-3-642-14743-2>
- Patton, J. L., Brown, D., Lewis, E., Santos, J., Makhlin, A., Colgate, J. E., & Peshkin, M. (2007). **Motility Evaluation of a Novel Overground Functional Mobility Tool for Post Stroke Rehabilitation.** *International Conference on Rehabilitation Robotics (ICORR), 00(c)*.
- Paul, R. P. (1972). *Technical Report AIM-177 : Modelling, Trajectory Calculation and Servoing of A Computer Controlled Arm, Stanford Artificial Intelligence Laboratory (Issue November)*.
- Peng, J., Ghosh, D., Zhang, F., Yang, L., Wu, J., Pang, J., Zhang, L., Yin, S., & Jiang, Y. (2022). Advancement of epigenetics in stroke. *Frontiers in Neuroscience, 16(October)*. <https://doi.org/10.3389/fnins.2022.981726>
- Pennycott, A., Wyss, D., Vallery, H., Klamroth-Marganska, V., & Riener, R. (2012). Towards more effective robotic gait training for stroke rehabilitation: A review. *Journal of NeuroEngineering and Rehabilitation, 9(1)*. <https://doi.org/10.1186/1743-0003-9-65>
- Piepmeyer, J. M., & Jenkins, N. R. (1988). Late neurological changes following traumatic spinal cord injury. *Journal of Neurosurgery, 69(3)*, 399–402. <https://doi.org/10.3171/jns.1988.69.3.0399>
- Pietrusinski, M., Cajigas, I., Severini, G., Bonato, P., & Mavroidis, C. (2014). Robotic gait rehabilitation trainer. *IEEE/ASME Transactions on Mechatronics, 19(2)*, 490–499. <https://doi.org/10.1109/TMECH.2013.2243915>
- Pirondini, E., Coscia, M., Marcheschi, S., Roas, G., Salsedo, F., Frisoli, A., Bergamasco, M., & Micera, S. (2016). Evaluation of the effects of the Arm Light Exoskeleton on movement execution and muscle activities: A pilot study on healthy subjects. *Journal of*

*NeuroEngineering and Rehabilitation*, 13(1), 1–21. <https://doi.org/10.1186/s12984-016-0117-x>

Pons, J. L. (2010). The Promise of an Emerging Field: Rehabilitation Exoskeletal Robotics. *IEEE Engineering in Medicine and Biology Magazine*, June, 57–63.

Ponsford, J., Kolb, B., Cioe, J., Willmott, C., Glisky, E., Nadeau, S., Gonzalez Rothi, L., Aimola Davies, A., Turner, G., Levine, B., & Alderman, N. (2004). Cognitive and Behavioral Rehabilitation. In *Journal of Head Trauma Rehabilitation* (Vol. 20).

Popovic, M. B. (2019). *Biomechatronics*. Academic Press.

Radjou, N., & Prabhu, J. (2015). *Frugal Innovation : How to Do Better with Less*. Profile Books.

Rehmat, N., Zuo, J., Meng, W., Liu, Q., Xie, S. Q., & Liang, H. (2018). Upper limb rehabilitation using robotic exoskeleton systems: a systematic review. *International Journal of Intelligent Robotics and Applications*, 2(3), 283–295. <https://doi.org/10.1007/s41315-018-0064-8>

Rosen, J., & Ferguson, P. W. (Eds.). (2020). *Wearable Robotics : Systems and Applications*. Academic Press.

Rosenberg, J. M. (1986). *Jeffrey Rosenberg-Dictionary of Artificial Intelligence and Robotics-Wiley*, John Wiley & Sons.

Rupal, B. S., Rafique, S., Singla, A., Singla, E., Isaksson, M., & Virk, G. S. (2017). Lower-limb exoskeletons: Research trends and regulatory guidelines in medical and non-medical applications. *International Journal of Advanced Robotic Systems*, 14(6). <https://doi.org/10.1177/1729881417743554>

Russell Esposito, E., Schmidtbauer, K. A., & Wilken, J. M. (2018). Experimental comparisons of passive and powered ankle-foot orthoses in individuals with limb reconstruction. *Journal of NeuroEngineering and Rehabilitation*, 15(1), 1–11. <https://doi.org/10.1186/s12984-018-0455-y>

Sadeghnejad, S., Abadi, V. S. E., & Jafari, B. (2022). Chapter 8 Rehabilitation Robotics : History

, Applications , and Recent Advances. In O. Boubaker (Ed.), *Medical and Healthcare Robotic (Issue December)*. Academic Press.

Saglia, J. A., Tsagarakis, N. G., Dai, J. S., & Caldwell, D. G. (2009a). **A high performance 2-dof over-actuated parallel mechanism for ankle rehabilitation.** *Proceedings - IEEE International Conference on Robotics and Automation, June*, 2180–2186. <https://doi.org/10.1109/ROBOT.2009.5152604>

Saglia, J. A., Tsagarakis, N. G., Dai, J. S., & Caldwell, D. G. (2009b). A High Performance 2-dof Over-Actuated Parallel Mechanism for Ankle Rehabilitation. *The International Journal of Robotics Research, September*. <https://doi.org/10.1177/0278364909104221>

Saglia, J. A., Tsagarakis, N. G., Dai, J. S., & Caldwell, D. G. (2013). Control Strategies for Patient-Assisted Training Using the Ankle Rehabilitation Robot ( ARBOT ). *IEEE/ASME Transactions on Mechatronics, 18(6)*, 1799–1808. <https://doi.org/10.1109/TMECH.2012.2214228>

Sakuta, K., Murayama, Y., & Iguchi, Y. (2016). Endovascular therapy in acute ischemic stroke. *Respiration and Circulation, 64(6)*, 609–615. <https://doi.org/10.1161/strokeaha.115.011426>

Salkind, N. J., Frey, B. B., Dougherty, D. D., Teasdale, K. R., & Hil-Kapturczak, N. (Eds.). (2010). *Encyclopedia of Research Design*. SAGE Publications.

Sanchez, R. J., Wolbrecht, E., Smith, R., Liu, J., Rao, S., Cramer, S., Rahman, T., Bobrow, J. E., Reinkensmeyer, D. J., & Shah, P. (2005). **A pneumatic robot for re-training arm movement after stroke: Rationale and mechanical design.** *Proceedings of the 2005 IEEE 9th International Conference on Rehabilitation Robotics, 2005*, 500–504. <https://doi.org/10.1109/ICORR.2005.1501151>

Sankai, Y. (2010). HAL: Hybrid assistive limb based on cybernics. *Springer Tracts in Advanced Robotics, 66(STAR)*, 25–34. [https://doi.org/10.1007/978-3-642-14743-2\\_3](https://doi.org/10.1007/978-3-642-14743-2_3)

Saver, J. L. (2006). Time is brain - Quantified. *Stroke, 37(1)*, 263–266. <https://doi.org/10.1161/01.STR.0000196957.55928.ab>

Sawicki, G. S., & Ferris, D. P. (2009). A pneumatically powered knee-ankle-foot orthosis ( KAFO

- ) with myoelectric activation and inhibition. *Journal of NeuroEngineering and Rehabilitation*, **16**, 1–16. <https://doi.org/10.1186/1743-0003-6-23>
- Scataglini, S., Imbesi, S., & Marques, G. (2022). *Internet of Things for Human-Centered Design (Vol. 1011)*. Springer Singapore. <https://doi.org/10.1007/978-981-16-8488-3>
- Schmidt, H., Hesse, S., Bernhardt, R., & Krüger, J. (2005). Haptic Walker—A Novel Haptic Foot Device. *ACM Transactions on Applied Perception*, **2**(2), 166–180. <https://doi.org/10.1145/1060581.1060589>
- Schmidt, H., Werner, C., Bernhardt, R., Hesse, S., & Krüger, J. (2007). Gait rehabilitation machines based on programmable footplates. *Journal of NeuroEngineering and Rehabilitation*, **7**, 1–7. <https://doi.org/10.1186/1743-0003-4-2>
- Scivoletto, G., Morganti, B., & Molinari, M. (2005). Early versus delayed inpatient spinal cord injury rehabilitation: An Italian study. *Archives of Physical Medicine and Rehabilitation*, **86**(3), 512–516. <https://doi.org/10.1016/j.apmr.2004.05.021>
- Scott, S. H. (1999). Apparatus for measuring and perturbing shoulder and elbow joint positions and torques during reaching. *Journal of Neuroscience Methods*, **89**(2), 119–127. [https://doi.org/10.1016/S0165-0270\(99\)00053-9](https://doi.org/10.1016/S0165-0270(99)00053-9)
- Sharkawy, A., Koustoumpardis, P., Sharkawy, A., Dynamics, P. K., & Control, C. (2019). Dynamics and Computed-Torque Control of a 2-DOF manipulator. *International Journal of Advanced Science and Technology*, **28**(12), 201–212.
- Siciliano, B., Khatib, O., & Groen, F. (2010). Robotics Research The 13th International Symposium ISRR. In M. Kaneko (Ed.), *Springer Tracts in Advanced Robotics*. Springer Verlag.
- Singh, R., Pathak, V. K., Sharma, A., Chakraborty, D., Saxena, K. K., Prakash, C., Buddhi, D., & Salem, K. hazim. (2023). Caster Walker GAIT Trainer (CGT): A robotic assistive device. *Robotics and Autonomous Systems*, **159**, 104302. <https://doi.org/10.1016/j.robot.2022.104302>
- Singla, A., Dhand, S., Dhawad, A., & Virk, G. S. (2019). Toward human-powered lower limb

exoskeletons: A review. *Advances in Intelligent Systems and Computing*, **741**(February), 783–795. [https://doi.org/10.1007/978-981-13-0761-4\\_75](https://doi.org/10.1007/978-981-13-0761-4_75)

Smania, N., Geroïn, C., Vale, N., & Gandolfi, M. (2018). The End-Effector Device for Gait Rehabilitation. In G. Sandrini, V. Homberg, L. Saltuari, N. Smania, & A. Pedrocchi (Eds.), *Biosystems & Biorobotics (Volume 19): Advanced Technologies for the Rehabilitation of Gait and Balance Disorders*. Springer International Publishing.

Song, Z., Yi, J., Zhao, D., & Li, X. (2005). A computed torque controller for uncertain robotic manipulator systems: Fuzzy approach. *FUZZY Sets and Systems*, **154**, 208–226. <https://doi.org/10.1016/j.fss.2005.03.007>

Stauffer, Y., Allemand, Y., Bouri, M., Fournier, J., Clavel, R., Metrailler, P., Brodard, R., & Reynard, F. (2009). The WalkTrainer - A new generation of walking reeducation device combining orthoses and muscle stimulation. *IEEE Transactions on Neural Systems and Rehabilitation Engineering*, **17**(1), 38–45. <https://doi.org/10.1109/TNSRE.2008.2008288>

Susko, T. G. (2015). *MIT Skywalker: A Novel Robot for Gait Rehabilitation of Stroke and Cerebral Palsy AM Patients*. MASSACHUSETTS INSTITUTE OF TECHNOLOGY February.

Sutyasadi, P. (2022). Control Improvement of Low-Cost Cast Aluminium Robotic Arm Using Arduino Based Computed Torque Control. *Jurnal Ilmiah Teknik Elektro Komputer Dan Informatika*, **8**(4), 650–659. <https://doi.org/10.26555/jiteki.v8i4.24646>

Takahashi, K., Domen, K., Sakamoto, T., Toshima, M., Otaka, Y., Seto, M., Irie, K., Haga, B., Takebayashi, T., & Hachisuka, K. (2016). Efficacy of Upper Extremity Robotic Therapy in Subacute Poststroke Hemiplegia: An Exploratory Randomized Trial. *Stroke*, **47**(5), 1385–1388. <https://doi.org/10.1161/STROKEAHA.115.012520>

Tiboni, M., Borboni, A., Vérité, F., Bregoli, C., & Amici, C. (2022). Sensors and Actuation Technologies in Exoskeletons: A Review. *Sensors*, **22**(3). <https://doi.org/10.3390/s22030884>

Tong, R. K.-Y. (2018). *Wearable Technology in Medicine and Health Care*. Academic Press.

- Tran, V. T., & Ravaud, P. (2016). Frugal innovation in medicine for low resource settings. *BMC Medicine*, *14*(1). <https://doi.org/10.1186/s12916-016-0651-1>
- Tsoi, Y. H., Xie, S. Q., & Mallinson, G. D. (2009). **Joint Force Control of Parallel Robot for Ankle Rehabilitation**. *2009 IEEE International Conference on Control and Automation Christchurch, New Zealand, December 9-11, 2009*, 1856–1861.
- Tucker, Mi. R., Olivier, J., Pagel, A., Bleuler, H., Bouri, M., Lamercy, O., Millán, J. D. R., Riener, R., Vallery, H., & Gassert, R. (2015). Control strategies for active lower extremity prosthetics and orthotics: a review. *Journal of NeuroEngineering and Rehabilitation*, *12*, 1.
- van Nunen, M. P. M. (2013). *Recovery of walking ability using a robotic device [Vrije Universiteit]*. [https://research.vu.nl/files/42114296/complete\\_dissertation.pdf](https://research.vu.nl/files/42114296/complete_dissertation.pdf)
- Veneman, J. F., Kruidhof, R., Hekman, E. E. G., Ekkelenkamp, R., Van Asseldonk, E. H. F., & Van Der Kooij, H. (2007). Design and evaluation of the LOPES exoskeleton robot for interactive gait rehabilitation. *IEEE Transactions on Neural Systems and Rehabilitation Engineering*, *15*(3), 379–386. <https://doi.org/10.1109/TNSRE.2007.903919>
- Venkatasubramanian, N., Yoon, B. W., Pandian, J., & Navarro, J. C. (2017). Stroke epidemiology in south, east, and south-east asia: A review. *Journal of Stroke*, *19*(3), 286–294. <https://doi.org/10.5853/jos.2017.00234>
- Wall, J., & Colley, T. (2003). Preventing pressure ulcers among wheelchair users: preliminary comments on the development of a self-administered risk assessment tool. *Journal of Tissue Viability*, *13*(2). [https://doi.org/10.1016/s0965-206x\(03\)80035-9](https://doi.org/10.1016/s0965-206x(03)80035-9)
- Walsh, C. J., Pasch, K., & Herr, H. (2006). **An autonomous, underactuated exoskeleton for load-carrying augmentation**. *IEEE International Conference on Intelligent Robots and Systems, May 2014*, 1410–1415. <https://doi.org/10.1109/IROS.2006.281932>
- Webster, J. B., & Murphy, D. P. (2009). *Atlas of Orthoses and Assistive Devices (5th ed.)*. Elsevier. <https://doi.org/10.1145/1640233.1640248>

- Wehner, M., Quinlivan, B., Aubin, P. M., Martinez-Villalpando, E., Baumann, M., Stirling, L., Holt, K., Wood, R., & Walsh, C. (2013). **A lightweight soft exosuit for gait assistance.** *Proceedings - IEEE International Conference on Robotics and Automation*, 3362–3369. <https://doi.org/10.1109/ICRA.2013.6631046>
- Welage, N., & Liu, K. P. Y. (2011). Wheelchair accessibility of public buildings: A review of the literature. *Disability and Rehabilitation: Assistive Technology*, **6(1)**, 1–9. <https://doi.org/10.3109/17483107.2010.522680>
- Whalley Hammell, K. (1995). *Spinal Cord Injury Rehabilitation (1th ed.)*. Springer.
- Whittle, M. W. (2007). *An Introduction to Gait Analysis (4th ed.)*. Elsevier.
- Xie, S. Q., & Jamwal, P. K. (2011). Expert Systems with Applications An iterative fuzzy controller for pneumatic muscle driven rehabilitation robot. *Expert Systems With Applications*, **38(7)**, 8128–8137. <https://doi.org/10.1016/j.eswa.2010.12.154>
- Xue, X., Yang, X., Deng, Z., Tu, H., Kong, D., Li, N., & Xu, F. (2022). Global Trends and Hotspots in Research on Rehabilitation Robots: A Bibliometric Analysis From 2010 to 2020. *Frontiers in Public Health*, **9(January)**, 1–17. <https://doi.org/10.3389/fpubh.2021.806723>
- Yang, Z., Wu, J., Mei, J., Gao, J., & Huang, T. (2008). *Mechatronic Model Based Computed Torque Control of a Parallel Manipulator*. **5(1)**, 123–128. <https://doi.org/10.5772/5650>
- Yeung, L., & Tong, R. K. (2018). Lower Limb Exoskeleton Robot to Facilitate the Gait of Stroke Patients. In *Wearable Technology in Medicine and Health Care (Issue 1)*. Elsevier Inc. <https://doi.org/10.1016/B978-0-12-811810-8.00005-1>
- Yoshizawa, N. (2012). **Active AFO with ankle joint brake friction control using force observer.** *Proceedings of the Annual International Conference of the IEEE Engineering in Medicine and Biology Society, EMBS*, 1900–1903. <https://doi.org/10.1109/EMBC.2012.6346324>
- Zeilig, G., Weingarden, H., Zwecker, M., Dudkiewicz, I., Bloch, A., & Esquenazi, A. (2012). Safety and tolerance of the ReWalk™ exoskeleton suit for ambulation by people with

complete spinal cord injury: A pilot study. *Journal of Spinal Cord Medicine*, **35(2)**, 96–101. <https://doi.org/10.1179/2045772312Y.0000000003>

Zhang, D., & Wei, B. (2017). A review on model reference adaptive control of robotic manipulators. *Annual Reviews in Control*, **43**, 188–198. <https://doi.org/10.1016/j.arcontrol.2017.02.002>

Zhang, J. fan, Dong, Y. ming, Yang, C. jun, Geng, Y., Chen, Y., & Yang, Y. (2010). 5-Link model based gait trajectory adaption control strategies of the gait rehabilitation exoskeleton for post-stroke patients. *Mechatronics*, **20(3)**, 368–376. <https://doi.org/10.1016/j.mechatronics.2010.02.003>

Zhang, X., Yue, Z., & Wang, J. (2017). Robotics in Lower-Limb Rehabilitation after Stroke. *Behavioural Neurology*, **2017**. <https://doi.org/10.1155/2017/3731802>

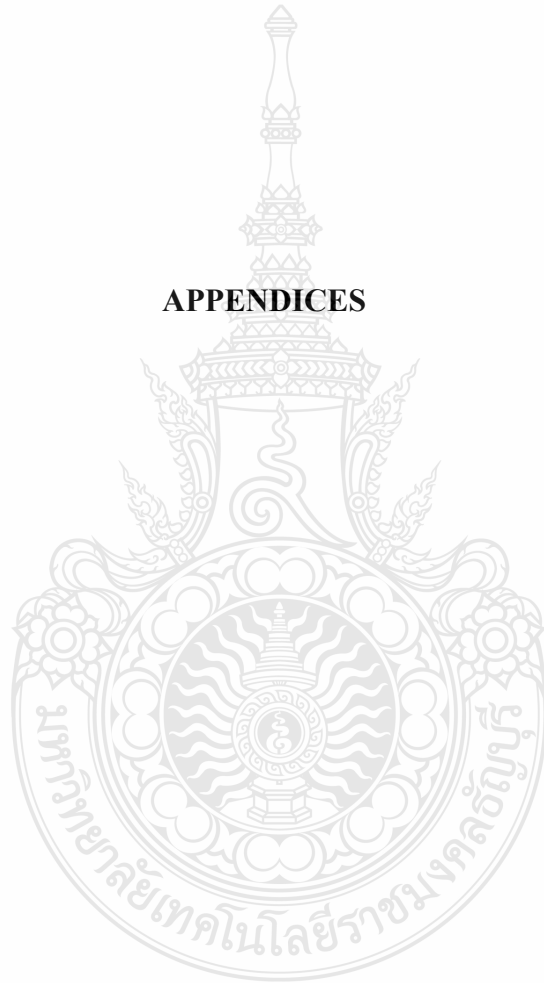
Zipes, D. P., Libby, P., Bonow, R. O., Mann, D. L., Tomaselli, G. F., & Braunwald, E. (Eds.). (2019). *Braunwald's Heart Disease : A Textbook of Cardiovascular Medicine (11th ed.)*. Elsevier.

Zoss, A. B., Kazerooni, H., & Chu, A. (2006). Biomechanical design of the Berkeley Lower Extremity Exoskeleton (BLEEX). *IEEE/ASME Transactions on Mechatronics*, **11(2)**, 128–138. <https://doi.org/10.1109/TMECH.2006.871087>

Zoss, A., Kazerooni, H., & Chu, A. (2005). **On the mechanical design of the Berkeley Lower Extremity Exoskeleton (BLEEX)**. *2005 IEEE/RSJ International Conference on Intelligent Robots and Systems, IROS*, 3465–3472. <https://doi.org/10.1109/IROS.2005.1545453>



**APPENDICES**





**APPENDIX A**  
**MICROCONTROLLER SOURCE CODE**

```

Int hip[] =
{6525,6523,6518,6508,6498,6486,6474,6462,6450,6434,6418,6402,6386
,6365,6344,6322,6301,6274,6247,6220,6193,6160,6128,6095,6062,6024
,5986,5948,5910,5867,5825,5782,5739,5691,5642,5594,5545,5491,5438
,5384,5330,5271,5212,5152,5093,5028,4962,4897,4831,4761,4691,4621
,4551,4477,4402,4328,4253,4175,4097,4019,3941,3861,3781,3700,3620
,3538,3457,3375,3293,3211,3129,3047,2965,2883,2801,2718,2636,2554
,2472,2389,2307,2225,2143,2061,1979,1897,1816,1734,1652,1570,1489
,1407,1325,1244,1162,1081,999,917,835,753,671,590,508,427,345,263
,181,99,17,-64,-146,-227,-308,-389,-471,-552,-633,-713,-794,-
874,-954,-1033,-1113,-1192,-1271,-1349,-1427,-1504,-1582,-1658,-
1734,-1809,-1885,-1958,-2032,-2105,-2178,-2249,-2320,-2390,-
2461,-2529,-2597,-2664,-2732,-2798,-2863,-2929,-2994,-3057,-
3120,-3182,-3245,-3306,-3367,-3427,-3488,-3546,-3605,-3663,-
3721,-3777,-3834,-3890,-3946,-3999,-4053,-4106,-4159,-4210,-
4261,-4311,-4362,-4409,-4456,-4502,-4549,-4592,-4635,-4678,-
4721,-4759,-4796,-4834,-4871,-4903,-4935,-4966,-4998,-5023,-
5047,-5072,-5096,-5113,-5130,-5146,-5163,-5171,-5179,-5187,-
5195,-5192,-5189,-5185,-5182,-5168,-5154,-5139,-5125,-5100,-
5074,-5049,-5023,-4985,-4946,-4908,-4869,-4819,-4768,-4718,-
4667,-4603,-4540,-4476,-4412,-4337,-4262,-4186,-4111,-4023,-
3935,-3847,-3759,-3661,-3562,-3464,-3365,-3256,-3146,-3037,-
2927,-2809,-2691,-2573,-2455,-2329,-2203,-2076,-1950,-1818,-
1686,-1553,-1421,-1284,-1147,-1009,-872,-732,-592,-452,-312,-
171,-
30,112,253,393,534,674,814,952,1091,1229,1367,1502,1637,1772,1907
,2038,2169,2299,2430,2556,2683,2809,2935,3056,3177,3298,3419,3534
,3649,3763,3878,3986,4094,4202,4310,4411,4513,4614,4715,4808,4901
,4993,5086,5171,5256,5340,5425,5501,5577,5653,5729,5795,5862,5928
,5994,6051,6109,6166,6223,6270,6317,6363,6410,6448,6485,6523,6560
,6587,6614,6640,6667,6686,6705,6724,6743,6759,6775,6791,6807,6810
,6812,6815,6817,6813,6808,6804,6799,6790,6780,6771,6761,6748,6736
,6723,6710,6694,6679,6663,6647,6631,6615,6599,6583,6567,6551,6534
,6518,6504,6490,6475,6461,6448,6434,6421,6407,6397,6387,6376,6366
,6359,6352,6345,6338,6332,6327,6321,6326,6334,6340,6345,6350,6370
,6385,6400,6420,6441,6470,6501,6510,6520,6525};

//int knee[] =
{1205,1303,1401,1499,1597,1692,1786,1881,1975,2076,2176,2277,2377
,2480,2582,2685,2787,2891,2995,3098,3202,3299,3396,3493,3590,3674
,3758,3841,3925,3992,4060,4127,4194,4244,4294,4344,4394,4429,4465
,4500,4535,4555,4576,4596,4616,4623,4630,4636,4643,4638,4633,4628
,4623,4607,4592,4576,4560,4535,4509,4484,4458,4426,4395,4363,4331
,4294,4257,4219,4182,4142,4103,4063,4023,3981,3940,3898,3856,3814
,3772,3730,3688,3647,3606,3564,3523,3482,3442,3401,3360,3320,3281
,3241,3201,3162,3123,3084,3045,3007,2970,2932,2894,2858,2821,2785
,2748,2712,2676,2640,2604,2569,2533,2498,2462,2427,2392,2357,2322

```

```
,2288,2254,2220,2186,2154,2121,2089,2056,2026,1995,1965,1934,1907
,1880,1852,1825,1802,1780,1757,1734,1717,1700,1682,1665,1655,1645
,1634,1624,1621,1617,1614,1610,1614,1619,1623,1627,1639,1650,1662
,1673,1693,1712,1732,1751,1777,1803,1829,1855,1889,1922,1956,1989
,2030,2071,2111,2152,2200,2248,2296,2344,2399,2454,2509,2564,2625
,2686,2746,2807,2875,2943,3010,3078,3152,3226,3300,3374,3457,3540
,3623,3706,3797,3888,3978,4069,4174,4279,4383,4488,4604,4721,4837
,4953,5085,5217,5349,5481,5629,5777,5925,6073,6238,6403,6568,6733
,6915,7098,7280,7462,7659,7856,8053,8250,8461,8671,8882,9092,9313
,9535,9756,9977,10205,10433,10661,10889,11119,11349,11578,11808,1
2034,12260,12485,12711,12925,13139,13353,13567,13765,13963,14161,
14359,14535,14710,14886,15061,15211,15361,15511,15661,15785,15908
,16032,16155,16248,16341,16433,16526,16590,16653,16717,16780,1681
3,16847,16880,16913,16917,16921,16924,16928,16905,16881,16858,168
34,16784,16733,16683,16632,16557,16483,16408,16333,16236,16139,16
042,15945,15824,15704,15583,15462,15323,15183,15044,14904,14744,1
4583,14423,14262,14083,13904,13725,13546,13350,13153,12957,12760,
12547,12334,12120,11907,11680,11453,11225,10998,10757,10517,10276
,10035,9786,9537,9287,9038,8794,8551,8307,8063,7805,7547,7289,703
1,6775,6520,6264,6008,5760,5511,5263,5014,4776,4539,4301,4063,383
8,3614,3389,3164,2962,2761,2559,2357,2182,2006,1831,1655,1513,137
1,1228,1086,979,872,765,658,589,521,452,383,343,303,263,223,216,2
10,203,196,220,244,267,291,357,423,489,555,637,720,802,900,1000,1
100};
```

```
#include <Encoder.h>
Encoder myEnc(2, 7);

//pin A and pin B (DT/CLK) of encoder connected to pin 2 and 3 of
arduino

const int setpoint = 0;

//analog pin input for potentiometer setpoint

int i_hip;

float p, i, d, sp, out, sp_vel;

float error_old = 0;

float error_dydx = 0;

float error_integral = 0;

float pid = 0;
```

```

float error = 0;

int pwm;

long oldPosition = -999;

//~~~~~
~~~~~

Encoder myEnc1(3, 4); //pin A and pin B (DT/CLK) of encoder
connected to pin 2 and 3 of arduino

const int setpoint1 = 0;

//pin analog input for potentiometer setpoint

int i_knee;

float p1, i1, d1, sp1, out1;

float error_old1 = 0;

float error_dydx1 = 0;

float error_integral1 = 0;

float pid1 = 0;

float error1 = 0;

int pwm1;

long oldPosition1 = -999;

//~~~~~
~~~~~

float e[403];

float e_last[403];

float old_e_last;

float
PIDILC,Kp_ILC,Kd_ILC,PD_ILC[403],U_ILC,old_PD_ILC[403],U_TOT;

int k,m,flag1,flag2;

int gaitFlag = 0;

void setup()

```

```

{
    // initialize the serial communications:
    Serial.begin(9600);
}

void loop()
{
    long newPosition = myEnc.read();
    out = newPosition;
//hip
//  p = 0.05;//0.45
//  i = 0.001;//0.05
//  d = 0.02;//0.4
//  Kp_ILC = 0.015;
//  Kd_ILC = 0.02;
//knee
//  p = 0.07;//0.45
//  i = 0.001;//0.05
//  d = 0.04;//0.4
//  Kp_ILC = 0.022;
//  Kd_ILC = 0.03;
    //  sp = analogRead(setpoin);
    //  sp = map(sp, 0, 1023, 0, 240);
    //  sp = 12500; //45 degree exo data 12500 encoder pulse
    sp = hip[gaitFlag];
//  i_hip ++;
//  if (i_hip == 404) {
//      i_hip = 0;

```

```

// }

error = sp - out;
e[k]=error;

//PID
error_integral += error;

if (error_integral > 150)
{
    error_integral = 150;
}
else if (error_integral < -150)
{
    error_integral = -150;
}
pid = (error * p) + (error_integral * i) + (error_dydx * d);
pid = pid / 2;
error_dydx = error - error_old;
error_old = error;
//ILC
PD_ILC[k] = Kp_ILC*e_last[k] + Kd_ILC*(e_last[k]-old_e_last);
old_e_last = e_last[k];
U_ILC = PD_ILC[k] + old_PD_ILC[k];
// old_PD_ILC = PD_ILC;
//end of ILC
//Total signal is PID signal plus ILC signal
U_TOT = pid + U_ILC;
//Count each point along the trajectory

```

```

gaitFlag = gaitFlag + 1;
k++;
//reseting the count when the final destination is reach
if(gaitFlag == 402) {
    gaitFlag = 0;
    k=0;
//Save previous error along trajectory for the next iteration of
ILC routine
    for (m=0; m <= 402; m++){
        e_last[m] = e[m];
        old_PD_ILC[m] = PD_ILC[m];
    }
}
if (error < 1 and error > -1)
{
    pid = 0;
}
PIDILC = U_TOT;
pwm = abs(PIDILC);
if (pwm > 255) {
    pwm = 255;
}
if (pwm < 0) {
    pwm = 0;
}
if (PIDILC > 0)
{

```



```

    analogWrite(9, 0);

    analogWrite(10, pwm);

}

if (PIDILC < 0)

{

    analogWrite(9, pwm);

    analogWrite(10, 0);

}

//~~~~~
~~~~~

// long newPosition1 = myEncl.read();

// out1 = newPosition1;

// p1 = 0.45;

// i1 = 0.05;

// d1 = 0.4;

//

// // sp = analogRead(setpoin);

// // sp = map(sp, 0, 1023, 0, 240);

// // sp1 = -12500;

// sp1 = knee[i_knee];

// i_knee ++;

// if (i_knee == 404) {

//     i_knee = 0;

// }

// error1 = sp1 - out1;

```

```

//
// //PID
// error_integrall += error1;
//
// if (error_integrall > 150)
// {
//     error_integrall = 150;
// }
// else if (error_integrall < -150)
// {
//     error_integrall = -150;
// }
//
// pid1 = (error1 * p1) + (error_integrall * i1) + (error_dydx1
* d1);
// pid1 = pid1 / 2;
// error_dydx1 = error1 - error_old1;
// error_old1 = error1;
//
// if (error1 < 1 and error1 > -1)
// {
//     pid1 = 0;
// }
//
// pwm1 = abs(pid1);
// if (pwm1 > 255) {
//     pwm1 = 255;
// }

```

```

// if (pwm1 < 0) {
//   pwm1 = 0;
// }
//
// if (pid1 > 0)
// {
//   analogWrite(5, 0);
//   analogWrite(6, pwm1);
// }
// if (pid1 < 0)
// {
//   analogWrite(5, pwm1);
//   analogWrite(6, 0);
// }
//~~~~~
//~~~~~
// i_knee++;
  Serial.print(sp);
  Serial.print(",");
  Serial.println(out);
// Serial.print(",");
// Serial.println(i_knee);
// Serial.print(",");
// Serial.println(out1);
  delay(50);
}

```



**APPENDIX B**  
**INTERNATIONAL PUBLICATIONS**

Parikesit, E, Maneetham D. Control of robot-assisted gait trainer using hybrid proportional integral derivative and iterative learning control. *International Journal of Electrical and Computer Engineering (IJECE)*. Vol. 12, No. 6, December 2022, pp. 5967~5978. DOI: 10.11591/ijece.v12i6.pp5967-5978

Parikesit, E, Maneetham D. Two-link lower limb exoskeleton model control enhancement using computed torque. *International Journal of Electrical and Computer Engineering (IJECE)*. Vol. 13, No. 6, December 2023, pp. 6204~6215. DOI: 10.11591/ijece.v13i6.pp6204-6215



## Biography



<b>Name-Surname</b>	Elang Parikesit
<b>Date of Birth</b>	March 30, 1970
<b>Address</b>	39 Rangsit, Thanyaburi District, Chang Wat Pathum Thani, 12110
<b>Education</b>	Doctoral Degree in Mechatronics Engineering (D.Eng) – Rajamangala University of Technology Thanyaburi, 2020-2023. Master Degree in Electrical Engineering (M.T), - Institut Teknologi Bandung (ITB), 2009-2012. Bachelor Degree in Electrical Engineering (S.T),- Universitas Diponegoro, 1989-1997.
<b>Work Experience</b>	Universitas Sanata Dharma, Yogyakarta, Indonesia, Lecturer (1999-now)
<b>Telephone</b>	+66 991835303 / +62 83840729336
<b>e-mail Address</b>	<b>elang_p@mail.rmutt.ac.th,</b> <b>elang@usd.ac.id</b>